Dissertation zur Erlangung des Doktorgrades

der Fakultät für Chemie und Pharmazie

der Ludwig-Maximilians-Universität München

Sorafenib Response in Hepatocellular Carcinoma Therapy

–

Introducing New Possibilities with Cdk5 Inhibition

Maximilian Alexander Ardelt

aus Aschaffenburg, Deutschland

2018

Erklärung

Diese Dissertation wurde im Sinne von §7 der Promotionsordnung vom 28. November 2011 von Frau Prof. Dr. Angelika M. Vollmar betreut.

Eidesstattliche Versicherung

Diese Dissertation wurde eigenständig und ohne unerlaubte Hilfe erarbeitet.

München, den 30.07.2018

Maximilian Alexander Ardelt

Dissertation eingereicht am:	26.06.2018
1. Gutachter:	Prof. Dr. Angelika M. Vollmar
2. Gutachter:	Prof. Dr. Johanna Pachmayr
Mündliche Prüfung am:	17.07.2018

To my family

CONTENTS

CONTENTS

SUMMARY

SUMMARY

Hepatocellular carcinoma (HCC) is the second most common cause of cancer related death worldwide, only surpassed by lung cancer. Late diagnosis and a high degree of chemoresistance lead to a poor survival prognosis for HCC patients, with a 5 year survival rate of only 5%. The only approved first line therapy for late stage HCC patients is the multityrosine kinase inhibitor Sorafenib. Clinical trials confirmed, that Sorafenib treatment led to a survival benefit of 3 months, however treatment efficacy is limited by poor response rates, numerous adverse effects and evasive cancer cell signaling. Especially the compensatory activation of growth factor receptor signaling is a major problem restricting the clinical benefit of Sorafenib. Therefore the search for new therapeutic options to improve the efficacy of Sorafenib is of great importance.

Here we investigate the inhibition of cyclin dependent kinase 5 (Cdk5) as a promising combination strategy to improve Sorafenib response in HCC. Combination of Sorafenib with Cdk5 inhibition (genetic knockdown by shRNA or CRISPR/Cas9 and pharmacologic inhibition) synergistically impaired HCC progression *in vitro* and *in vivo* by inhibiting both tumor cell proliferation and migration. Importantly, these effects were mediated by a novel mechanism for Cdk5: A LC-MS/MS based proteomic approach revealed that Cdk5 inhibition interferes with intracellular trafficking, a process crucial for cellular homeostasis and growth factor receptor signalling. Cdk5 inhibition resulted in an accumulation of enlarged vesicles and respective cargos in the perinuclear region, considerably impairing the extent and quality of growth factor receptor signalling (**Figure 1**). Thereby, Cdk5 inhibition offers a comprehensive approach to globally disturb growth factor receptor signalling that is superior to specific inhibition of individual growth factor receptors.

In conclusion, Cdk5 inhibition represents an effective approach to improve Sorafenib response and to prevent Sorafenib treatment escape in HCC. Notably, Cdk5 is an addressable target frequently overexpressed in HCC and with Dinaciclib a clinically tested Cdk5 inhibitor is readily available. Thus, our study provides evidence for clinically evaluating the combination of Sorafenib and Dinaciclib to improve the therapeutic situation for advanced-stage HCC patients.

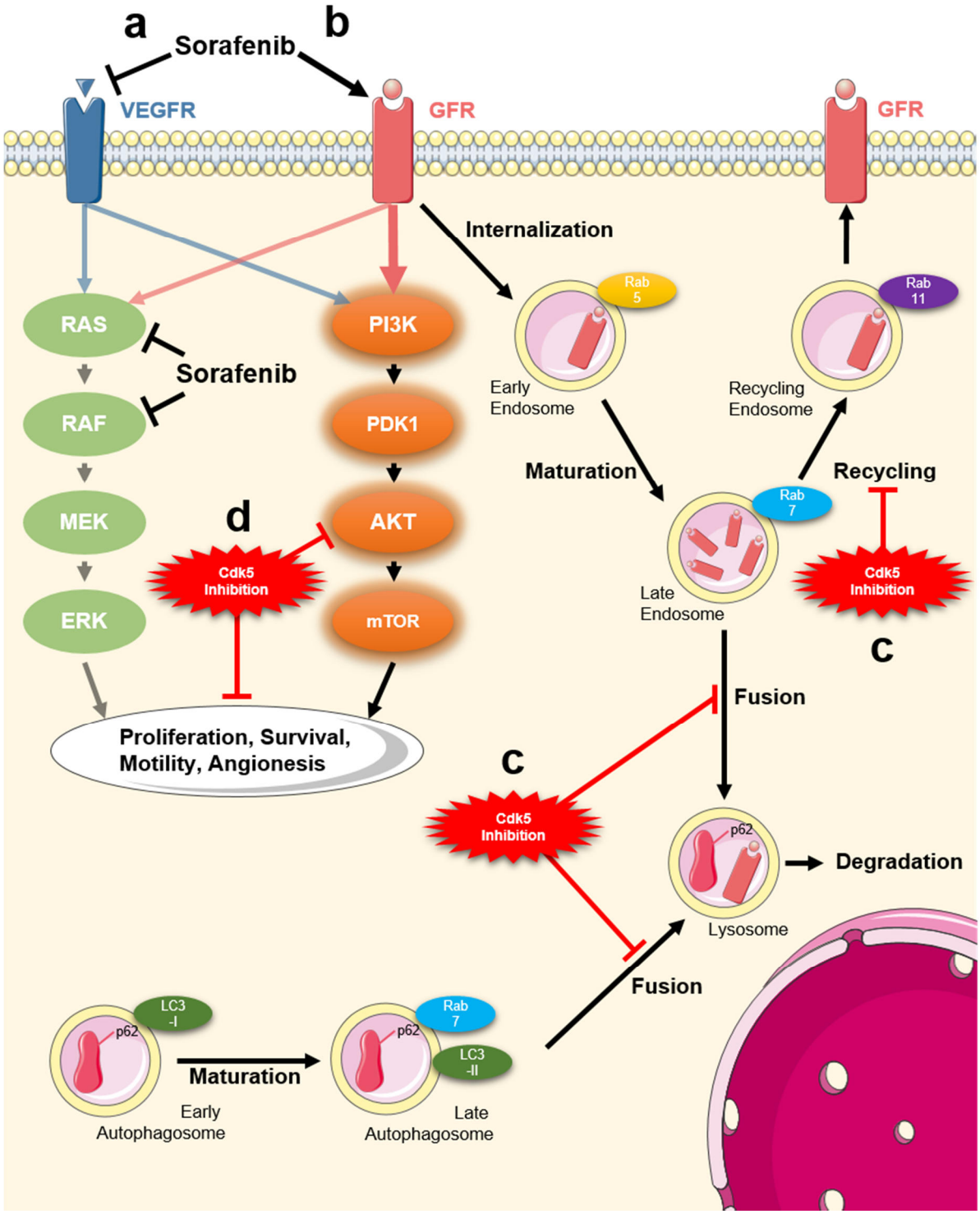

Figure 1 – Cdk5 inhibition prevents compensatory activation of PI3K/Akt pathway by interfering with intracellular trafficking. (**a**) The treatment of HCC cells with Sorafenib causes an inhibition of VEGFR and its downstream targets RAS and RAF. (**b**) In turn, this leads to the compensatory activation of growth factor receptor signaling, which allows tumor cells to maintain proliferation and migration, mediated via the PI3K/AKT pathway. After activation, growth factor receptors have to be trafficked via the endosomal system and are either degraded via lysosomes or recycled via endosomes. (**c**) We uncovered that Cdk5 inhibition interferes with intracellular trafficking leading to an increase in vesicle size and an accumulation of respective cargos. (**d**) Thereby an inhibition of Cdk5 prevents the Sorafenib induced compensatory activation of growth factor receptors and respective downstream targets and enhances the anti-tumor effects of Sorafenib.

INTRODUCTION

1 INTRODUCTION

1.1 Hepatocellular Carcinoma

1.1.1 Pathogenesis and Risk Factors

Even with extensive research in the field of hepatocellular carcinoma (HCC), it still remains one of the most common and lethal cancers worldwide.[1,2] HCC accounts for one third of all cancer related deaths and represents the leading cause of death in liver cirrhosis patients.[3] This is primarily due to high chemoresistance and difficult diagnosis in early stages. Mainly, HCC arises on the basis of a manifested chronic liver disease.[4] Chronic infections with hepatitis B virus (HBV) and exposure to oncogenic substances like aflatoxin B1 are the main cause for HCC in eastern Asia and large parts of Africa. The main risk factors in western countries are infections with hepatitis C virus (HCV) and alcohol abuse with non-alcoholic fatty liver disease and diabetes as minor risk factors.[5] The presented risk factors ultimately lead to liver cirrhosis which contributes to the development of HCC and is present in 80-90% of HCC patients.[6]
The molecular background on which HCC develops is very heterogeneous.[7] Mutations of various oncogenes and tumor suppressor proteins like p53 are commonly found in HCC tissue compared to healthy liver tissue.[8] Numerous signaling pathways are altered in HCC, like the Wingless (Wnt) signaling cascade, that is known to be associated with the development of several cancer types[9] and to support HCC progression.[10] The diversity of molecular alterations complicates the establishment of effective chemotherapy.

1.1.2 Staging and treatment

HCC patients are commonly classified according to the Barcelona clinic liver cancer (BCLC) staging system or the Child Pugh system (**Figure 2**).[11,12] The determined stage of disease is crucial for the treatment strategy and the prognosis is strongly dependent on the gravity of the initial liver disease.[13] For patients diagnosed with early stage HCC curative treatment options like surgical liver resection, orthotopical liver transplantation or radio frequency ablation are available.[14] Especially liver transplantations result in excellent prognoses for patients, because the underlying liver disease is cured in the process.[15] However, it is needless to say that the demand for donor organs greatly overtakes the supply. Transarterial chemoembolization (TACE) is the method of choice for intermediate stage HCC patients.[16] Nonetheless, HCC is commonly diagnosed at an advanced stage, where curative treatment is no longer feasible.[17] Therapy resistance against conventionally used chemotherapeutics, like DNA damaging agents, narrow the options for drug based treatments.[18] Therefore patients diagnosed with

advanced stage HCC face a poor prognosis with a median overall survival of 6.5-10.7 months. The only available treatment option to increase the median overall survival is the multityrosine kinase inhibitor Sorafenib, which is considered the first line treatment for unresectable HCC.[19]

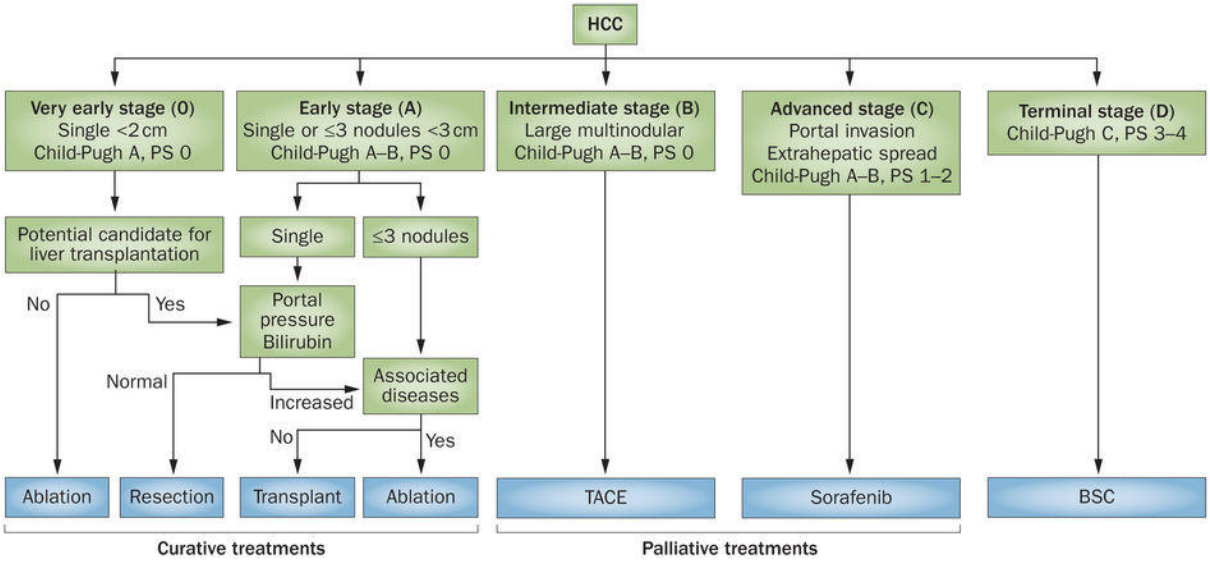

Figure 2 – Barcelona Clinic Liver Cancer and Child-Pugh staging system. Adapted from Forner et al.[20]

1.2 Sorafenib in HCC therapy

Sorafenib is an orally available multi-tyrosine kinase inhibitor and represents the only approved systemic treatment option for advanced HCC (**Figure 3**).[21] Tumor growth and angiogenesis are inhibited by targeting Raf, RET, FMS-like tyrosine kinase 3 (FLT3), c-Kit, vascular endothelial growth factor receptor (VEGFR) -1, -2 and -3 and platelet derived growth factor receptor (PDGFR) α and β.[22] Thereby Sorafenib directly targets the Ras/mitogen-activated protein kinase (MAPK)/extracellular signaling-regulated kinase (Erk) pathway, which is involved in tumor cell proliferation and angiogenesis and is frequently increased in HCC (**Figure 4**).[23]

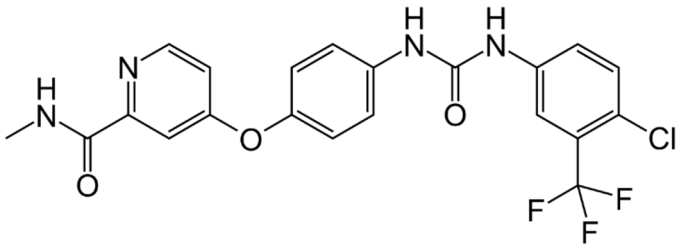

Figure 3 – Chemical structure of Sorafenib.

The clinical efficiency of Sorafenib was evaluated in two large phase III clinical trials, the SHARP (Sorafenib Hepatocellular carcinoma assessment randomized protocol) trial, conducted in Europe and America, and a similar trial performed in Asia.[19,24] Both revealed a significant increase in median overall survival as well as time to radiologic progression in the Sorafenib group compared to the placebo group. However, the increase in median overall survival only amounts to about 3 months, which is a great achievement, but leaves room for improvement. In addition, treatment success was restricted by low response rates and severe side effects including hand-foot skin reaction, diarrhea and fatigue. These adverse reactions often demand for dose reduction or, at worst, a complete termination of treatment.[25] Therefore various attempts were made to improve the effect of Sorafenib via combinational therapy, though with very little success.[21]

Hence, the identification of new targets for the treatment of HCC is of substantial importance and might be the key to improve the therapeutic effect of Sorafenib. A study conducted by our group could show that the cyclin-dependent kinase 5 (Cdk5) is frequently overexpressed in HCC tissue and represents a promising drug target. An inhibition of Cdk5 sensitized HCC cells for the treatment with conventional chemotherapeutics and we therefore judged Cdk5 as a potential candidate to support Sorafenib treatment.[26]

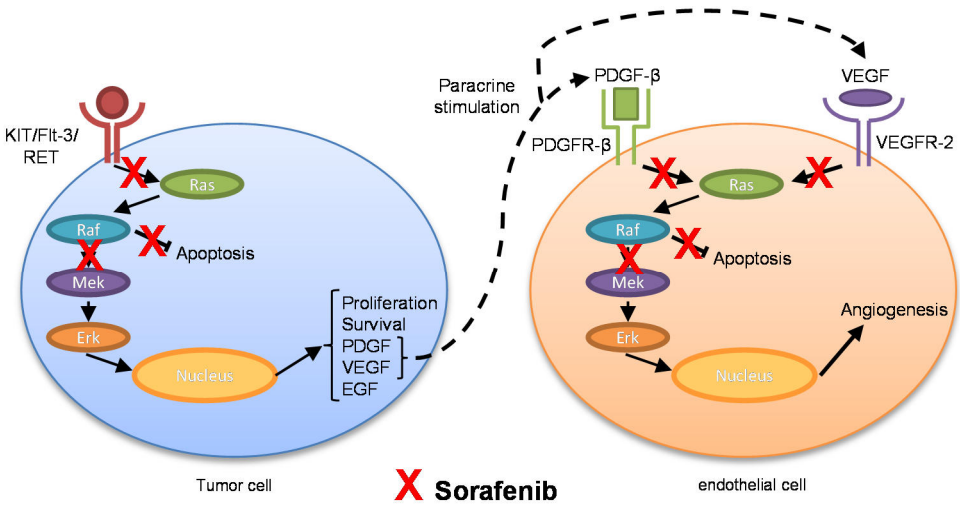

Figure 4 – Mechanism of action for Sorafenib.

1.3 Cyclin Dependent Kinase 5

Cyclin dependent kinase (Cdk) 5 can be described as an unusual member of the cyclin dependent kinase family, a group of serine/threonine kinases controlled by cyclins with major influence on cellular progression by regulating multiple steps of the cell cycle.[27] Cdk5 however is neither regulated by cyclins nor is it involved in cell cycle control, despite sharing 60% structural identity with Cdk1 and Cdk2.[28]

In the early 1990s, Cdk5 was discovered in neurons and was long thought to be neuron specific.[29] In the central nervous system (CNS) Cdk5 plays an essential role in neuronal development, migration and function.[30] The importance of Cdk5 for brain development is most likely seen in mice with a knockout of Cdk5 or its activators p35 and p39, which die perinatally due to disruption of the neuronal layering throughout the brain.[31] Additionally, Cdk5 regulates memory processes and learning by influencing synaptic transmission and axon guidance and is accountable for mediating drug addiction by affecting dopaminergic signal transmission pathways (**Figure *5***).[30,32]

Numerous reports also show that Cdk5 is involved in the development of various neurodegenerative diseases.[33] The binding of Cdk5 to p25, the truncated form of its activator p35, leads to abnormal kinase activity and thus to increased phosphorylation and activation of Cdk5 downstream targets. An overactivation of the Cdk5 signaling cascade is related to the pathogenesis of Alzheimer's and Parkinson's disease.[34-36]

1.3.1 Regulation and Dysregulation of Cdk5

Like other Cdks, Cdk5 is activated by its binding to the respective catalytic subunits, which are in the case of Cdk5 not the eponymous cyclins, but the two non-cyclin Cdk5 specific proteins p35 and p39.[30] The Cdk5 activators share an amino acid homology of 57% and are both regulated by transcription and ubiquitin-mediated degradation.[28] Notably, despite their sequence similarity, the absence of p39 can be compensated by p35, but not vice versa.[37] An amino-terminal myristoylation motif defines the subcellular distribution and binds p35 and p39 to the plasma membrane and cytoskeleton and therefore activated Cdk5 is most likely to be found in the cell periphery.[38] In addition to the interaction with p35/p39, it was believed that a phosphorylation of Cdk5 at residue Tyr15, a target domain for the upstream kinases Fyn and c-Abelson (c-Abl) increased kinase activity.[39,40] However, Kobayashi et al. showed that in neuronal cells a phosphorylation of Tyr15 does not influence kinase activity.[41]

Cdk5 activity has to be tightly controlled, because aberrant activation and thus hyperphosphorylation of downstream targets is associated with the pathogenesis of neurodegenerative diseases. For instance, reports indicate that Cdk5 is involved in the hyperphosphorylation of the microtubule associated protein tau, which marks a crucial

pathological event in Alzheimer's disease.[42] Abnormal activation is primarily caused by the binding of Cdk5 to p25, the N-terminally truncated form of p35 generated by calpain-mediated proteolytic cleavage.[43] Besides a 5-10-fold increase in half-life compared to p35, p25 lacks the myristoylation motif, which leads to a mislocalization of the activated Cdk5-p25 complex to the wrong intracellular section and therefore to aberrant target phosphorylation (**Figure 5**).[44]

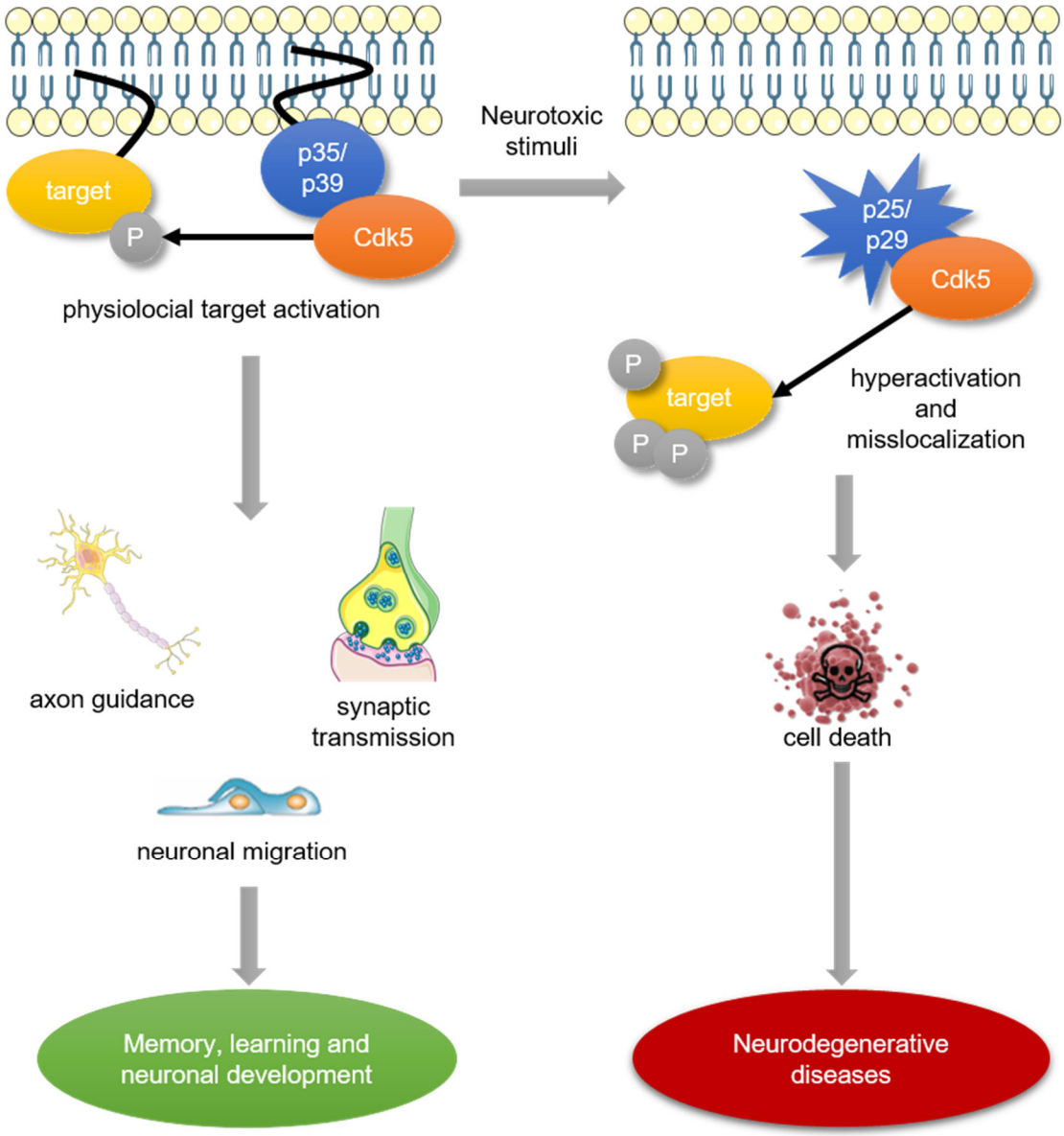

Figure 5 - Overview of function and dysregulation of Cdk5 in neurons. Adapted from Liebl et al.[30]

1.3.2 Function of Cdk5 in Cancer

Most of the knowledge about Cdk5 stems from the study of neuronal cells. Nevertheless, in the last decade it has been shown that Cdk5 also plays a role in non-neuronal tissue.[43] Along this line Cdk5 has been associated with human cancer progression.[45] Accumulating evidence is indicating that Cdk5 is expressed in human cancers, where it is linked to increased cancer risk and severity.[46,47] For instance, increased levels of Cdk5 or its activators p35/p25 correlate with advanced cancer stages and poor prognosis in non-small cell lung cancer (NSCLC), brain, nasopharyngeal and breast cancer.[48-51] Cdk5 was shown to play a key role in the regulation of pathways necessary for cancer progression. For example, the retinoblastoma protein (Rb)/E2F pathway is activated by Cdk5 in medullary thyroid carcinoma (MTC), thus promoting cancer cell proliferation and cell cycle progression.[52,53] In prostate cancer, Cdk5 phosphorylates signal transducer and activator of transcription 3 (STAT3) and androgen receptor (AR), thereby directly contributing to the dysregulation of these pathways and cancer progression.[54,55] Another important aspect of tumor progression is angiogenesis, where new blood vessels are generated from pre-existing ones to manage the increased need for oxygen and nutrients of solid tumors. The formation of blood vessels is initiated by endothelial cells, where Cdk5 is not only expressed but is a key regulator of proliferation and migration.[56-58] Therefore, Cdk5 inhibition has come into focus as a potential strategy to inhibit cancer growth by disturbing angiogenesis, thus starving the tumor.

In keeping with the latter notion, our group could discover a vital role for Cdk5 in HCC.[26] Not only is Cdk5 overexpressed in HCC tissue compared to healthy liver tissue, it also regulates tumor cell survival by influencing DNA damage response. By exploiting the impact of Cdk5 on DNA damage regulation with pharmacological inhibitors or genetic downregulation, HCC cells could be sensitized to the treatment with DNA damaging agents. By combining Cdk5 inhibition with DNA damaging agents, HCC cell proliferation could be inhibited *in vitro* as well as *in vivo*. However, DNA damaging agents are only approved for the treatment of patients with intermediate stage HCC.[20] In the therapeutic schedule of advanced stage HCC patients, DNA damage inducing agents received little attention up to this point, because high degree of treatment resistance limited therapeutic success.

1.3.3 Pharmacological Inhibition of Cdk5

Cyclin-dependent kinases are attractive targets for cancer therapy because of their pivotal role in cell cycle regulation and cellular progression.[59] As neoplastic cells show a high degree of proliferation and cell division, inhibiting growth by arresting cell cycle progression would mean a certain specificity for cancer cells.[60] Nonetheless, the development of Cdk5 inhibitors started on a different basis. The pivotal role of Cdk5 in the pathogenesis of neurodegenerative

diseases led to the endeavor to design specific Cdk5 inhibitors.[33] Due to the high sequence similarity within the Cdk family this presents a difficult task as most inhibitors target a variety of Cdks.[30] The first Cdk5 inhibitors were Olomoucine and Roscovitine (**Figure 6a, b**), a synthetic derivate of Olomoucine, which target the ATP-binding pocket, an adequately conserved domain throughout the Cdk family. Despite having the highest relative selectivity for Cdk5, Roscovitine further targets Cdk1, Cdk2 and Erk 1, 2 and 8.[61] Nevertheless, Roscovitine provided promising preclinical results as an anti-cancer agent, but clinical trials remained unconvincing. With the intension of increasing selectivity for Cdk5 for the application in neurodegenerative diseases, indolinone D (Boehringer-Ingelheim)[62] and 4-amino-imidazoles (Pfizer)[63] were developed.

The refinement of Cdk inhibitors led to the development of Dinaciclib (**Figure 6c**), a novel potent small molecule inhibitor with high selectivity for Cdk 5, 2, 1 and 9 (IC_{50} = 1, 1, 3 and 4 nmol/l respectively).[64] Recent reports already showed that Dinaciclib revealed promising effects in various types of cancer. Especially in hematological malignancies Dinaciclib showed encouraging results. Collectively, Cdk5 is a promising target for cancer therapy with a variety of inhibitors available, which have already been established in clinical context.

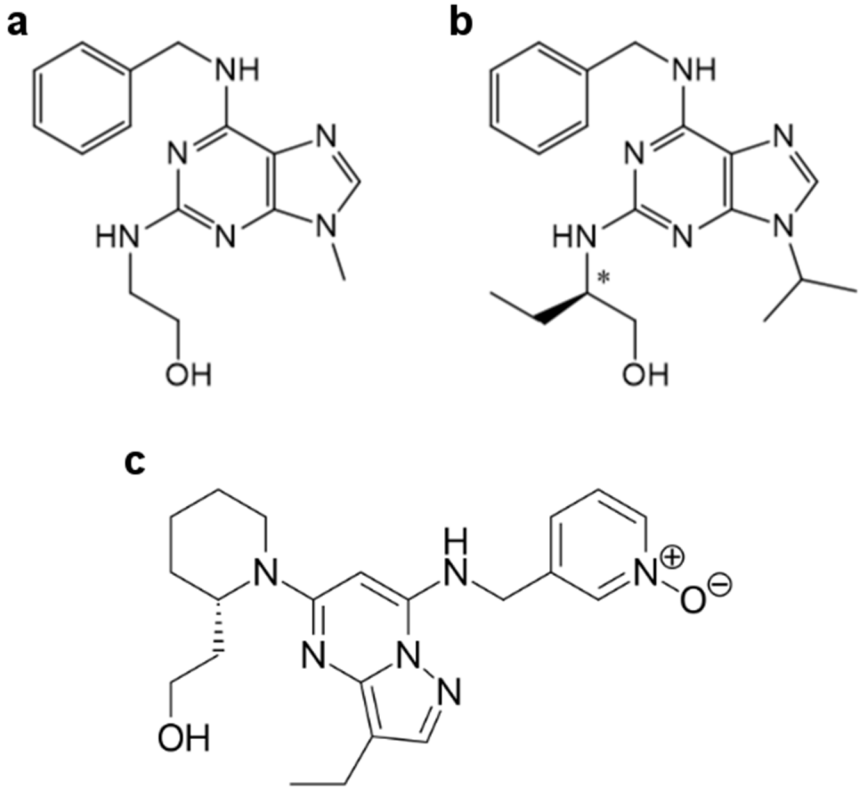

Figure 6 - Structure of Olomucine (a), Roscovitine (b) and Dinaciclib (c).

1.4 Aim of the Study

Background:

- The multikinase inhibitor Sorafenib still represents the only approved first line therapy for advanced-stage HCC patients. However, due to low response rates, severe side effects, and tumor progression, clinical effectiveness is limited and patients face a poor prognosis. So far, new therapies or combination approaches to improve Sorafenib failed.
- Sorafenib treatment is limited by chemoresistance and compensatory activation of survival signalling and growth factor receptors signaling
- Compounds that directly address specific growth factor receptors have failed to improve Sorafenib responsiveness
- Cdk5 is frequently overexpressed in HCC and regulates tumor cell survival by influencing DNA damage response
- Cdk5 inhibition can be used to sensitize HCC cells for the treatment with DNA damaging agents

The aim of this study was to evaluate if Cdk5 inhibition can be utilized to prevent Sorafenib induced treatment escape. Therefore, the functional effects of Cdk5 inhibition in combination with Sorafenib on tumor cell proliferation and migration were investigated *in vitro* as well as *in vivo*. Further, the underlying mechanism behind the sensitizing effect of Cdk5 inhibition was elucidated.

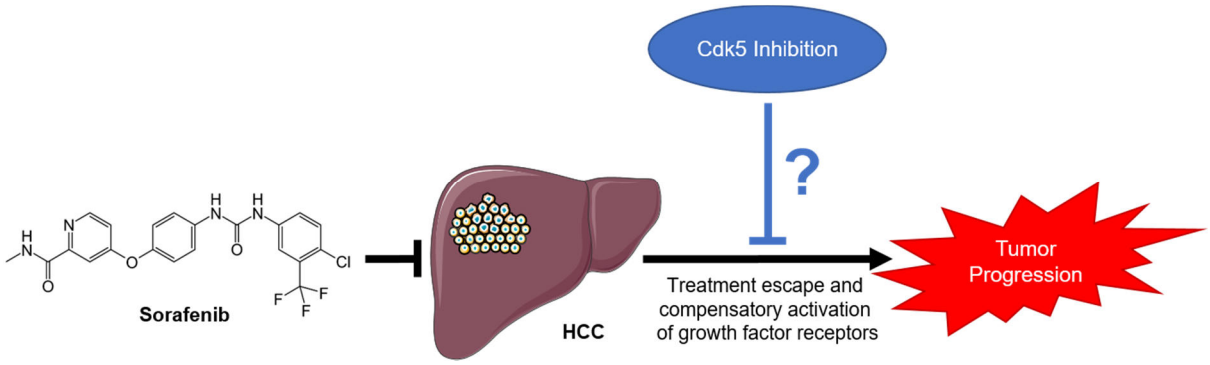

Figure 7

MATERIALS AND METHODS

2 MATERIALS AND METHODS

2.1 Materials

2.1.1 Compounds

(R)-Roscovitine was obtained from Sigma-Aldrich. Sorafenib was obtained from Enzo Life Sciences. Dinaciclib and Gefitinib were obtained from Selleckchem. LGR1407 was kindly provided by Libor Havlíček, Isotope Laboratory (Institute of Experimental Botany AS CR, Prague, Czech Republic).

2.1.2 Reagents and Technical Equipment

Table 1 - Biochemicals, inhibitors, dyes and cell culture reagents

Reagent	Producer
Bovine serum albumin (BSA)	Sigma-Aldrich, Taufkirchen, Germany
Bradford reagent Roti® Quant	Bio-Rad, Munich, Germany
CellTiter-Blue® reagent	Promega, Mannheim, Germany
Collagen G	Biochrom AG, Berlin, Germany
Complete®	Roche Diagnostics, Penzberg, Germany
CyQUANT® Cell Proliferation Assay Kit	Life Technologies, Eugene, USA
Dimethylsulfoxide (DMSO)	Sigma-Aldrich, Taufkirchen, Germany
Dithiothreitol (DTT)	Sigma-Aldrich, Taufkirchen, Germany
Dulbecco's Modified Eagle Medium (DMEM)	PAA Laboratories, Pasching, Austria
ECL Plus WB Detection reagent	GE Healthcare, München, Germany
Ethylendiaminetetraacetic acid (EDTA)	Sigma Aldrich, Taufkirchen, Germany
Fetal calf serum (FCS)	Biochrom AG, Berlin, Germany
FluorSave® reagent mounting medium	Merck, Darmstadt, Germany
Glycerol	Applichem¸ Darmstadt, Germany
High-Capacity cDNA Reverse Transcription Kit	Applied Biosystems, Waltham, USA
Hoechst 33342	Sigma-Aldrich, Taufkirchen, Germany
ibidiTreat µ-slides	Ibidi GmbH, Munich, Germany
L-Glutamine	Sigma-Aldrich, Taufkirchen, Germany
Mayer's Hematoxylin Solution	Sigma-Aldrich, Taufkirchen, Germany
MEM Eagle Medium	PAA Laboratories, Pasching, Austria
MicroAmp® Fast Optical 96-Well Reaction Plate, 0.1 mL	Applied Biosystems, Waltham, USA
MicroAmp® Optical Adhesive Film	Applied Biosystems, Waltham, USA
Nitrocellulose membrane (0.2 µM)	Hybond-ECL™, Amersham Bioscience, Freiburg, Germany
Non-fat dry milk powder	Carl Roth, Karlsruhe, Germany
Page Ruler™ Prestained Protein Ladder	Fermentas, St. Leon-Rot, Germany
Penicillin/Streptomycin 100x	PAA Laboratories, Pasching, Austria

Reagent	Producer
Phenymethylsulfonyl fluoride (PMSF)	Sigma-Aldrich, Taufkirchen, Germany
Polyacrylamide	Carl Roth, Karlsruhe, Germany
Poly-D-lysine hydrobromide (mol wt 70,000-150,000)	Sigma-Aldrich, Taufkirchen, Germany
Polyvinylidene difluoride (PVDF) membrane (0.2 µM)	Hybond-ECL™, Amersham Bioscience, Freiburg, Germany
PowerUp™ SYBR® Green Master Mix	Applied Biosystems, Waltham, USA
Primers	metabion, Planegg, Germany
Propidium Iodide	Sigma-Aldrich, Taufkirchen, Germany
Puromycin	Sigma-Aldrich, Taufkirchen, Germany
RNeasy® Mini Kit (250)	QIAGEN, Hilden, Germany
Seahorse XF Glycolysis Stress Test Kit	Agilent Technologies, Santa Clara, USA
Seahorse XFe96 FluxPaks (inc. mini)	Agilent Technologies, Santa Clara, USA
Sodium chloride	Carl Roth, Karlsruhe, Germany
Sodium fluoride (NaF)	Merck, Darmstadt, Germany
Sodium orthovanadate (Na_3VO4)	ICN, Biomedicals, Aurora, OH, USA
Sodiumdodecylsulfate (SDS)	Carl Roth, Karlsruhe, Germany
Transwell Permeable Supports (8 µm pore polycarbonate inserts)	Corning Incorporated, New York, NY, USA
Tris Base	Sigma-Aldrich, Taufkirchen, Germany
Trypsin	PAN Biotech, Aidenbach, Germany
Tween 20	Sigma-Aldrich, Taufkirchen, Germany

Table 2 - Technical equipment

Name	Producer
Axioskop microscope	Zeiss, Jena, Germany
Axiovert 25/200 microscope	Zeiss, Jena, Germany
Canon 450D camera	Canon, Krefeld, Germany
Canon DS 126181 camera	Canon, Krefeld, Germany
ChemiDoc™ Touch Imaging System	Bio-Rad Laboratories GmbH
FACSCalibur	Becton Dickinson, Heidelberg, Germany
TCS SP8 confocal laser scanning microscope	Leica Microsystems, Wetzlar, Germany
Mikro 22R centrifuge	Hettich, Tuttlingen, Germany
Nanodrop® Spectrophotometer	PEQLAB Biotechnologie GmbH
Olympus DP25 camera	Olympus, Hamburg, Germany
Olympus BX41 microscope	Olympus, Hamburg, Germany
QuantStudio™ 3 Real-Time PCR System	Applied Biosystems
Seahorse XF^e96 Analyzer	Agilent Technologies
SpectraFluor Plus™	Tecan, Crailsheim, Germany
Vi-Cell™ XR	Beckman Coulter, Fullerton, CA, USA
xCELLigence System	Roche Diagnostics, Mannheim, Germany
Zeis LSM 510 Meta confocal laser scanning microscope	Zeis, Jena, Germany

2.2 Cell culture

2.2.1 Solutions and Reagents

The following solutions and reagents were used for the cultivation of HCC cells.

Table 3 - Solutions and reagents for cell culture

PBS (pH 7.4)	
NaCl	132.2 mM
Na_2HPO_4	10.4 mM
KH_2PO_4	3.2 mM
H_2O	

PBS+Ca^{2+}/Mg^{2+} (pH 7.4)	
NaCl	137 mM
KCl	2.68 mM
Na_2HPO_4	8.10 mM
KH_2PO_4	1.47 mM
$MgCl_2$	0.25 mM
H_2O	

Growth medium	
DMEM/MEM Eagle	500 ml
FCSgold (not heat-inactivated)	50 ml

Freezing medium	
DMEM	70%
FCSgold (not heat-inactivated)	20%
DMSO	10%

Trypsin/EDTA (T/E)	
Trypsin	0.05%
EDTA	0.20%
PBS	

Collagen G	
Collagen G	0.001%
PBS	

2.2.2 Cell Lines

HUH7 and Hep3B cells were obtained from Japanese Collection of Research Biorescources (JCRB) and ATCC, respectively. RIL175 cells were kindly provided by Simon Rothenfußer (Center of Integrated Protein Science Munich (CIPS-M) and Division of Clinical Pharmacology, Department of Internal Medicine IV, Klinikum der Universität München). For the cultivation of HUH7 and RIL175 DMEM supplemented with 10% fetal calf serum(FCS) was used, while Hep3B cells were cultured in MEM Eagle supplemented with 10% FCS. All cells were cultured at 37°C with 5% CO^2 in constant humidity in an incubator. Before cell seeding, all culture flasks, multiwell-plates and dishes were coated with collagen G (0.001% in PBS).

2.2.3 Passaging

When cells reached confluency, they were either subcultured 1:2-1:10 in 75cm^2 culture flasks or seeded in multiwell-plates or dishes for further experiments. For the detachment of cells, they were washed with prewarmed PBS and afterwards incubated with trypsin/ethylene diamine tetraacetic acid (EDTA) for 2-3 min at 37°C. Tryptic digestion was stopped by adding growth medium. To prepare the cells for plating, trypsin/EDTA was removed by centrifugation (1000 rpm, 5 min, 20°C) and replaced by fresh growth medium.

2.2.4 Freezing and Thawing

For long term storage, cells were detached as described previously and resuspended in ice-cold freezing medium (containing 20% FCS and 10% DMSO). Aliquots of 1.5 ml (equal to 3x10^6 cells) were transferred into cryovials. After an initial storage at -80°C for 24h, cryovials were moved to liquid nitrogen for long term storage. For the thawing process, cryovials were warmed to 37°C and the cell suspension was immediately dissolved in prewarmed growth medium. Through centrifugation (1000 rpm, 5 min, 20°C) excessive DMSO was removed by replacing freezing medium with fresh growth medium.

2.3 Transfection Experiment – Cdk5 shRNA

For the transduction of HUH7 and Hep3B cells with Cdk5 shRNA and nt shRNA Cdk5 MISSION® shRNA Lentiviral Transduction Particles (Vector: pLKO.1-puro; SHCLNV-NM_004935; Clone ID: (1) TRCN0000021465, (2) TRCN0000021466, (3) TRCN0000021467, (4) TRCN0000194974, (5) TRCN0000195513; Sigma-Aldrich) and MISSION® pLKO.1-puro Non-Mammalian shRNA Control Transduction Particles (SHC002V; Sigma-Aldrich) as a control were used according to the manufacturer's protocol. Both cell lines were transduced with a multiplicity of infection (MOI) of one. Successfully transduced cells were selected by adding 2µg/ml puromycin to the medium. After the initial selection, puromycin concentration was reduced to 1µg/ml for further cultivation to ensure the stable transfection with Cdk5 and nt shRNA. Through Western Blot analysis the most efficient and well tolerated clones were selected.

2.4 Genome Editing Using the CRISPR/Cas9 System

2.4.1 DNA Isolation and Guide RNA Design

For the knockout of Cdk5 in murine RIL175 cells the CRISPR/cas9 system was used as described previously.[65] We decided to introduce an InDel-mutation into exon 2 of the Cdk5 gene. Genomic DNA was isolated from wild-type RIL175 cells using the QuickExtract DNA extraction solution according to the manufacturer's protocol. The genomic region of interest was amplified with the appropriate primers (**Table 4**) via PCR by using the Phusion® high fidelity DNA polymerase kit as described by the manufacturer. Correct amplification was checked by agarose gel electrophoresis (2% agarose in Tris/Borate/EDTA buffer, 150 V, 45 min). Sequencing services were provided by Eurofins Genomics GmbH (Ebersberg, Germany).

Table 4 - Sequencing primers

Name	Sequence
Cdk5_PCR_F	5'- CTTCCTGCATTTCTCGTCCC-3'
Cdk5_PCR_R	5'- CTACAACATGCAAGGGGGTA-3'
Cdk5_Sequencing_F	5'- GAGTTTATGGCAGATTCTCC-3'

For the generation of single guide RNAs (sgRNAs) the CRISPOR-Tefor online designing tool was used as described previously.[66] The three top-ranked sgRNAs were used for further experiments (**Table 5**).

Table 5 - sgRNA sequences/cloning oligomers

Name	Sequence
Cdk5_sgRNA1_top	5'-CACCGTTGTGGCTCTGAAGCGTGTC-3'
Cdk5_sgRNA1_bottom	5'-AAACGACACGCTTCAGAGCCACAAC-3'
Cdk5_sgRNA2_top	5'-CACCGGCTCTGAAGCGTGTCAGGC-3'
Cdk5_sgRNA2_bottom	5'-AAACGCCTGACACGCTTCAGAGCC-3'
Cdk5_sgRNA3_top	5'-CACCGTGTGTTCAAGGCTAAAAACC-3'
Cdk5_sgRNA3_bottom	5'-AAACGGTTTTTAGCCTTGAACACAC-3'

2.4.2 Cloning and Transformation of E.coli

In the next step, the three top-ranked sgRNAs were cloned via the BbsI restriction site into the eSpCas9(1.1)-2A-Puro using the T4 DNA ligase protocol provided by the manufacturer (New England BioLabs, Frankfurt a.M., Germany). Therefore cloning oligomers were annealed using a PCR cycler (5 min at 95°C, ramp down to 25°C) and diluted (1:200 in H_2O) (**Table 6**).

Table 6 - Oligo-Annealing-Mix

Reagent	Volume [µl]
sgRNA_top (100 µM)	1
sgRNA_bottom (100 µM)	1
T4 ligation buffer	1
H_2O	7

eSpCas9(1.1)-2A-Puro was cloned by introducing the T2A-puromycin resistance cassette from PX459 into eSpCas9(1.1) via FseI and NotI (both plasmids were a gift from Feng Zhang, Addgene plasmids #62988 and #71814, respectively).[67] For the insertion of the annealed oligomers the desired plasmid (eCas9_Puro2.0, c=464,9 ng/µl) has to be opened with a suited restriction enzyme. Therefore a restriction enzyme mix was prepared and incubated at 37°C for 30 min (**Table 7**).

Table 7 - restriction enzyme mix

Reagent	Volume [µl]
eCas9_Puro2.0 plasmid (150 ng)	0.323 µl
FD buffer (10x)	1.5
FD BpiI (restriction enzyme)	1
H_2O	Ad 15

For the assembly of annealed oligomers and opened plasmid a ligation mix containing T4 DNA ligase was prepared and incubated at RT for 30 min (**Table 8**). For the removal of not ligated plasmid the PlasmidSafe ATP-dependent DNase was used according to the manufacturer's protocol and incubated at 37°C for 30 min and at 70°C for 30 min (**Table 9**). Obtained plasmids were stored at -20°C before the transformation of E.coli.

Table 8 - ligation mix

Reagent	Volume [µl]
Restricted plasmid	10
Annealed oligomers (diluted)	2
T4 ligation buffer (10x)	2
T4 DNA ligase	1
H2O	5

Table 9 - PlasmidSafe Exonuclease mix

Reagent	Volume [µl]
Ligation product	11
PlasmidSafe buffer (10x)	1.5
ATP (25 mM)	0.6
PlasmidSafe Exonuclease	1
H_2O	Ad 15

For the replication of plasmid-DNA, competent DH5α-E.coli were transformed with the respective sgRNA plasmids. After addition of plasmid-DNA, E.coli were first kept on ice for 10 min before being heat-shocked at 42°C for 45 s and returned to ice for 2 min. The bacterial suspension was then plated on an agar plate with ampicillin and stored at 37°C over night. On the next day 3-5 colonies were picked per plasmid and amplified in 5 ml LB (+) medium containing 100 µg/ml ampicillin. Plasmids were then isolated by mini-prep using the Qiaprep Spin Miniprep kit as described by the manufacturer. Correct insertion and amplification was confirmed by restriction analysis (restriction enzyme: EheI) and sequencing (U6-F-primer: 5'-GAGGGCCTATTTCCCATGATTCC-3') before selected plasmids were amplified and isolated using the QIAGEN plasmid Maxiprep Kit according to the manufacturer's protocol.

2.4.3 Transfection and Evaluation of Genome Targeting Efficiency

RIL175 cells were cultured in 6-well plates to a confluency of 60-70% before being transfected with respective plasmids (sgRNA1, 2 and 3) using Lipofectamine™ 3000 as described by the manufacturer. An eGFP-plasmid was used to evaluate transfection efficiency after 24 hours, before puromycin (2µg/ml) was added for another 48 hours. After removal of puromycin, cells were left to recover until reaching sufficient confluency for the analysis of genome targeting efficiency using T7 Endonuclease I according to the manufacturer's instructions. Cells transfected with the sgRNA plasmid with the highest genome targeting efficiency were subjected to clonal selection.

2.4.4 Clonal Selection and Knockout Verification

Clonal-density dilution was used to isolate clonal cell lines. Therefore cells were dissociated from the transfected wells and adjusted to a cell number of 0.6 cells/well before being seeded into 96-well plates. Cell aggregates were separated with a cell strainer prior to seeding. Single cell colonies were grown to confluency before DNA and whole cell proteins were isolated to check gene knockout via sequencing and Western blot analysis.

2.5 Western Blot Analysis

2.5.1 Cell Lysis

For the cell lysis cells were washed with ice-cold PBS before adding lysis buffer and freezing the cells at -80°C. The cells were then scraped off, transferred into Eppendorf tubes and centrifuged (14.000 rpm, 10 min, 4°C) in order to remove debris. To ensure equal amounts of protein in all samples, protein concentration was measured using Bradford Assay and adjusted by adding 1x SDS sample buffer. The samples were then heated at 95°C for 5 min and kept at -20°C until Western blot analysis.

2.5.2 SDS-PAGE

For the separation of proteins a discontinuous SDS-polyacrylamide gel electrophoresis (SDS-PAGE) was used, as described by Laemmli.[68] Equal amounts of adjusted protein samples were loaded on the discontinuous polyacrylamide gels, which consist of a separation and a stacking gel, and were separated using a Mini PROTEAN 3 electrophoresis module. To ensure the best protein separation the concentration of Rotiphorese™ Gel 30 (acrylamide) in the separation gel was adjusted depending on the molecular weight of the proteins of interest. In the first step of electrophoresis the proteins were stacked at a current of 100 V for 21 min before being separated at 200 V for 45 min in the second step. To evaluate the molecular weight of the proteins the received bands were compared to the prestained protein ladder PageRuler™ or the Spectra Multicolor High Range Protein Ladder™.

2.5.3 Tank Electroblotting and Protein Detection

After separation, the proteins were transferred onto a nitrocellulose membrane by electro tank blotting.[69] Before usage the membrane was equilibrated with 1x tank buffer for 15 min. After equilibration a blotting sandwich (cathode – pad – blotting paper – separation gel – nitrocellulose membrane – blotting paper – pad – anode) was prepared and mounted in the

Mini Trans-Blot® system, which was filled with 1x tank buffer. The proteins were transferred using a constant current of 100 V for 90 min.

To block the unspecific binding sites, the membrane was incubated in 5% non-fat dry milk powder for 2 h before being incubated with the primary antibody overnight at 4°C. The excess of primary antibody was washed away in four washing steps with TBS-T, before the incubation with the secondary antibody for 2 h at RT. Secondary antibody were HRP-coupled and chemiluminescence was detected by adding ECL substrate and analysed with a ChemiDoc touch device.

Table 10 - Solutions and reagents for Western blot analysis

Lysis buffer	
Tris/HCl	50 mM
NaCl	150 mM
Nonidet NP-40	1%
Sodium deoxycholate	0.25%
SDS	0.10%
activated Na_2VO_4	300 µM
NaF	1 mM
β-glycerophosphate	3 mM
pyrophosphate	10 mM
H_2O	
add before use:	
Complete® EDTAfree	4 mM
PMSF	1 mM
H_2O_2	600 µM

5x SDS sample buffer	
Tris/HCl pH 6.8	3.125 M
Glycerol	50%
SDS	5%
DTT	2%
Pryonin Y	0.025%
H_2O	

Separation gel 7.5%/10%/12%/15%	
Rotiphorese™ Gel 30	25%/33%/ 40%/50%
Tris (pH 8.8)	375 mM
SDS	0.1%
TEMED	0.1%
APS	0.05%
H_2O	

Stacking gel	
Rotiphorese™ Gel 30	17%
Tris (pH 6.8)	125 mM
SDS	0.1%
TEMED	0.2%
APS	0.1%
H_2O	

Electrophoresis buffer	
Tris	4.9 mM
Glycine	38 mM
SDS	0.1%
H_2O	

Tank buffer	
Tris base	48 mM
Glycine	39 mM
Methanol	20%
H_2O	

Table 11 - primary antibodies for Western blot

Antigen	Product no.	Provider	Dilution	In
Akt	#9272	Cell Signaling Technology	1:1,000	BSA 5%
actin	MAB1501	Millipore	1:1,000	Blotto 1%
p-Akt (Ser473)	#9271	Cell Signaling Technology	1:500	BSA 5%
p44/42 MAPK (Erk)	#9102	Cell Signaling Technology	1:1,000	BSA 5%
p-Erk (Thr 202/Tyr204)	#9106	Cell Signaling Technology	1:1,000	BSA 5%
Erk	#9102	Cell Signaling Technology	1:1000	BSA 5%
EGFR	#2239	Cell Signaling Technology	1:1,000	BSA 5%
p-EGFR (Tyr 1068)	#2234	Cell Signaling Technology	1:1,000	BSA 5%
Cdk5	AHZ0492	Invitrogen	1:1,000	Blotto 1%
p-H2A.X	#2577	Cell Signaling Technology	1:1,000	BSA 5%
p62 (Sequestosome 1)	#8025	Cell Signaling Technology	1:1000	BSA 5%
LC3	#4108	Cell Signaling Technology	1:1000	BSA 5%
LIN28B	#4196	Cell Signaling Technology	1:1000	BSA 5%

Table 12 - secondary antibodies for Western blot

Antibody	Product no.	Provider	Dilution	In
Goat anti-mouse IgG1: HRP	BZL07046	Biozol	1:1,000	Blotto 1%
Goat anti-rabbit: HRP (H+L)	111-035-144	Dianova	1:1,000	Blotto 1%

2.6 Quantitative Real-Time PCR Analysis

For the isolation of mRNA from cell culture samples the Qiagen RNeasy Mini Kit (Qiagen, Hilden, Germany) was used according to the manufacturer's protocol. Concentration of mRNA in each sample was determined with the NanoDrop® ND-1000 spectrophotometer (Nanodrop Technologies, Erlangen, Germany). For the creation of cDNA templates out of mRNA by reverse transcription the High-Capacity cDNA Reverse Transcription Kit (Applied Biosystems, Foster City, CA, USA) was used as described by the manufacturer. The Real-Time-Polymerase chain reaction was performed with the ABI 7300 Real Time PCR System (Applied Biosystems, Foster City, CA, USA) using SYBR Green Master Mix (ThermoFisher Scientific, Germering, Germany) and respective primers. Actin was used as a housekeeping gene. In order to evaluate changes in mRNA levels the ΔΔCT method was used as described earlier.[70]

2.7 Proliferation Assay

The proliferation of HCC cells was evaluated using the xCELLigence system provided by Roche Diagnostics. The respective cell lines were seeded at the given density in 100 µl growth medium in equilibrated 16-well E-plates (HUH7: 2,000 cells per well; Hep3B: 4000 cells per well). After an initial incubation of 24 h without any compounds, cells were either treated with different substances for 72 h or left untreated as a control (4 wells per experimental condition). Through impedance measurement, the xCELLigence system evaluates the cell index, a dimensionless parameter, which is proportional to the cell number and recorded every hour. After normalizing the cell index to the start point of treatment, the doubling time could be evaluated by the xCELLigence software.

Synergism was evaluated using the Bliss independence model.[71] Therefore, the Bliss Value (BV) was evaluated by comparing the effects of drug A (E_A) and drug B (E_B) with the effect of the combination of both drugs (E_{AB}) according to the following formula:

$$BV = \frac{E_{\mathrm{AB}}}{(E_{\mathrm{A}} + E_{\mathrm{B}}) - (E_{\mathrm{A}} \times E_{\mathrm{B}})}$$

Synergistic effects were assumed with BV>1, antagonistic effects with BV<1 and additive effects with BV=1.

2.8 Migration/Invasion Assays

To examine the migratory ability of HCC cells under the influence of various compounds, cells were first seeded into 6-well plates and either left untreated or pretreated with the indicated agent for 24 h. After pretreatment cells were trypsinized, centrifuged (1000 rpm, 5 min, RT) and resuspended in DMEM or DMEM containing chemotherapeutic agents. 100,000 cells per condition were seeded into collagen G coated Transwell® Permeable Supports (8µm pore polycarbonate inserts), which were then placed into a 24-well plate containing 700µl DMEM (negative control) or DMEM containing 10% FCS per well. Cells were allowed to migrate for 16 h (HUH7) or 24 h (Hep3B) before being stained with crystal violet. Cells which remained on the upper side of the insert were removed with cotton swabs. Cells which migrated through the polycarbonate filter were photographed using a Zeiss Axiovert 25 microscope and a Canon 450D camera. Five pictures of each sample were used to count the number of migrated cells. Cell counting was performed by using ImageJ with the particle counter plugin. For the evaluation of invasive capabilities the Transwell® Permeable Supports were coated with Matrigel to simulate extracellular matrix.

2.9 Cell Cycle and Apoptosis Analysis

Cell cycle analysis and evaluation of apoptosis rates was performed as described by Nicoletti et al.[72] In detail, cells were seeded at a densitiy of 80,000 cells per well into 24 well plates and treated with Sorafenib (5µM) for 24, 48 and 72h. After incubation cells were trypsinized, washed with PBS and centrifuged (600 g, 4°C, 10 min). Further cells were permeabilized and stained by adding fluorochrome solution (FS) containing propidium iodide, to evaluate DNA content. After an overnight incubation at 4°C, cells were analysed by flow cytometry on a FACSCalibur device.

The fluorescence intensity, which is indicative for the DNA content of the cells permits to draw conclusions about the rate of apoptosis and cell cycle phase. The cell cycle is divided into mitosis (M phase) and interphase, which is again subdivided into G1/G0-phase, S-phase and G2-phase. Each of these phases is characterized by their DNA content and thereby their fluorescence intensity, which results in characteristic histogram plots (**Figure 8**). In apoptotic cells the DNA is fragmented, which results in low fluorescence (sub-G1 peak). For the determination of cell populations in different cell cycle phases and the percentage of apoptotic cells the FlowJo 7.6 analysis software (Tree Star Inc., Ashland, USA) was used.

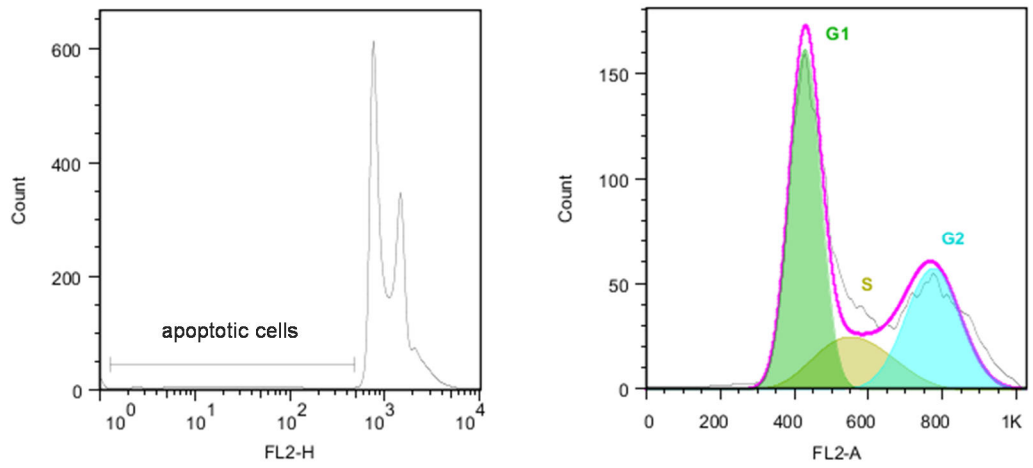

Figure 8 - Analysis of apoptotic cells and cell cycle

2.10 Clonogenic Assay

For the evaluation of long term cell survival, cells were seeded into 6-well plates and treated with the respective compounds for 24 h. After the incubation cells were trypsinized and reseeded at a density of 10,000 cells per well into a 6-well plate. After an incubation of 7 d, viable cells were stained with crystal violet solution for 10min (RT), before being washed with distilled water. Bound dye was solubilized by adding 1ml dissolving buffer and the absorbance at 550 nm was measured in a plate-reading photometer. Through the ability of a single cell to form a colony after treatment, which is indicated by the amount of bound dye, the efficacy of a cytotoxic agent can be determined.

2.11 Immunohistochemistry

For the evaluation of proliferating cells in tumors derived from nt and Cdk5 shRNA HUH7 cells in a xenograft mouse model, 5 µM sections of tumor tissue were used for immunohistochemical staining. Therefore the slides were first deparaffinized in xylene for 15 min and rehydrated by descending concentrations of ethanol (20 min in 100% ethanol, 20 min in 95% ethanol). Thereafter the sections were boiled in sodium citrate buffer (10 mM sodium citrate, 0.05% Tween 20, pH 6.0) for antigen retrieval, before endogenous peroxidase was blocked by incubation in 7.5% hydrogen peroxide for 10 min. Between the individual steps the slides were washed two times with PBS. As an indicator for proliferating cells the primary antibody for Ki67 was applied in a dilution of 1:100 in PBS for 1 h at room temperature. The Vectastain® Universal Elite ABC Kit was used for antibody detection according to the manufacturer's protocol and AEC was used as a chromogen. The slides were then counterstained with hematoxylin for 1 min before being washed with distilled water. The sections were embedded

in FluorSave™ Reagent mounting medium and covered with glass coverslips. Images were collected with an Olympus BX41 microscope and an Olympus DP25 camera.

2.12 Immunostaining

2.12.1 Colocalization

For immunostaining experiments nt and Cdk5 shRNA HUH7 cells were seeded into 8-well ibiTreat µ-slides. Cells were then washed with ice-cold PBS+ $Ca^{2+/}Mg^{2+}$ once and fixed in 4% paraformaldehyde for 15 min, before being washed with PBS once. In order to permeabilize the cells 0.2% Triton X-100 was applied for 20 min. Unspecific antibody binding sites were blocked by incubation with 0.2 % BSA in PBS for 20 min. Afterwards cells were incubated with primary antibodies against EGFR and EEA1 for 1 h. Thereafter cells were washed with PBS and incubated with Alexa Fluor® 488 and 546 secondary antibodies together with 5 µg/µl Hoechst 33342 in PBS containing 0.2% BSA for 30 min. Each well was then covered with FluorSave™ reagent mounting medium and glass coverslips. Images were taken with a Leica SP8 confocal laser scanning microscope.

2.12.2 EGFR surface localization

For the analysis of EGFR localized exclusively at the cell surface, nt and Cdk5 shRNA HUH7 cells were seeded into 8-well ibiTreat µ-slides and treated with Sorafenib as indicated. After incubation cells are immediately put on ice and incubated with a primary antibody targeting the extracellular domain of the EGFR (1:150, Calbiochem, GR01) for 1 h at 4°C. After antibody staining cells were washed twice with ice-cold PBS and fixed in 4% paraformaldehyde for 8 min on ice. Thereafter cells were washed with PBS and incubated with Alexa Fluor® 488 secondary antibody together with 5 µg/ml Hoechst 33342 in PBS containing 0.2% BSA for 30 min. Each well was then covered with FluorSave™ reagent mounting medium and glass coverslips. Images were taken with a Leica SP8 confocal laser scanning microscope.

2.12.3 EGF Uptake and Chase

In order to analyze the uptake of EGF into the cell and its subsequent elimination via degradation and recycling, nt and Cdk5 shRNA cells were seeded in 8-well ibiTreat µ-slides and treated with 100 ng/ml EGF Rhodamine for various time points. In the chase experiments, EGF Rhodamine was removed after 30 min of incubation, cells were washed twice with prewarmed PBS and incubated for various time points in medium without FCS. After incubation and chase, cells are immediately put on ice, washed twice with ice-cold PBS and incubated

with acid wash solution (acetic acid 0.2M, NaCl 0.5M, pH 2.0) for 5 min to remove excessive EGF. Cells were then washed with PBS twice and fixed in 4% paraformaldehyde. Thereafter cells were incubated with 5µg/ml Hoechst 33342 in PBS containing 0.2% BSA for 30 min. Each well was then covered with FluorSave™ reagent mounting medium and glass coverslips. Images were taken with a Leica SP8 confocal laser scanning microscope.

2.12.4 Live Cell Imaging/Time Lapse Microscopy

nt and Cdk5 shRNA HUH7 cells were seeded in 8-well ibiTreat µ-slides at a density of 5 x 10^4 and transfected with either EGFR-GFP (a gift from Alexander Sorkin, Addgene plasmid #32751), pLenti-MetGFP (a gift from David Rimm, Addgene plasmid #37560) or Alpha 5 integrin-GFP (a gift from Rick Horwitz, Addgene plasmid #15238) using DharmaFECT 1 transfection reagent (ThermoFisher Scientific, Waltham, MA). Cells were imaged using a Leica SP8 confocal laser scanning microscope. Frames were taken every 0.75 s for a total of 10 min. For the quantification of vesicle size two types of objects have been considered: small vesicles (present in both conditions) and “ring shaped” vesicles (present only in Cdk5 shRNA HUH7 cells). The ParticleSizer Plugin of Fiji after background removal is used to recognize the small vesicles, while a Circular Hough Transform based algorithm implemented by the Matlab imfindcircles function is used to recognize the “ring shaped” vesicles only in the Cdk5 knockdown condition after background removal. If the two kinds of vesicles are overlapping only the donut shaped ones will be considered.

2.13 Proteomic Analysis via LC-MS/MS

2.13.1 Stimulation

Cells were seeded at a density of 0.35*10^6 cells per well into 6-well plates and stimulated with Sorafenib (0.5 µM, 5 µM, 24 h). After incubation cells were washed five times with PBS and detached with trypsin/EDTA as described in *Passaging.* To remove excessive trypsin/EDTA cells were centrifuged (1000 rpm, 5 min, 4°C). Cell pellets were resuspended in 100 µl ice-cold PBS and stored at -80°C until further processing.

2.13.2 Sample Processing

Per 1*10^5 cells 20 µl of 8 M urea / 0.4 M NH_4HCO_3 was added. Cells were lysed using an ultrasonic device (Sonoplus GM3200 with BR30 cup booster, Bandelin, Berlin, Germany) applying 10,000 kJ. For further homogenization, samples were centrifuged through QIA-Shredder devices (Qiagen, Hilden, Germany). Protein concentrations were determined by

Bradford assays and adjusted to 0.6 mg/ml with 8 M urea/0.4 M NH_4HCO_3. To cleave bisulfide bonds, 25 µg of total protein was incubated with DTE at a concentration of 4.5 mM for 30 min and free sulfhydryl residues were blocked with iodoacetamide (final concentration 10 mM) for 30 min in the dark. After dilution with water to a concentration of 1 M urea, 0.5 µg porcine trypsin (Promega, Madison, WI, USA) was added and incubated overnight at 37 °C.

2.13.3 Liquid-Chromatography Mass Spectrometry

Chromatography of peptides was performed on an EASY-nLC 1000 chromatography system (Thermo Scientific, Waltham, MA, USA) coupled to an Orbitrap XL instrument (Thermo Scientific). 2.5 µg of peptides diluted in 0.1 % formic acid (FA) were transferred to a trap column (PepMap100 C18, 75 µm x 2 cm, 3 µm particles, Thermo Scientific) and separated at a flow rate of 200 nL/min (Column: PepMap RSLC C18, 75 µm x 50 cm, 2 µm particles, Thermo Scientific) using a 260 min linear gradients from 5 % to 25 % solvent B (0.1 % formic acid, 100 % ACN) and a consecutive 60 min linear gradient from 25 % to 50 % solvent B. For data acquisition, a top five data dependent CID method was used.

2.13.4 Proteomic Data Processing

For the quantitative analysis of the data obtained from the mass spectrometry screen the MaxQuant and Perseus software packages (provided by Max Planck Institute of Biochemistry, Munich) were used.

2.14 Glycolysis Stress Test

Nt and Cdk5 shRNA HUH7 cells were seeded at a density of 1.5 x 10^4 into a XF^e96 microplate and grown for 24 h prior to Sorafenib treatment (0.5 µM, 5 µM, 24 h). The Seahorse Glycolysis Stress Test Kit was used in combination with the Seahorse XFe96 Analyzer (Agilent Technologies, Santa Clara, CA) as described by the manufacturer. Results were normalized to DNA content measured with CyQuant® GR dye solution (ThermoFisher Scientific, Waltham, MA) according to the manufactures protocol. Data analysis was performed with Wave 2.3.0 software and Seahorse XF Glycolysis Stress Test Report Generator (Agilent Technologies, Santa Clara, CA).

2.15 Human HCC Microarrays

Tissue microarrays (TMA), containing human HCC samples and matched surrounding non-tumor tissue were produced. Tissue staining and histological scoring was performed by Prof. Dr. Doris Mayr and Dr. Veronika Kanitz (Institute of Pathology, Ludwig-Maximilians Universitiy, Munich). The TMAs included 115 patients which had been treated with liver transplantation or partial hepatectomy at the University Clinic Munich Großhadern between 2008 and 2013. The formalin-fixed, paraffin-embedded blocks were cut into 2 mm thick slices and mounted on SuperFrost Plus microscope slides (Menzel Gläser, Braunschweig, Germany). After deparaffinization and rehydration all slides were Hematoxilien-Eosin stained in a standard manner (Vector Laboratories, Burlingame, CA, USA). Several blank-slides were set aside for immunohistochemical stainings.
Staining for EGFR was performed by using a Ventana Benchmark XT autostainer using the XT UltraView diaminobenzidine kit (Ventana Medical Systems). The Ventana EGFR-antibody clone 3C6 (ready to use) was used.
EGFR-staining of the TMA section was assessed using the immunoreactive score as described[73]: 0 – absent; 1-4 –weak; 5-8 – moderate; 9-12 – strong expression.
Images were obtained with a digital network microscope Leica DMD108 (Leica Biosystems Nussloch, Germany).

2.16 In vivo Experiments

All experiments were performed according to German legislation of animal protection and approved by the local government authorities (animal test request number: 55.2-1-54-2532-22-2016). All *in vivo* experiments were performed by M. Ulrich, C. Atzberger and K. Loske.

2.16.1 Ectopic Tumor Model

20 female SCID „CB17/Icr-PrkdcSCID/IcrIcocrl" mice, six weeks old, purchased from Charles River, were used. For the implantation of tumors, nt and Cdk5 shRNA HUH7 cells were cultured to confluency of about 70% before being harvested as described in (Passaging) and $3.3*10^6$ cells in 100 µl PBS were injected into the flank of SCID mice. The animals were checked regularly for tumor progression and tumor volume was evaluated using a digital measuring slide to measure the three parameters, length (a), width (b) and height (c). The total volume was determined by the formula $a*b*c*\pi/6$ (with $\pi/6$ as a correction factor for tumor shape). Sorafenib was injected intraperitoneally (100 µl, solvent: 5% DMSO, 10% Solutol, 85% PBS). Therefore mice were fixed by hand and turned to allow access to the ventral side, before the solution was administered with a 25 G needle. Treatment with Sorafenib was started ten

days after implantation with 10 mg/kg/d Sorafenib injected daily for seven days. 18 days after the implantation all mice were sacrificed through cervical dislocation. An exponential growth model was used to model tumor volume, where the tumor volume at a given time t (N(t)) is a function of the starting volume N(0), the time of growth t and of the growth rate α: $N(t) = N(0) \times \exp^{\alpha x t}$. Modelling was performed using a non-linear mixed effects modelling with the software NONMEM 7.3.

2.16.2 Dissemination Assay - Dinaciclib

20 female C57BL/6 albino "C57BL/6BrdCrHsd-Tyrc" mice, six weeks old, purchased from Envigo, were used. The mice were pretreated intraperitoneally with 10 mg/kg Dinaciclib or solvent (5% DMSO, 10% Solutol, 85% PBS) three times (48, 24, and 0.5 hours) before cell injection. We intravenously injected 2 x 10^5 Ril175-luc cells into the tail vein and imaged the mice after intraperitoneal injection of 6 mg luciferin/mouse on day three after the cell injection using the IVIS Lumina system (PerkinElmer). The tumor signal per defined region of interest was calculated with the Living Image 4.4 software (Caliper Life Sciences) as photons/second/cm^2 (total flux/area).

2.16.3 Dissemination Assay – Cdk5 KO

20 female C57BL/6 albino "C57BL/6BrdCrHsd-Tyrc" mice, six weeks old, purchased from Envigo, were used. We intravenously injected 2 x 10^5 Ril175-luc cells (either wild-type or Cdk5 KO) into the tail vein and imaged the mice after intraperitoneal injection of 6 mg luciferin/mouse on day three after the cell injection using the IVIS Lumina system (PerkinElmer). The tumor signal per defined region of interest was calculated with the Living Image 4.4 software (Caliper Life Sciences) as photons/second/cm2 (total flux/area).

2.17 Statistical Analysis

All listed experiments were conducted at least three times unless otherwise indicated in the figure legends. The given data is presented as mean ± SEM and statistical significance was considered if $P \leq 0.05$. The statistical analysis was performed with GraphPad Prism software version 5.04 (GraphPad Software, San Diego, USA).

RESULTS

3 RESULTS

3.1 Combination of Cdk5 inhibition and Sorafenib Synergistically Decreases HCC Cell Proliferation *in vitro* and *in vivo*

In order to evaluate the effects of Cdk5 inhibition on Sorafenib treatment we used HUH7 and Hep3B cells and combined Sorafenib with the established Cdk5 inhibitors Roscovitine and Dinaciclib as well as the experimental Cdk5 inhibitor LGR1407.[74] Due to strong similarities among Cdks, inhibitors often lack specificity and target multiple Cdks. Therefore we used a genetic knockdown of Cdk5 via shRNA interference in both cell lines to confirm that our results are Cdk5 dependent.

Proliferation as well as clonogenic survival assays showed that the combination of Sorafenib treatment with either genetic knockdown of Cdk5 (**Figure 9a, b**) or pharmacological inhibition (**Figure 9c-e**) synergistically reduced HCC cell proliferation. For the evaluation of synergism two different models, *Combination Subthresholding* and *Bliss Independence*, were used.[75] In both models the combination of Cdk5 inhibition with Sorafenib revealed synergistic effects compared to single treatments. Respective Bliss values are indicated in Figure 9.

This sensitizing effect could also be confirmed in an HCC xenograft mouse model. Mice that were subcutaneously injected with Cdk5 shRNA HUH7 cells and treated with Sorafenib showed strongly reduced tumor size and weight compared to controls or single treatments (**Figure 10a**). Tumor volume was observed over time and respective data subjected to a non-linear mixed effects modelling technique, which revealed a synergistic effect of the combination of Sorafenib and Cdk5 inhibition resulting in a significantly reduced tumor growth rate (**Figure *10*b**). The reduced tumor size and decreased tumor growth rate can be attributed to a significant reduction of proliferating cells in the tumors, as shown by immunohistochemistry staining of Ki67 in tumor sections (**Figure 10c**).

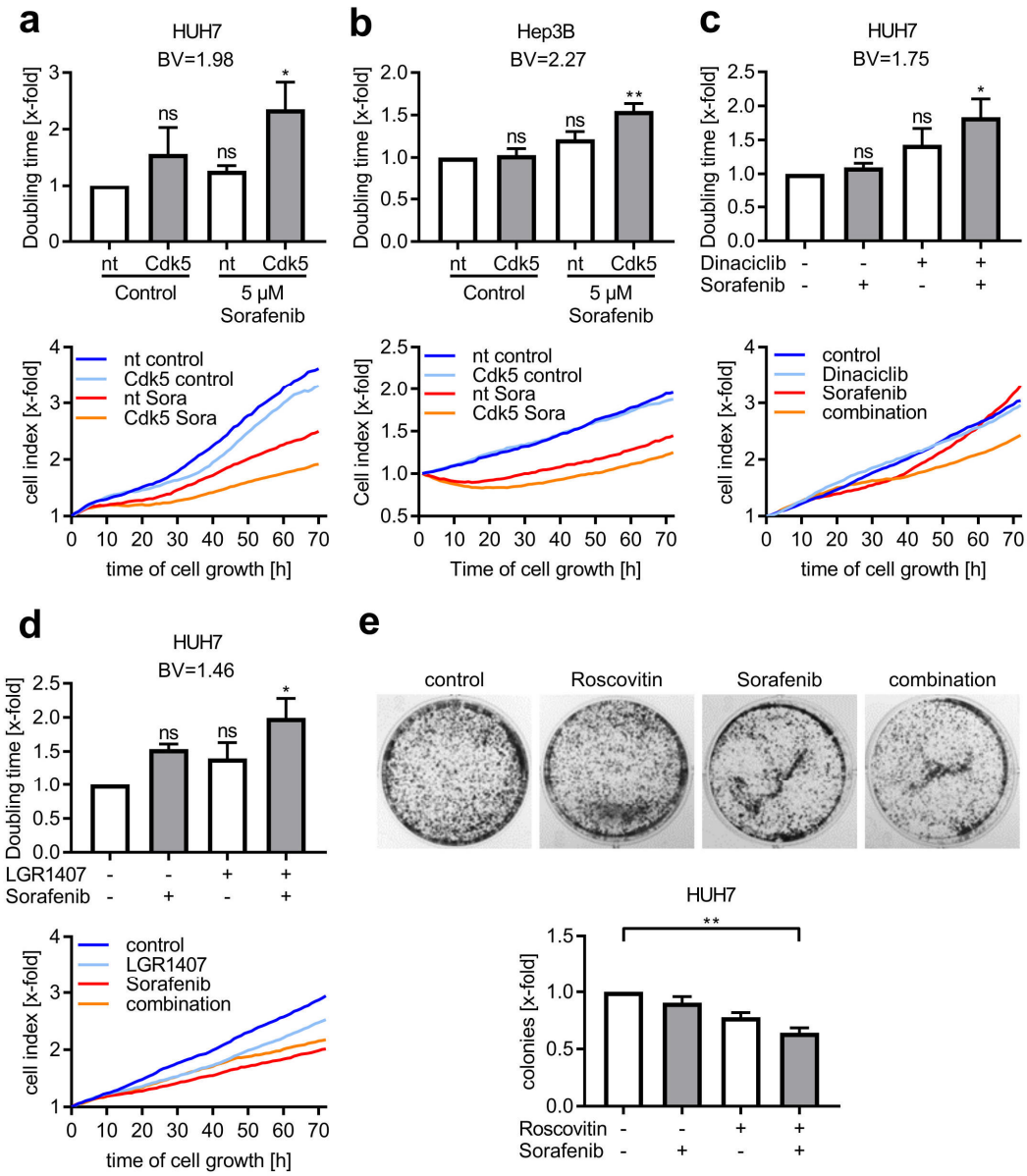

Figure 9 - The influence of Cdk5 on HCC growth *in vitro*. (**a**) Proliferation of nt and Cdk5 shRNA HUH7 cells after treatment with Sorafenib is shown. Corresponding doubling time is shown. One Way ANOVA, Tukey **P*<0.05, *n*=3, Bliss Value = 1.98. (**b**) Proliferation of nt and Cdk5 shRNA Hep3B cells treated with Sorafenib is shown. Corresponding doubling time is shown. One Way ANOVA, Tukey ***P*<0.01, *n*=3, Bliss Value = 2.27. (**c**) Proliferation of HUH7 cells treated with either Sorafenib, Dinaciclib or a combination of both is shown. Corresponding doubling time is shown. One Way ANOVA, Tukey **P*<0.05, *n*=3, Bliss Value = 1.75. (**d**) Proliferation of HUH7 cells treated with either Sorafenib, LGR1407 or a combination of both is shown. Corresponding doubling time is shown. One Way ANOVA, Tukey **P*<0.05, *n*=3, Bliss Value = 1.46. (**e**) Clonogenic survival of HUH7 cells treated with either Sorafenib or Roscovitin or a combination of both is shown. One Way ANOVA, Tukey ***P*<0.01, *n*=3.

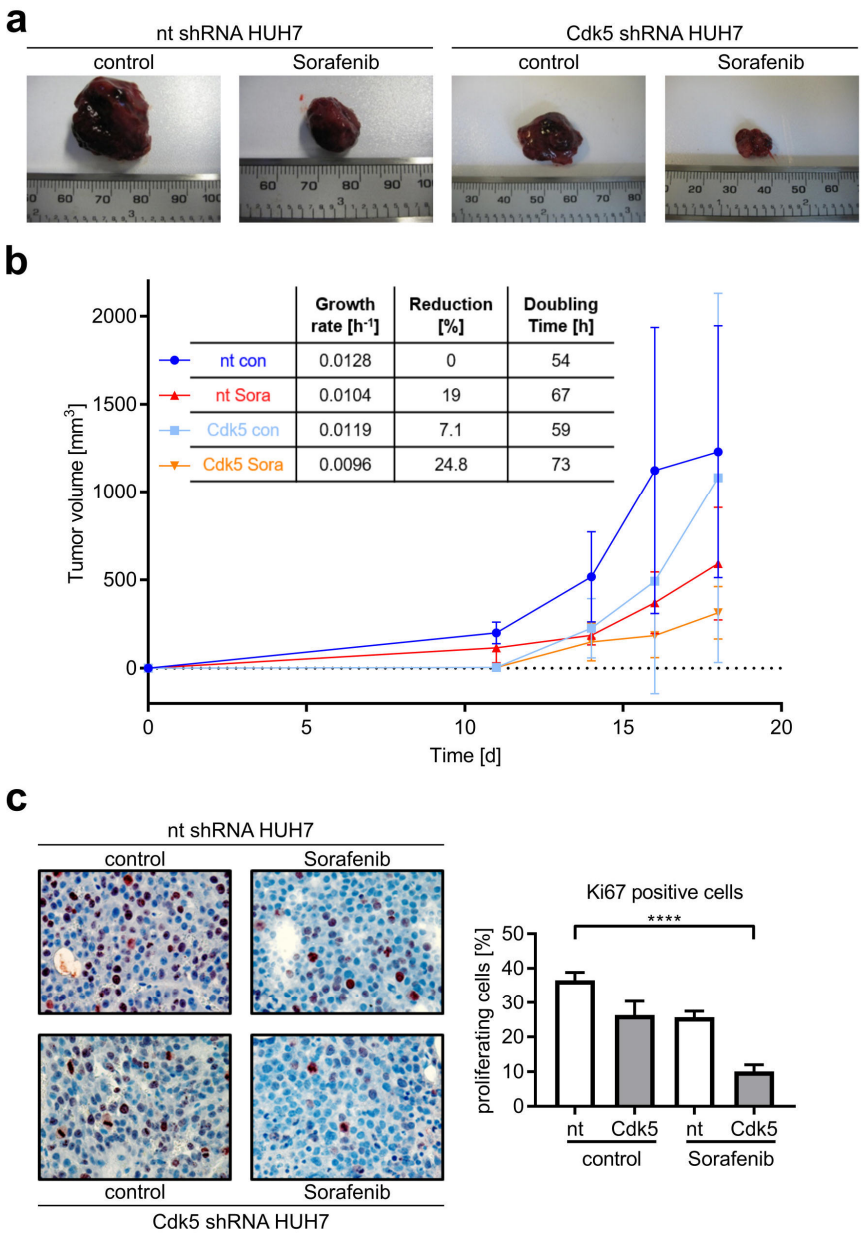

Figure 10 - Cdk5 inhibition reduces HCC growth *in vivo*. (**a**) Tumors of nt and Cdk5 shRNA HUH7 cells grown in SCID mice that were either treated with Sorafenib or solvent are shown (n=6). (**b**) Tumor volume over the treatment period of 18 days is shown. Table shows the evaluated growth rates that were determined by applying an exponential tumor growth model. (**c**) Immunostaining of respective tumors from (**a**) for Ki67 (red) and hematoxylin (nuclei, blue) is shown. The bar graph indicates proliferating cells evaluated by counting Ki67-positive cells. One Way ANOVA, Tukey ****P<0.0001, n=6.

3.2 Cdk5 Inhibition Prevents Sorafenib Induced HCC Cell Migration

Aside from the anti-proliferative effect, Sorafenib as well as Cdk5 inhibition significantly reduced HCC cell migration (**Figure 11a**). Strikingly, in the past various reports have shown that by targeting angiogenesis tumors gain a higher level of malignancy and invasiveness. These observations are often linked to dose reductions and treatment termination, which frequently occur under Sorafenib treatment.

As a matter of fact, our results show that treatment of HUH7 and Hep3B cells with Sorafenib in a concentration 10-fold lower than used in the proliferation experiments (0.5 µM) led to an overall increase of migration (**Figure 11b-f**) and invasion (**Figure 11g**). This increase in motility is independent from proliferation as Sorafenib does not influence proliferation in the given concentration (**Figure 11h**). An inhibition of Cdk5, either via genetic knockdown (**Figure 11a,b and e**) or pharmacological intervention (**Figure 11c,d and f**) reduced the overall migration/invasion to a level significantly lower than the control and further prevented the Sorafenib-induced increase in migration and invasion.

The anti-migratory effect of Cdk5 could also be confirmed in two *in vivo* dissemination assays. Firstly, C57BL/6 mice were treated with Dinaciclib daily for 2 days before RIL175 cells expressing luciferase were injected into the tail vein. Luminescence measurements three days after injection showed, that mice treated with Dinaciclib showed a significantly reduced dissemination of tumor cells into the lung (**Figure 12a**).

Secondly, we used RIL175 cells with a Cdk5 knockout (Cdk5 KO) generated with the CRISPR-Cas9 system to confirm that the effect was Cdk5 dependent (**Figure 12b**). Therefore, either RIL175 wild-type cells or RIL175 Cdk5 KO cells were injected into the tail vein of C57BL/6 mice. After three days, luminescence measurement revealed an even greater effect on dissemination by Cdk5 KO compared to Dinaciclib treated mice (**Figure 12c**).

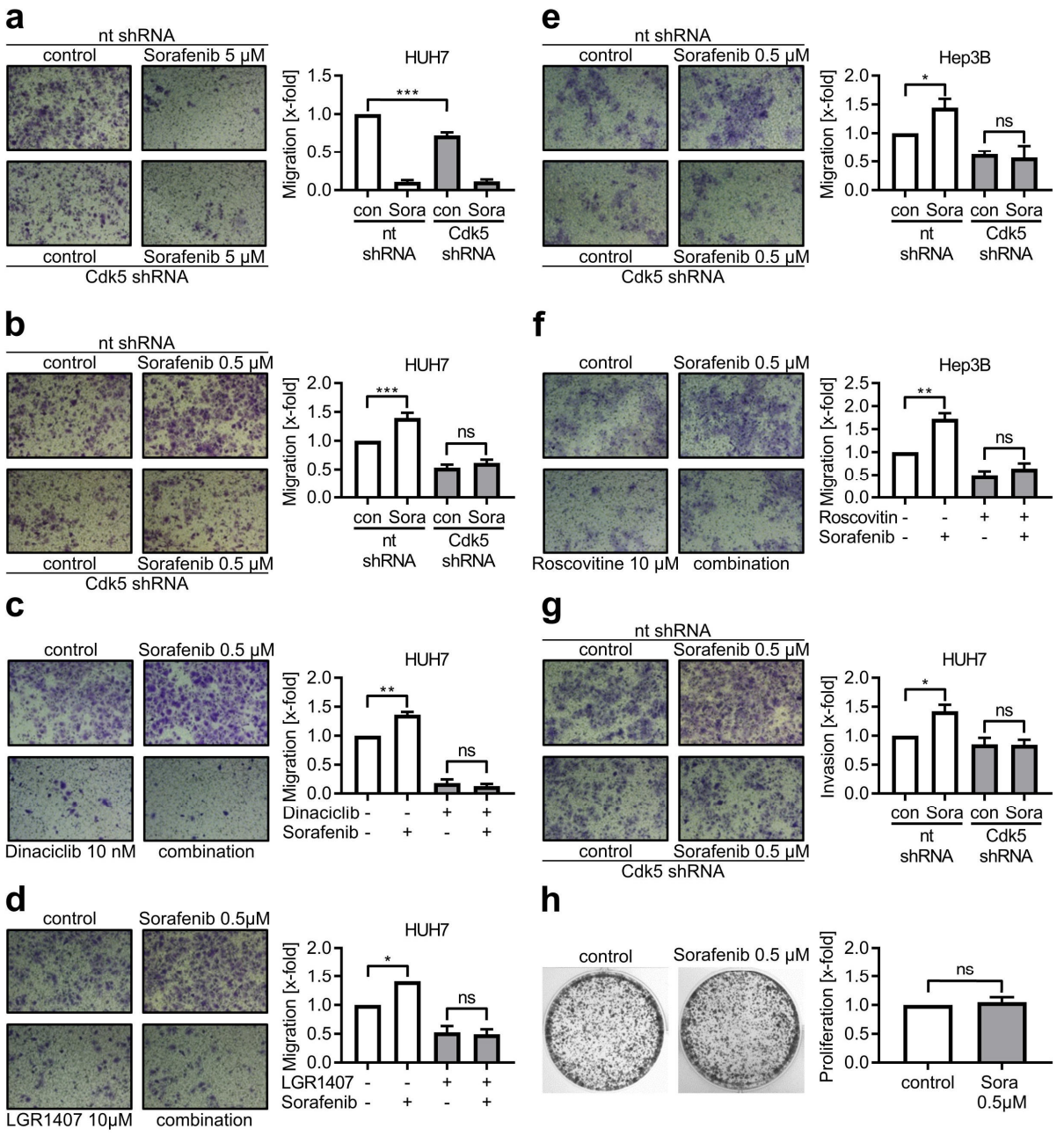

Figure 11 - Cdk5 inhibtion prevents cancer cell migration induced by Sorafenib treatment in low concentrations. (**a-f**) Transwell migration of nt and Cdk5 shRNA HUH7 (**a,b**), wild-type HUH7 (**c,d**), nt and Cdk5 shRNA Hep3B cells (**e**) and wild-type Hep3B cells (**f**) that were pretreated with the respective compounds in the indicated concentrations is shown. (**g**) Invasion of nt and Cdk5 shRNA HUH7 cells that were pretreated with Sorafenib is shown. (**a-g**) Respective pictures of migrated cells are shown together with bar diagrams showing the number of migrated cells normalized to the control. One Way ANOVA, Tukey **P*<0.05, ***P*<0.01, ****P*<0.001, n=3. (**h**) Clonogenic survival of HUH7 cells treated with Sorafenib is shown. t-test **P*<0.05, n=3.

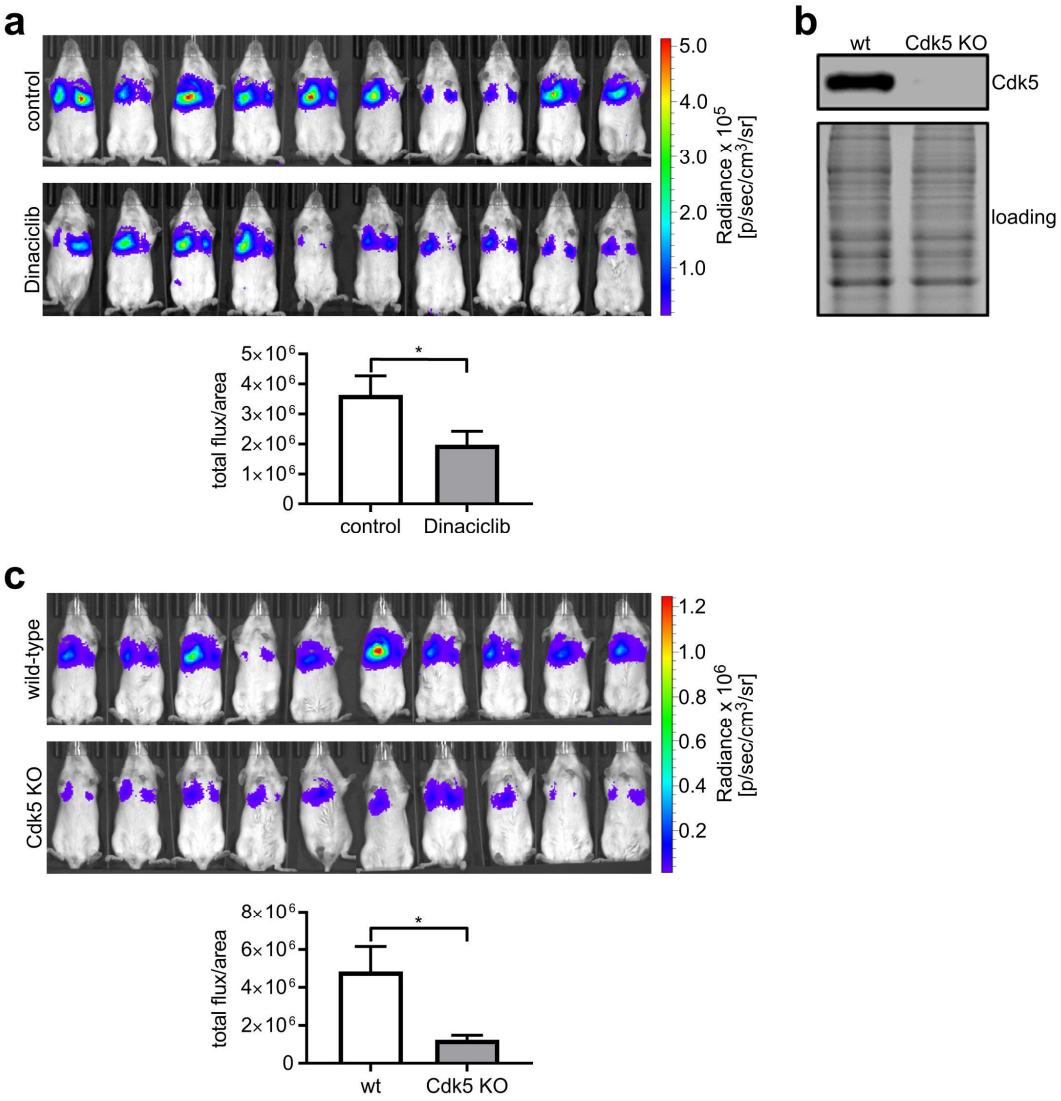

Figure 12 - Cdk5 inhibition reduces HCC metastasis *in vivo*. (**a**) Non-invasive images of tumor bearing mice either treated with Dinaciclib or solvent are shown. Bar diagram shows corresponding signal intensities. t-test, *P<0.05, n=10. (**b**) Non-invasive images of tumor bearing mice either injected with RIL175 wild-type cells or RIL175 Cdk5 KO cells are shown. Bar diagram shows corresponding signal intensities. t-test, *P<0.05, n=10. (**c**) Western Blot showing the protein levels of Cdk5 in RIL175 wild-type cells and RIL175 Cdk5 KO cells generated via the CRISPR-Cas method.

3.3 The Influence of Sorafenib Treatment and Cdk5 knockdown on HCC cells – A Proteomic Evaluation

A previous study conducted by our group showed that Cdk5 inhibition sensitized HCC cells to the treatment with DNA damaging agents by influencing DNA damage response, which ultimately led to apoptosis. However, the synergistic effect observed by Sorafenib treatment combined with Cdk5 inhibition is not caused by alterations in DNA damage response, as indicated by unchanged phosphorylation of the DNA damage marker H2A.X (**Figure 13a**), or apoptosis (**Figure 13b**).

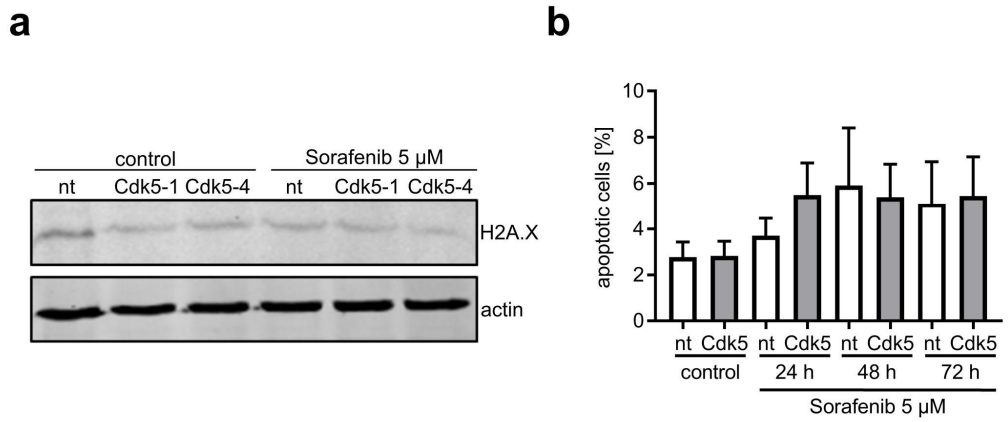

Figure 13 - Influence of Cdk5 inhibition and Sorafenib on DNA damage and apoptosis. (**a**) Immunoblot of nt and Cdk5-1/4 shRNA HUH7 cells treated with Sorafenib and probed for phosphorylated H2A.X is shown. (**b**) Evaluation of apoptotic cells by flow cytometry in Sorafenib treated nt and Cdk5 shRNA HUH7 cells.

To get a clue on how Cdk5 inhibition sensitizes HCC cells for Sorafenib treatment, we decided to use a LC-MS/MS based whole cell proteomics approach, where we compared the differential expression of proteins caused by Cdk5 knockdown alone or in combination with Sorafenib. In total, over 2000 proteins were identified, out of which 52 proteins were significantly influenced by Cdk5 knockdown, while 48 proteins were changed in abundance by the combination of Cdk5 knockdown and Sorafenib. Significant alterations in protein abundance were indicated by a log2-fold change > |0.6| and a P-value<0.05 (**Figure 14a, b** and **Supplementary Figure 1a, b**). Selected protein hits were subsequently analysed on mRNA level using RT-qPCR analysis (**Supplementary Figure 2a, b**).

a

Protein names	Gene names	x-fold change	t-test p-value
Mannosyl-oligosaccharide 1,2-alpha-mannosidase IA	MAN1A1	0,38	0,01787
E3 ubiquitin-protein ligase RBX1	RBX1	0,42	0,00217
Hypoxanthine-guanine phosphoribosyltransferase	HPRT1	0,56	0,00087
Ladinin-1	LAD1	0,56	2,49E-05
Importin subunit alpha-1	KPNA2	0,57	8,39E-05
Alpha-fetoprotein	AFP	0,58	0,01497
Myotrophin	MTPN	0,60	0,03885
Carbonic anhydrase 2	CA2	0,61	0,00129
Protein lin-28 homolog B	LIN28B	0,62	4,33E-06
Adenine phosphoribosyltransferase	APRT	0,63	0,01299
Histone-binding protein RBBP4	RBBP4	0,64	0,00520
Tumor protein D54	TPD52L2	0,65	0,01133
Epiplakin	EPPK1	0,65	0,00879
DNA topoisomerase 2-alpha	TOP2A	0,65	0,00258
26S proteasome non-ATPase regulatory subunit 14	PSMD14	0,65	0,00128
Neutral amino acid transporter B(0)	SLC1A5	0,65	0,04813
F-box only protein 2	FBXO2	0,65	0,00032
Glucose-6-phosphate 1-dehydrogenase	G6PD	1,52	7,27E-08
D-dopachrome decarboxylase	DDT	1,52	0,00114
Sodium/potassium-transporting ATPase subunit alpha-1	ATP1A1	1,52	0,00598
Redox-regulatory protein FAM213A	FAM213A	1,53	0,04823
Cytochrome c oxidase subunit 7A2, mitochondrial	COX7A2	1,53	0,01589
4F2 cell-surface antigen heavy chain	SLC3A2	1,55	0,00226
Microsomal glutathione S-transferase 1	MGST1	1,55	0,02072
Angiotensinogen	AGT	1,56	0,02933
Sodium/potassium-transporting ATPase subunit beta-1	ATP1B1	1,58	0,00112

Protein names	Gene names	x-fold change	t-test p-value
LETM1 and EF-hand domain-containing protein 1, mitochondrial	LETM1	1,59	0,00634
Homogentisate 1,2-dioxygenase	HGD	1,62	4,09E-06
Calcium-regulated heat stable protein 1	CARHSP1	1,62	0,00014
Multidrug resistance protein 1	MDR1	1,62	0,01178
PDZ and LIM domain protein 7	PDLIM7	1,63	0,00496
Oxidoreductase HTATIP2	HTATIP2	1,65	0,03960
Ras-related protein Rab-10	RAB10	1,65	0,02916
Isopentenyl-diphosphate Delta-isomerase 1	IDI1	1,65	0,00103
7-dehydrocholesterol reductase	DHCR7	1,67	0,00793
Neutral cholesterol ester hydrolase 1	NCEH1	1,67	0,00646
Sec1 family domain-containing protein 1	SCFD1	1,67	2,63E-05
Reticulocalbin-1	RCN1	1,70	0,00243
Myc box-dependent-interacting protein 1	BIN1	1,70	1,23E-06
Estradiol 17-beta-dehydrogenase 11	HSD17B11	1,78	0,00275
Sodium-coupled neutral amino acid transporter 2	SLC38A2	1,80	0,00531
Galectin-3	LGALS3	1,80	7,94E-05
Vimentin	VIM	1,84	0,00090
Transmembrane protein 33	TMEM33	1,85	0,00609
Histone H3;Histone H3.3;Histone H3.1t	H3F3B	1,89	0,04004
(3R)-hydroxyacyl-CoA dehydrogenase	HSD17B4	1,94	2,29E-05
Epidermal growth factor receptor	EGFR	2,04	7,02E-07
Sequestosome-1	SQSTM1	2,23	2,55E-05
Claudin-6	CLDN6	2,34	0,02977
Apolipoprotein B-100	APOB	2,35	2,66E-05
Aminopeptidase N	ANPEP	2,93	1,86E-08
Ferritin;Ferritin heavy chain	FTH1	3,67	0,03627

b

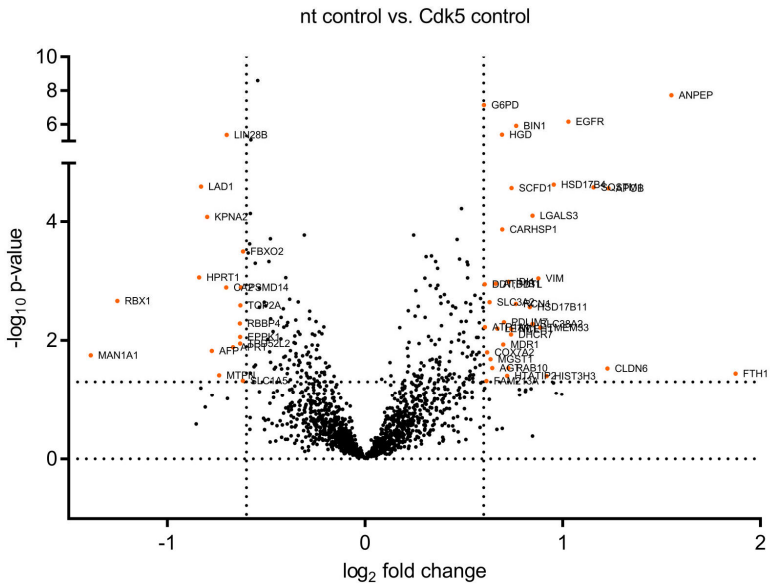

Figure 14 - Proteomic analysis of nt/Cdk5 shRNA HUH7 cells. (**a**) Table of proteins showing alterations of protein abundance (*P*-value < 0.05; log2-fold change > |0.6|) between untreated nt and Cdk5 shRNA control cells together with their respective gene names, x-fold changes (nt shRNA vs. Cdk5 shRNA) and *P*-values. (**b**) Volcano Plot visualizing the protein hits given in table **a**.

A protein-protein interaction (PPI) network analysis revealed significant interaction enrichment between the differentially regulated proteins indicating that they are biologically related (**Figure 15a** and **Supplementary Figure 1c**). A subsequent functional enrichment analysis of the PPI network uncovered a modulation of proteins involved in cellular metabolism (**Figure 15a**). In addition, we could detect an accumulation of proteins regulated via intracellular trafficking including proteins associated with autophagy like p62 and proteins trafficked via endocytosis like integrins and the epidermal growth factor receptor (EGFR) (**Figure 15b**), hinting at a critical role of these pathways in the sensitizing effect of Cdk5 inhibition to Sorafenib treatment. We therefore decided to evaluate the importance of each identified pathway.

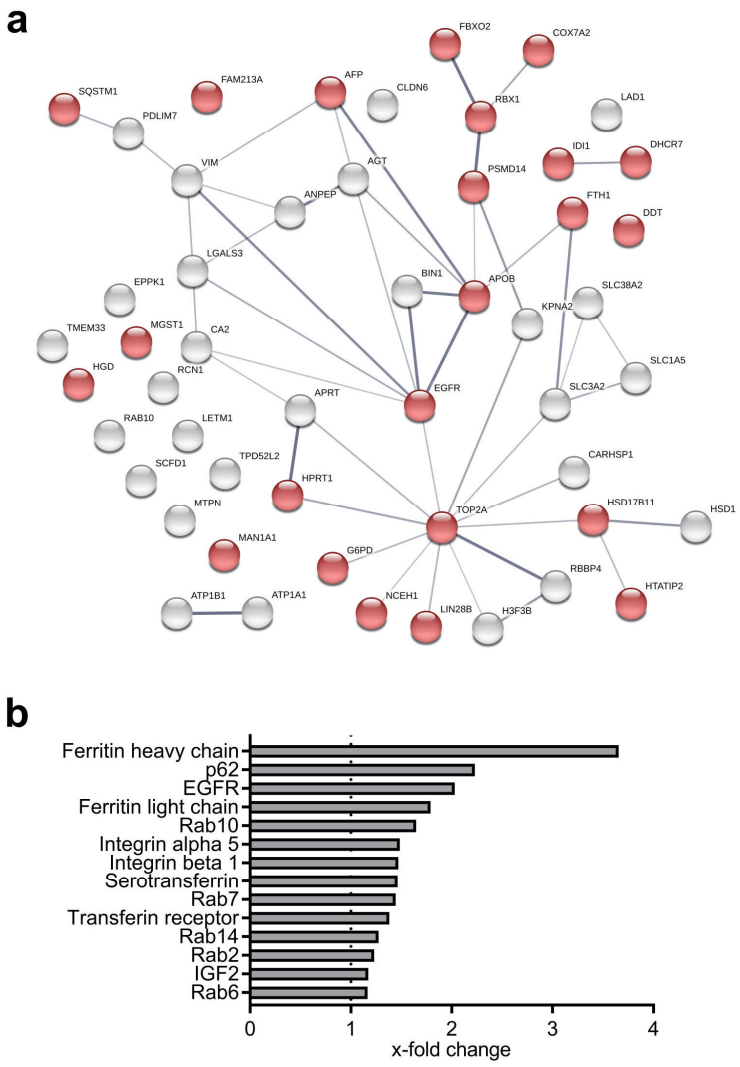

Figure 15 - Protein-protein interaction analysis. (**a**) Protein interaction map of protein hits given in table **a** created with string-db.org (protein-protein interaction enrichment *P*-value: 0.0016). Proteins involved in cellular metabolic processes are highlighted in red (false discovery rate: 0.0125). (**b**) The graph shows proteins associated with or regulated by endocytosis that were modulated by Cdk5 knockdown (x-fold change compared to nt shRNA is displayed).

Firstly, we decided to investigate cellular metabolism. Cancer cells critically depend on increased metabolic activity to satisfy their elevated energy consumption. A deregulation of numerous proteins involved in the regulation of metabolism led to the hypothesis that Cdk5 negatively influences cancer cell metabolism, thereby increasing the effects of Sorafenib. Especially the downregulation of LIN28 as shown by proteomic analysis (**Figure 14**) and confirmed by Western blot analysis and mRNA was of particular interest (**Figure 16a, b**). LIN28 is a critical regulator of glucose metabolism and is associated with HCC and liver disease.[76]

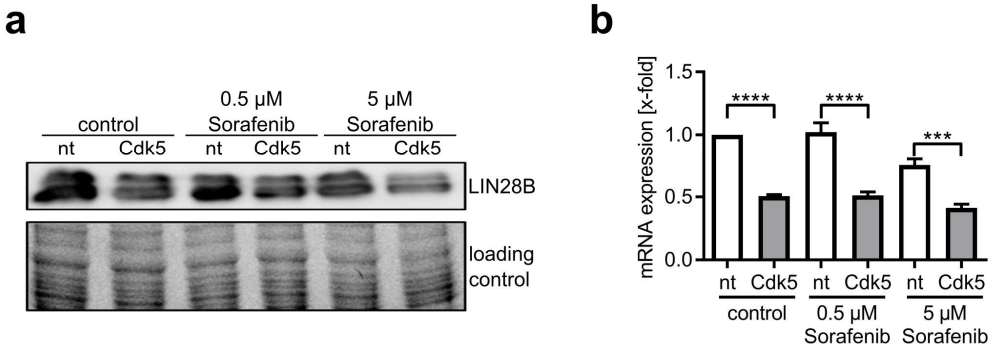

Figure 16 – LIN28 expression is reduced upon Cdk5 inhibition. (**a**) Immunoblot of nt and Cdk5 shRNA HUH7 cells treated with Sorafenib and probed for LIN28B is shown. (**b**) mRNA levels of LIN28B in nt and Cdk5 shRNA HUH7 cells treated with Sorafenib are shown. One Way ANOVA, Tukey ***P<0.001, ****P<0.0001, n=3.

As cellular metabolism is certainly not dependent on one protein alone but rather regulated by a variety of pathways and proteins we decided to take a wider approach and measured glycolysis and oxidative phosphorylation via the Seahorse XF^{e}96 Analyzer. The readout for glycolysis is displayed as extracellular acidification rate (ECAR), while oxidative phosphorylation is measured via oxygen consumption (OCR). We could show that Sorafenib indeed influenced cellular metabolism by reducing ECAR as well as OCR (**Figure 17a, b**). However there was no additional effect induced by Cdk5 inhibition (**Figure 17c-e**). Therefore we concluded that the sensitizing effect of Cdk5 inhibition was not due to impaired metabolic activity.

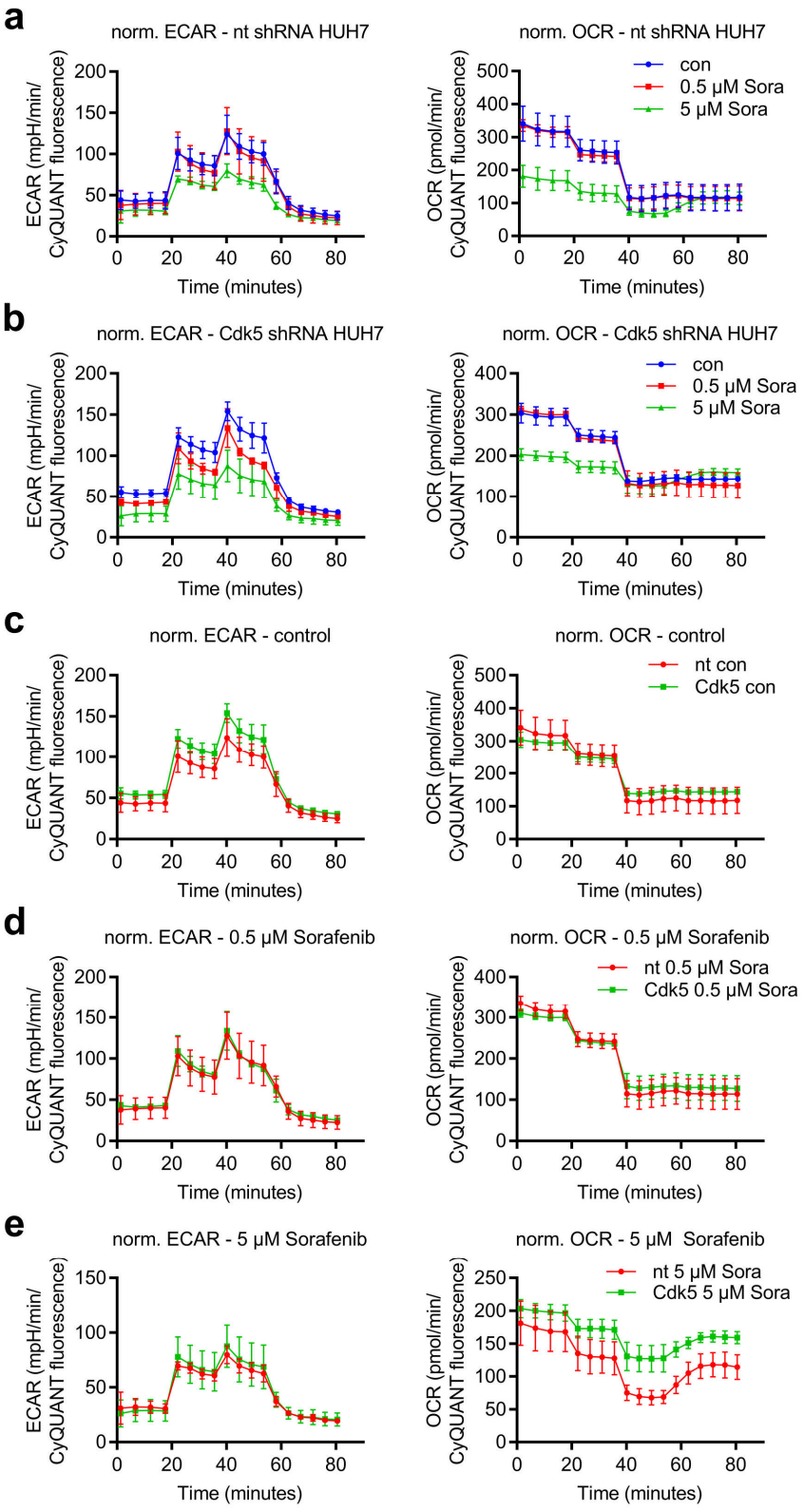

Figure 17 - Effect of Sorafenib and Cdk5 inhibition on cellular metabolism. Glycolysis Stress Test with nt and Cdk5 shRNA HUH7 cells that were pre-treated with Sorafenib before consecutive exposure to D-glucose, oligomycin and 2-DG is shown. ECAR and OCR were recorded using a Seahorse XFe96 Analyzer and normalized with CyQUANT® GR dye. (**a-e**) Normalized ECAR (left) and OCR (right) of untreated and Sorafenib treated nt and Cdk5 shRNA HUH7 cells are compared.

Secondly, an accumulation of p62/Sequestosome1, a marker for proteins destined for autophagy, indicated that the autophagic flux was disturbed by Cdk5 inhibition. Cdk5 knockdown cells displayed a significant upregulation of p62/Sequestosome1 as shown by proteomic analysis and western blot analysis (**Figure 14** and **Figure 18a, b**). The disturbance in autophagic flux could be confirmed by an increase of the LC3-II/I ratio upon Cdk5 inhibition, which is indicative of an accumulation of late autophagosomes and thereby a disturbance of the equilibrium between early and late autophagic vesicles (**Figure 18a, c**). The increase in p62/Sequestosome1 and LC3-II/I ratio can either be caused by an increase in autophagy or by a degradation block. Therefore an artificial degradation block was applied by using Concanamycin A, an inhibitor of vesicle fusion (**Figure 18d**). The LC3-II/I ratio in nt shRNA cells was increased in response to Concanamycin A, while Cdk5 shRNA cells remained unaffected, pointing to a degradation block in the autophagic cascade by Cdk5 knockdown (**Figure 18e, f**). Nevertheless, Sorafenib did neither affect p62/Sequestosome1 expression nor LC3 conversion. Thus the influence of Cdk5 on autophagic flux is unlikely mediating the sensitizing effect towards Sorafenib treatment.

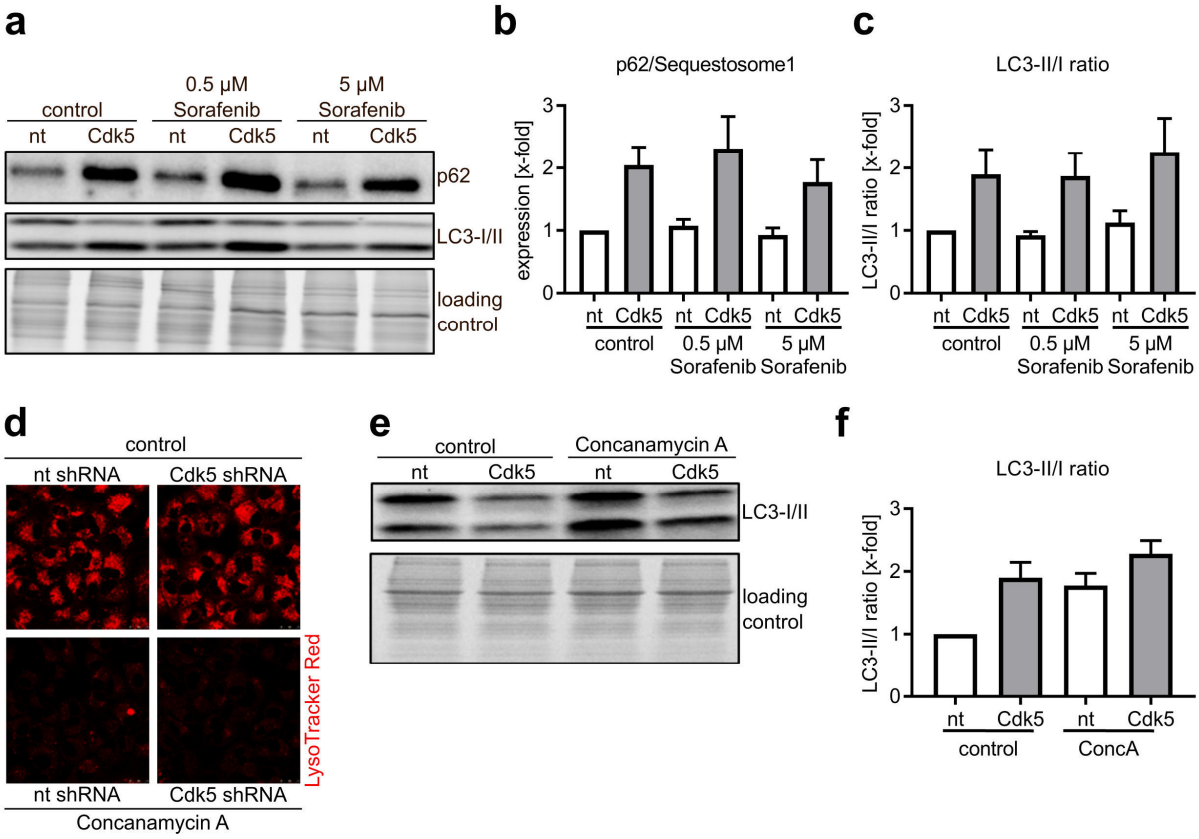

Figure 18 - Cdk5 influences autophagic flux. (**a**) Immunoblots from nt and Cdk5 shRNA HUH7 cells treated with Sorafenib probed with antibodies for p62/Sequestosome1 and LC3 are shown. (**b**) Quantitative evaluation of p62/Sequestosome1 from **a** is shown. (**c**) Ratio of LC3-II to LC3-I after quantitative evaluation from **a** is shown. (**d**) LysoTracker Red staining of nt and Cdk5 shRNA HUH7 cells after treatment with Concanamycin A (ConcA) is shown. (**e**) Immunoblot from nt and Cdk5 shRNA HUH7 cells treated with Concanamycin A and probed with antibodies for LC3-I/II is shown. (**f**) Ratio of LC3-II/I is shown after quantitative evaluation of immunoblots from **e**.

3.4 Cdk5 Influences EGFR Signaling

Interestingly, the proteomics screen showed that Cdk5 inhibition induced an upregulation of proteins involved in or transported via intracellular trafficking (**Figure 15b**). This finding suggested that Cdk5 inhibition interferes with intracellular trafficking, thereby leading to an accumulation of respective cargos. Out of the identified cargo proteins, especially the EGFR was of particular interest, as an increase of growth factor receptors levels usually leads to more aggressive tumor progression.[77] In order to elucidate the controversy between elevated EGFR levels on the one hand and growth inhibition on the other hand, we decided to use the EGFR as an example to investigate the effect of Cdk5 inhibition and Sorafenib treatment on the compensatory activation of growth factor receptors.

Activation of growth factor signaling including EGF-, IGF-, FGF-, or HGF-signaling in response to Sorafenib treatment was described as a mechanism of HCC treatment evasion.[78-80] Building on these findings our results confirm the compensatory activation of EGFR upon Sorafenib treatment. While the Ras/Raf/MEK/ERK pathway was inhibited as shown by decreased ERK1/2 phosphorylation, the phosphorylation of the growth factor downstream target AKT and EGFR itself was induced by Sorafenib (**Figure 19a-c**).

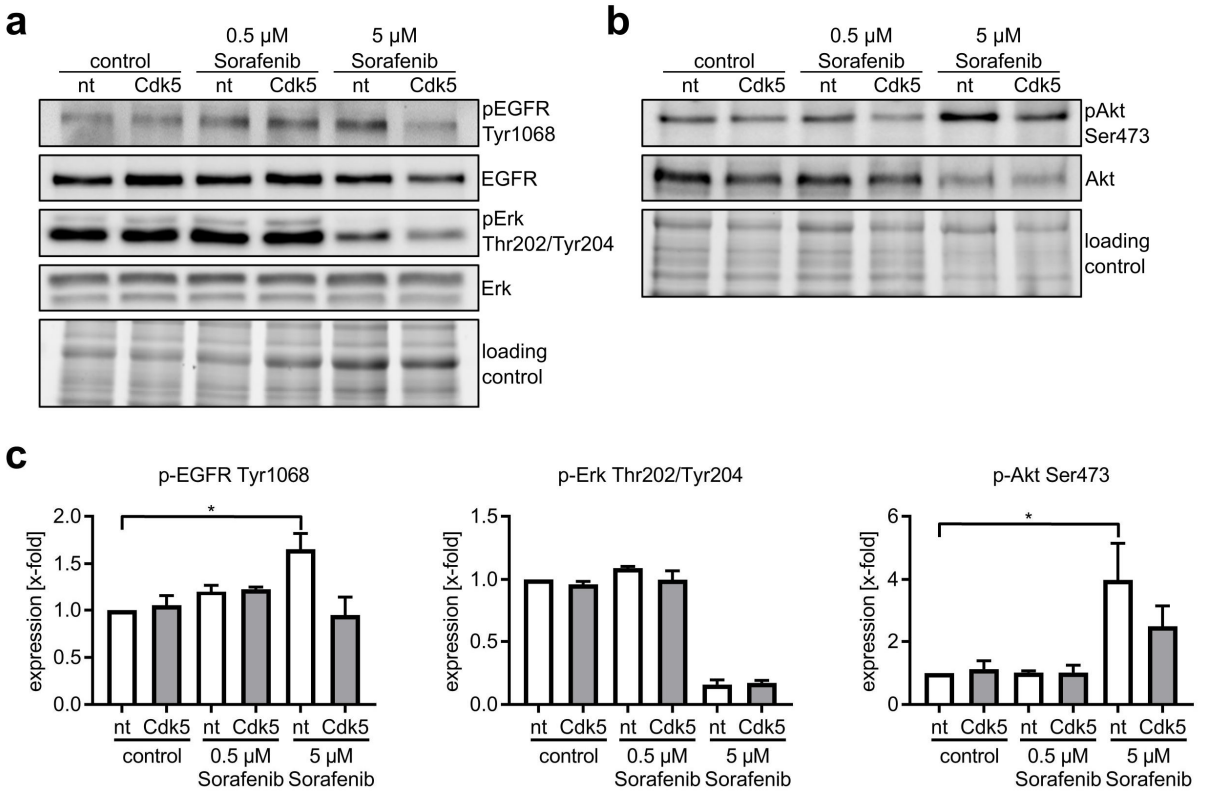

Figure 19 - Influence of Cdk5 inhibition on EGFR activity. (**a,b**) Immunoblots from nt and Cdk5 shRNA HUH7 cells treated with Sorafenib probed with antibodies for phosphorylated EGFR (p-EGFR), EGFR, phosphorylated Erk (p-Erk), Erk, phosphorylated Akt (p-Akt) and Akt are shown. (**c**) Quantitiative evaluations of p-EGFR, p-Erk and p-Akt from **a,b** are shown. One Way ANOVA, Tukey *P<0.05, n=3.

Moreover, we could show that upon Sorafenib treatment the surface levels of EGFR are significantly increased, making cells more receptive for an activation of EGFR (**Figure *20*a, b**).

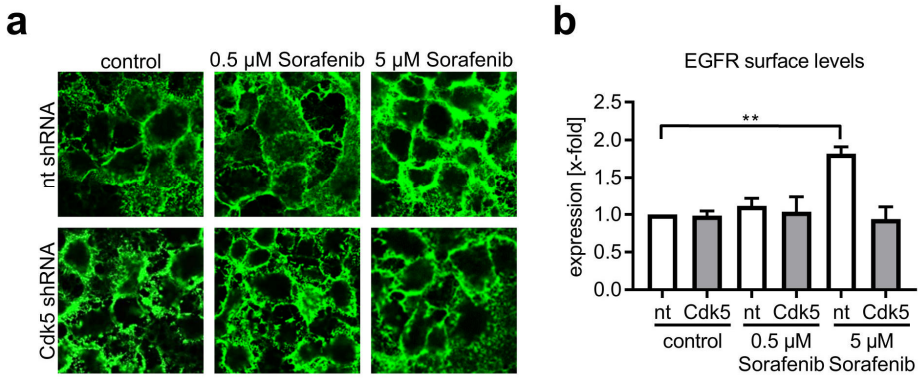

Figure 20 - Sorafenib increases surface levels of EGFR. (**a**) Immunostaining for EGFR with an antibody specific to the extracellular domain in nt and Cdk5 shRNA HUH7 cells after Sorafenib treatment is shown. (**b**) Relative evaluation of fluorescence intensity from **a** is shown. One Way ANOVA, Tukey $^{**}P<0.01$, $n=3$.

We therefore concluded that HCC cells use an activation of EGFR and PI3K/AKT signaling to compensate the Sorafenib induced impairment of the Ras/Raf/MEK/ERK pathway, implying that this dysregulation might be responsible for the poor therapeutic response to Sorafenib treatment (**Figure 21**).

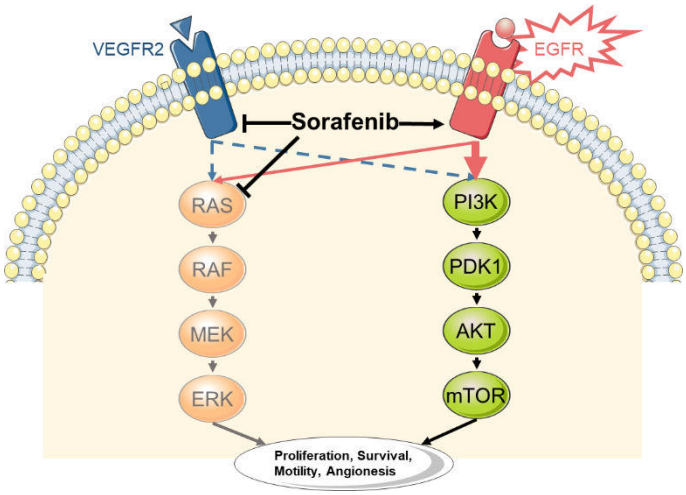

Figure 21 - Compensatory activation of EGFR upon Sorafenib treatment.

Importantly, the compensatory activation of the EGFR cascade was prevented by Cdk5 inhibition. By simultaneously treating cells with Sorafenib and Cdk5 inhibition, an induction of EGFR activity and consequently and activation of the PI3K/AKT pathway could be successfully avoided (**Figure 19**). Finally, the EGFR surface levels of Cdk5 knockdown cells remained unchanged upon Sorafenib treatment (**Figure 20**).

In order to more solidly confirm the interference with growth factor receptor activity as the mechanism mediating the sensitizing effect of Cdk5 inhibition, we investigated the effects of Sorafenib together with the EGFR inhibitor Gefitinib. Combination of Sorafenib and Gefitinib resulted in a significant reduction of proliferation similar to the combination of Cdk5 inhibition and Sorafenib (**Figure 22a**). Further we observed an analogous reduction in HCC cell migration by Gefitinib (**Figure 22b**). However, Cdk5 inhibition does not directly target EGFR kinase activity and even led to an increase of EGFR protein levels, indicating that Cdk5 inhibition acts through a mechanism different from conventional growth factor receptor inhibitors.

In summary, this set of evidence confirmed the compensatory activation of growth factor receptor pathways as a mechanism for HCC cells to evade Sorafenib treatment and sustain proliferative and migratory capacities. Importantly, Cdk5 inhibition can be used to prevent the compensatory feedback loop which activates the EGFR, despite not targeting the kinase activity of the EGFR directly, suggesting a different mode of action.

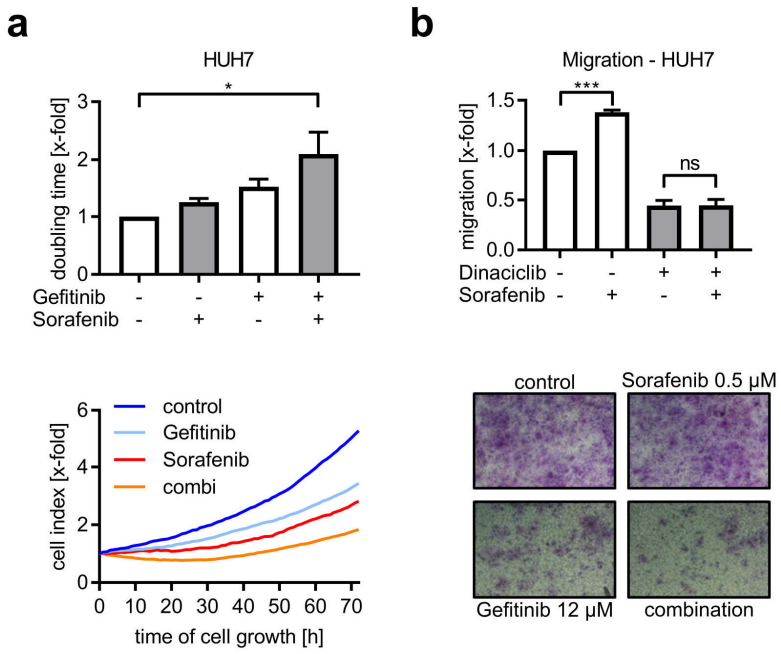

Figure 22 - Sorafenib and Gefitinib reduce HCC cell proliferation and migration. (**a**) Proliferation of HUH7 cells treated with either Sorafenib, Gefitinib or a combination of both is shown. Corresponding doubling time is shown. One Way ANOVA, Tukey *P<0.05, n=3. (**b**) Transwell migration of wild-type HUH7 cells that were pretreated with the respective compounds in the indicated concentrations before their ability to migrate was determined by Boyden Chamber assay. Representative pictures of migrated cells are shown together with bar diagrams showing the number of migrated cells normalized to the control. One Way ANOVA, Tukey ***P<0.001, n=3.

3.5 EGFR Expression Is High in Human HCC

In the clinical practice the assessment of EGFR expression in human tissue is not used as a diagnostic marker. However, our results show that EGFR signaling and distribution are important targets in HCC impaired by Cdk5 inhibition. A perturbation of these pathways may increase the efficacy of Sorafenib and overcome treatment resistance. Therefore we wanted to evaluate the clinical relevance of the EGFR in HCC by performing an immunohistochemistry staining of a tissue micro-array (TMA) containing HCC tumor tissue of 63 patients treated at the university hospital in Munich, Germany between 2008 and 2013. Staining and analysis of the HCC-TMA was performed in cooperation with Prof. Dr. med. Doris Mayr and Dr. med. Veronika Kanitz from the institute of pathology (LMU, Munich, Germany).

The evaluation of the TMA showed that expression of EGFR was increased in HCC patient tissue compared to healthy liver tissue (**Figure 23a**). About 63.4% of the patient tissues have EGFR positive cells, with 44.4% of tissues showing more than 80% EGFR positive cells (**Figure 23b**) and 44.8% demonstrating intermediate or strong EGFR staining intensity (**Figure 23c**). As EGFR staining is no common practice for HCC diagnostic we used the immunoreactive score (IRS) for breast cancer tissue as described by Remmele et al. as a scoring system.[73] The IRS takes the percentage of positively stained cells as well as the staining intensity into account revealing that 39.5% of patients show an intermediate or strong IRS (6-12), out of which 44% show the highest possible score (**Figure 23d**).

Next we tried to find a relation between EGFR expression and patient prognosis by correlating percentage of positive cells, staining intensity and IRS with tumor grading, r-classification, tumor stage, frequency of recurrence and cause of death. However, due to the size and heterogeneity of the observed patient population we could not find any correlation between the considered parameters (**Supplementary Table 1**).

Still, the outcome of our experiment proposes that the EGFR is frequently increased in human HCC and could be accountable for treatment evasion, which can be addressed by inhibiting Cdk5.

a

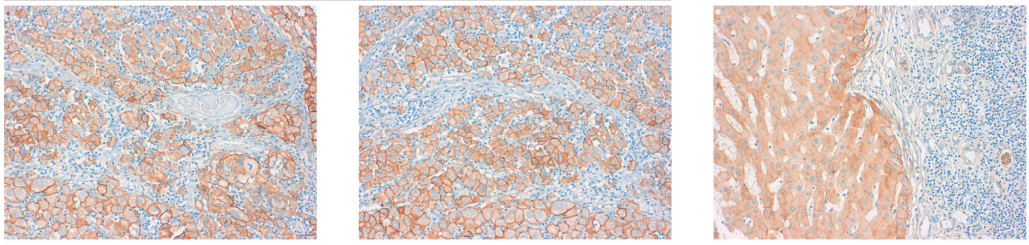

b

EGFR percentage

		frequency	percentage	valid percentage	cumulated percentage
valid	negative	20	31.7	31.7	31.7
	1-10%	2	3.2	3.2	34.9
	11-50%	5	7.9	7.9	42.9
	51-80%	5	7.9	7.9	50.8
	>80%	28	44.4	44.4	95.2
	missing	3	4.8	4.8	100
	total	63	100	100	

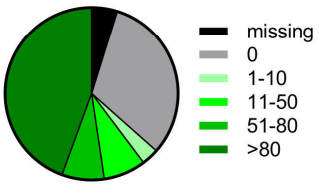

c

EGFR intensity

		frequency	percentage	valid percentage	cumulated percentage
valid	0	20	31.7	31.7	31.7
	weak	13	20.6	20.6	52.4
	interm.	13	20.6	20.6	73
	strong	14	22.2	22.2	95.2
	missing	3	4.8	4.8	100
	total	63	100	100	

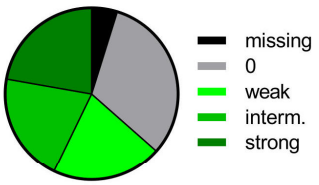

d

EGFR – IRS

		frequency	percentage	valid percentage	cumulated percentage
valid	0	20	31.7	31.7	31.7
	1	1	1.6	1.6	33.3
	2	5	7.9	7.9	41.3
	4	9	14.3	14.3	55.6
	5	3	4.8	4.8	60.3
	6	3	4.8	4.8	65.1
	8	9	14.3	14.3	79.4
	9	2	3.2	3.2	82.5
	12	11	17.5	17.5	100
	total	63	100	100	

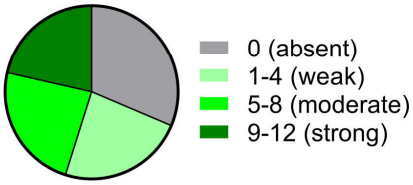

Figure 23 - EGFR expression is high in human HCC. (**a**) Immunostaining of patient tissue for EGFR. Pictures of EGFR expression in HCC tissue (left and middle) and healthy liver tissue (right) are shown. (**b**) Table showing percentage of EGFR positive cells in HCC tissue. (**c**) Table showing the staining intensity of EGFR in HCC tissue. (**d**) Table showing the immunoreactive score for EGFR in HCC tissue.

3.6 Cdk5 Is Essential for Intracellular Vesicle Trafficking

The previous experiments have shown that the prevention of a compensatory activation of the EGFR contributes to the sensitizing effect of Cdk5 on Sorafenib treatment. However, our results suggest a mechanism different from direct inhibitors of growth factor activity. In order to elucidate how Cdk5 inhibition influences the activation of the EGFR we focused on endocytosis, a process crucial for EGFR signaling. After being activated trough ligand binding, the EGFR has to be internalized and trafficked through early and late endosomes. The signaling is then either terminated by degradation via lysosomes or maintained by recycling via recycling endosomes.[81]

We used Rhodamine-labeled EGF to analyze receptor internalization, but there was no apparent effect of Cdk5 inhibition on the uptake of the EGF/EGFR complex (**Figure 24a**, **b**). In contrast, a pulse-chase experiment showed that Cdk5 inhibition significantly influenced EGFR elimination and led to delayed clearance of internalized receptor/ligand complex (**Figure *24*c, d**).

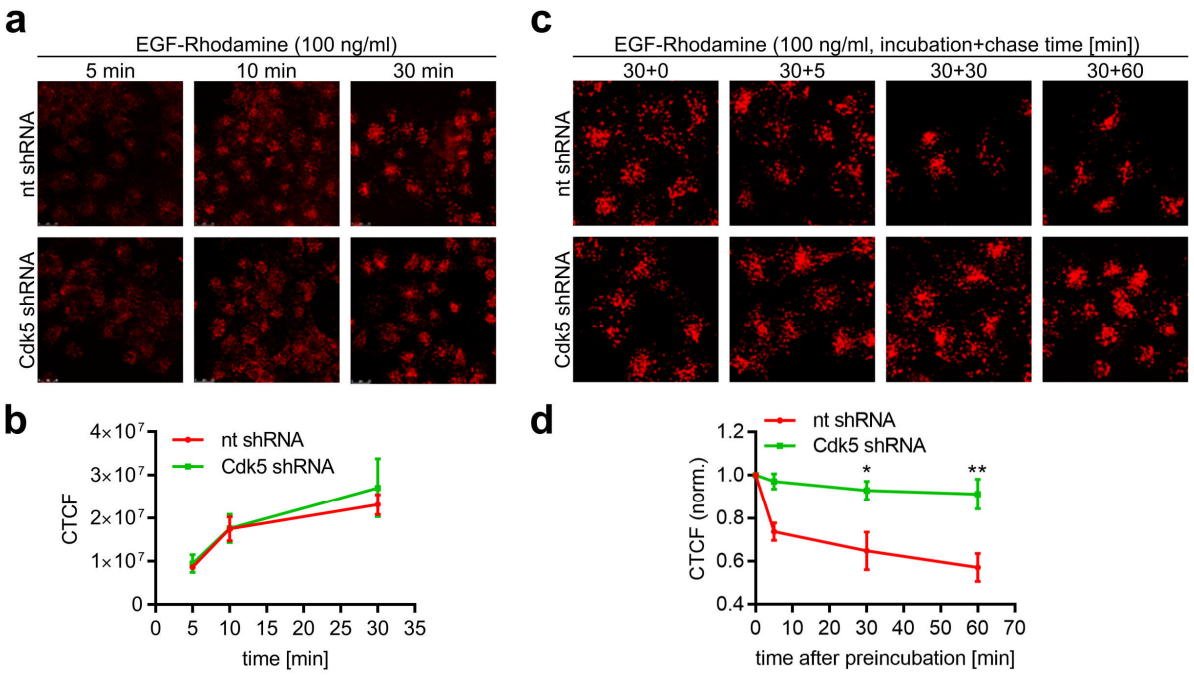

Figure 24 - Cdk5 inhibition influences EGFR elimination. (**a**) Images display nt and Cdk5 shRNA HUH7 cells that were treated with EGF-Rhodamine for various time points and analysed by confocal microscopy. (**b**) Quantitative evaluation of corrected total cell fluorescence (CTCF) of images from **a** is shown. For each condition 30 cells were analysed. (**c**) Images show nt and Cdk5 shRNA HUH7 cells that were incubated with EGF-Rhodamine before EGF-Rhodamine was removed and cells were chased for the given time points. (**d**) Quantitative evaluation of CTCF of images from **c** is indicated. One Way ANOVA, Tukey *P<0.05, **P<0.01, n=3.

These findings suggest that Cdk5 inhibition interferes with a late step of EGFR trafficking, which is in line with distinct EGFR clusters in the perinuclear region of Cdk5 shRNA cells (**Figure 25**).

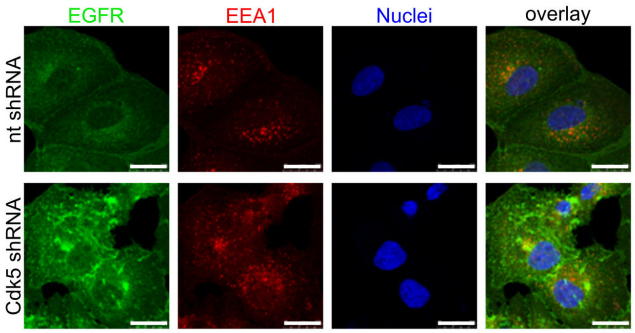

Figure 25 - Cdk5 inhibition leads to an accumulation of the EGFR. Immunostaining for EGFR (green), EEA1 (red) and Hoechst33342 (blue, nuclei) from nt and Cdk5 shRNA HUH7 cells are shown. Scale bar, 25 µm.

Next we performed live cell imaging of control and Cdk5 knockdown HUH7 cells expressing eGFP-tagged EGFR, to get a detailed insight into the effect of Cdk5 inhibition on endosomal trafficking of the EGFR. Analysis of vesicle dynamics and size revealed that vesicle trafficking was disturbed by Cdk5 inhibition. In nt shRNA cells there was an equal distribution of small EGFR-positive vesicles across the cell moving with high velocity and distinct directionality (**Figure 26a** and **Supplementary Video 1**). On the contrary, Cdk5 shRNA cells showed a significant amount of large, ring-shaped vesicles with impaired motility in close proximity to the nucleus (**Figure 26a** and **Supplementary Video 1**). Evaluation of vesicle size showed that vesicles larger than 0.8 µm^2 appear only in Cdk5 knockdown cells (**Figure *26*b**).

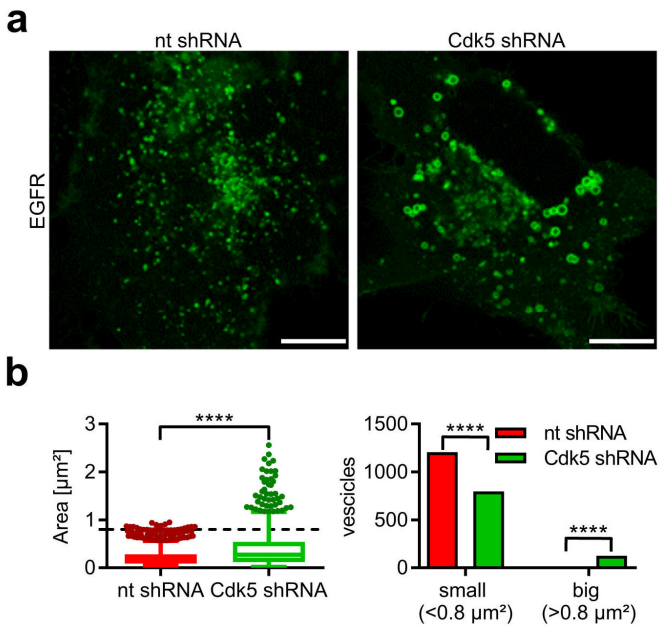

Figure 26 – Cdk5 influences EGFR trafficking. (**a**) Single frames from live cell imaging videos of nt and Cdk5 shRNA cells expressing GFP-EGFR are shown. Scale bar, 10 µm. (**b**) Box plot diagram and bar diagram show the distribution of vesicle size comparing nt and Cdk5 shRNA. Mann Whitney, ****P<0.0001, Chi-squared test, ****P<0.0001.

Strikingly, the effect of Cdk5 inhibition seems to affect the whole endocytic system, rather than being exclusive to EGFR, as Cdk5 knockdown also modulates size and motility of vesicles carrying integrin α5, a model protein for endocytic trafficking, and c-MET, the receptor for HGF (**Figure 27** and **Supplementary Video 2 and 3**). Specifically, the HGF-receptor is of significant importance in this context, because it belongs to the most prominent and frequently dysregulated growth factors in HCC.[82] Hence, our results indicate, that several important growth factor receptors, which are linked to HCC, can be targeted by inhibiting Cdk5.

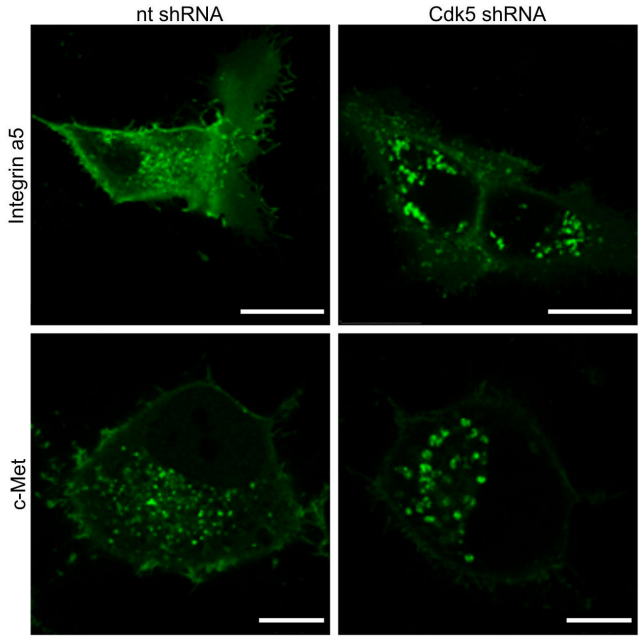

Figure 27 - Cdk5 inhibition influences intracellular trafficking. Single frames from live cell imaging videos of nt and Cdk5 shRNA HUH7 cells expressing either GFP-Integrin-α5 or GFP-cMet are shown. Scale bar, 25 µm (integrin α5), 10 µm (c-Met).

Taken together, our results indicate that Cdk5 inhibition has a global effect on intracellular trafficking by disturbing a late step in endocytosis as well as autophagy. This leads to an intracellular accumulation of various cargo proteins, which potentially impairs the extent and quality of signaling, with special focus on growth factor receptors. As a result, the inhibition of Cdk5 provides a global approach to prevent the compensatory activation of growth factor receptors commonly induced by Sorafenib and thereby offers a significant advantage over individual growth factor receptor targeting.

DISCUSSION

4 DISCUSSION

4.1 Sorafenib, the First Line Treatment for HCC

The treatment of late stage HCC patients radically changed with the approval of the multi-tyrosine kinase inhibitor Sorafenib in 2008. The first and only approved systemic chemotherapeutic agent for late stage HCC increased both median overall survival and time to radiologic progression by about three months. However, poor response rates and severe side effects overshadowed the therapeutic success of Sorafenib. Since then, various attempts have been made to increase the therapeutic effect of Sorafenib.

4.1.1 Sorafenib-Based Combination Therapies for HCC

Combining chemotherapeutics to enhance therapeutic success and reduce treatment-related toxicities is a common practice in cancer therapy. Along this line, a panel of experts proposed a framework of guidelines for the development of clinical studies investigating the combination of Sorafenib with other chemotherapeutics in HCC.[83] Since then, Sorafenib has been combined with fluoropyrimidines (Tegefur/Uracil, 5-Fluorouracil)[84,85], anthracyclines (Doxorubicin)[86,87] and mTOR inhibitors (Sirolimus and Everolimus)[88]. Only the combination with mTOR inhibitors showed a remarkable increase in overall survival (40 months), while the other studies failed to improve the situation for patients. However, the results of the aforementioned mTOR study need to be interpreted with caution, as the study aimed at patients recurring after liver transplantation, which makes overall survival and progression free survival difficult to compare to other studies. This concern is confirmed in a phase I trial investigating the Everolimus/Sorafenib combination in advanced-stage HCC patients, showing a median overall survival of only 7.4 months.[89] Further, the mentioned combination approaches not only failed to reduce therapy related adverse events but caused additional chemotherapy related side effects, therefore rendering them unsuitable for routine clinical practice.[21]

4.1.2 New First Line Treatments for HCC

Along with the attempts to increase the efficiency of Sorafenib, several clinical trials were conducted to establish a new first line therapy for advanced HCC. However, the results of the randomized phase III trials comparing Sorafenib against Sunitinib[90], Brivanib[91] and Linifanib[92] showed that each drug failed to meet the primary end point of increasing overall survival. The search for an effective second line therapy has been similarly un-successful, as Brivanib[93], Everolimus[94] and Ramucirumab[95] all failed to show significant influence on patient survival in global phase III trials after Sorafenib treatment has failed.

Recently, two new promising multityrosine kinase inhibitors, Regorafenib[96] and Lenvatinib[97], came into prospect as treatment options for HCC patients. Regorafenib treatment had remarkable impact on overall survival of patients progressing under Sorafenib treatment, thus providing the first effective second line therapy.[96] Lenvatinib reached overall survival rates similar to Sorafenib in a randomized phase III non-inferiority trial in advanced stage HCC patients while showing significant improvements in all secondary efficiency parameters, e.g. response rate, time to progression and progression free survival.[98] Lenvatinib thereby presents a reasonable alternative to Sorafenib as a first line treatment. Apart from inhibiting multiple tyrosine kinases, the interference with immune checkpoint signaling by targeting the programmed cell death protein 1 (PD-1) was discussed as a potential therapy for HCC.[99] On this basis, Nivolumab, a human monoclonal antibody against PD-1, was evaluated in clinical trials and recently approved as a second line therapy for HCC patients progressing under Sorafenib treatment.[100] However, Sorafenib is still expected to remain the standard of care. Therefore it is of paramount importance to search for ways to improve the impact of Sorafenib on HCC.

4.2 Treatment Escape of Sorafenib Is Caused by Compensatory Activation of Survival Signaling

The activation of parallel pathways to evade chemotherapeutic treatment is a common trait of cancer.[101] The evasion of Sorafenib treatment in HCC is mainly caused by the activation of the Ras/Raf/MEK/ERK pathway, the PI3K/AKT/mTOR pathway, histone deacetylases (HDACs), as well as growth factor receptors.[102]

4.2.1 Sorafenib Leads to an Upregulation of Parallel Pathways

Sorafenib directly inhibits the activity of the Ras/Raf/MEK/ERK pathway by targeting the Raf kinase. However, an inhibition of Raf kinase activity by Sorafenib triggers complementary and/or feed-back mechanisms in HCC, which partially restore the activity of ERK, thereby reducing the therapeutic impact of Sorafenib.[103,104] Along this line, a combination of Sorafenib with MEK inhibitors could show some efficacy in preclinical and clinical studies, particularly when Ras was mutated.[105] Further, increased levels of MAPK14 has been shown to be associated with poor Sorafenib response in HCC and inhibition of MAPK14 could restore sensitivity to Sorafenib.[106] The PI3K/AKT/mTOR pathway has been shown to be playing a crucial role in HCC, where it is activated in 30-50% of cases and renders HCC cells less sensitive to Sorafenib treatment.[107] In keeping with the latter notion, combining Sorafenib with PI3K/AKT/mTOR inhibitors showed favorable results in a phase 1/2 study[108], while other

studies report severe side effects and failure to improve patient survival.[89,109] The simultaneous inhibition of HDACs along with Sorafenib treatment started out positive with encouraging results in preclinical studies, but consecutive clinical trials revealed severe side effects and had to be terminated (reviewed in [102]).

4.2.2 Sorafenib Leads to Compensatory Activation of Growth Factor Receptor Pathways

The deregulation of growth factor receptor signaling pathways is commonly observed in cancer. High degrees of redundancy lead to an overactivation of one growth factor receptor pathway to overcome the malfunction of another pathway, leading to treatment evasion and tumor progression, which is often observed in HCC.[110] Compensatory activation of growth factor receptors results in an overactivation of Ras/Raf/MEK/ERK pathway and the PI3K/AKT/mTOR pathway, two pathways with a mutual dependency in HCC.[111] Upon Sorafenib treatment and thereby an inhibition of the Ras/Raf/MEK/ERK cascade, an activation of the PI3K/AKT/mTOR pathway is observed[112,113], which is associated with malignancy and metastasis.[114,115] These findings are in line with our results showing increased HCC cell migration and EGFR activation, and subsequent AKT signaling, upon Sorafenib treatment. By inhibiting Cdk5 the compensatory activation of the EGFR-AKT axis can be prevented, thereby sensitizing HCC cells towards Sorafenib treatment.

4.3 EGFR Signaling in HCC

From the family of growth factor receptors the EGFR was the first member to be linked to the development of cancer.[116] Since then, the role of EGFR in a variety of human malignancy was elucidated[117], which led to the development of numerous strategies to inhibit EGFR activity (reviewed in [118]). Our results demonstrate that EGFR expression is high in human HCC tissue. This is in line with previous studies showing that EGFR is frequently overexpressed in HCC and correlates with metastasis, tumor aggressiveness and poor patient survival.[77,119,120] Therefore, EGFR inhibition was evaluated as a therapeutic option for the treatment of HCC.

4.3.1 Preclinical Evaluation of EGFR Inhibitors for HCC Treatment

In preclinical studies the inhibition of EGFR activity with either Erlotinib, Gefitinib or Cetuximab showed encouraging results in HCC cell lines.[121] The chimeric EGFR-directed monoclonal antibody Cetuximab showed a significant growth reduction in p53 wild-type HepG2 cells and sensitized p53-mutated HUH7 cells for the treatment with Fluvastatin and Doxorubicin. Growth reduction was achieved via an arrest of cell cycle progression by increasing levels of Cdk

inhibitors p21 and p27 and elevated levels of apoptosis.[122] Treatment with Erlotinib or Gefitinib, two small molecule inhibitors of the tyrosine-kinase domain of the EGFR, resulted in reduced growth rate, increased apoptosis and cell cycle arrest in human HCC.[123,124] By inhibiting MAPK and STAT pathway activity, Erlotinib treatment led to an induction of a G1/G0 arrest, an increase in pro-apoptotic factors and a decrease in anti-apoptotic factors.[125]

Further, both Erlotinib and Gefitnib showed promising results in animal tumor models. In a diethylnitrosamine (DEN)-induced HCC tumor model, Erlotinib not only impeded the progression of cirrhosis but also prevented the development of HCC.[126] Similar to Erlotinib, Gefitinib led to a significant reduction of tumor size and metastasis in orthotopic HCC mouse models.[127] The tumor growth inhibiting effect of Gefitinib could even be enhanced by combinational treatment with the cytotoxic agent cisplatin.[128]

Taken together, the preclinical results for EGFR inhibition in HCC *in vitro* as well as in animal models established a reasonable basis for further clinical trials.

4.3.2 Clinical Trials Investigating EGFR Inhibitors in Human HCC

The inhibition of EGFR was already shown to be effective in other solid tumors like colorectal cancer and non-small cell lung cancer.[129,130] The efficacy in other solid tumors together with the promising preclinical results in HCC and the fact that EGFR is overexpressed in the majority of human HCC led to a series of clinical trials for the evaluation of EGFR inhibition as a therapeutic strategy in HCC patients. However, EGFR inhibition in patients with HCC only achieved modest results. While Lapatinib[131] and Gefitinib[132] treatment showed no benefits for HCC patients, Erlotinib as a single agent resulted in moderate effects.[133] Also Cetuximab had no effect on HCC progression if applied as a single agent[134] and only had minor effects in combination with Gemcitabine and Oxaliplatin.[135] Erlotinib was also tested in combination with the angiogenesis inhibitor Bevacizumab, but failed to achieve any clinical improvements for HCC patients.[136]

The most promising approach for the use of EGFR inhibitors in HCC was the combination with Sorafenib, as a combination of Sorafenib and Gefitinib showed encouraging results in HCC xenograft mouse models.[78] The combination of Sorafenib and Erlotinib was evaluated in the SEARCH (Sorafenib and Erlotinib, a Randomized Trial Protocol for the treatment of Patients witch Hepatocellular Carcinoma) trial, the only phase III clinical trial in HCC involving an EGFR inhibitor. However, the combination treatment failed to show a significant survival benefit for patients.[137] The failure of these clinical trials put the specific targeting the EGFR as reasonable approach for HCC treatment into doubt.

4.3.3 Growth Factor Receptor Signaling in HCC

The difficulties which arise by targeting a specific growth factor receptor are related to the high degree of redundancy in growth factor receptor signaling. The inhibition of an individual growth factor receptor frequently leads to a compensatory activation of other growth factor receptors and subsequent signaling pathways, ultimately resulting in treatment evasion. In human HCC a variety of growth factor receptors is deregulated and targeting a single growth factor receptor seems to be insufficient, as shown by several clinical studies. For example, there is accumulating evidence that the insulin-like growth factor-1 receptor (IGF1R) and the hepatocyte growth factor receptor (HGFR) are involved in the development of HCC.[121]

HGFR/c-MET was shown to be overexpressed in advanced HCC tissue and the role in the development of HCC was confirmed in mouse models.[120,138] The activation of a liver-specific inducible MET transgene led to HCC development in transgenic mice, while the deactivation decreased tumor size via apoptosis and reduced proliferation, thereby showing the direct involvement of c-MET in hepatocarcinogenesis.[139] Additionally, previous studies could show that phosphorylation of c-MET is mediated via an EGFR dependent pathway suggesting a simultaneous inhibition of EGFR and c-MET to increase clinical impact.[121,140] Likewise, the IGF1R is frequently overexpressed (33% of HCCs) and overactivated (52% of HCCs) in human HCC.[141] It was shown that EGFR activation was needed for IGF-2 mediated proliferation in HCC cells and that parallel inhibition of IGF1R and EGFR had a synergistic effect on HCC progression. Interestingly, hepatoma cells used an EGFR dependent pathway to compensate IGF1R inhibition underlining the interconnection of the two signaling pathways.[142]

Thus, it was thought that combining inhibitors for individual growth factor receptors would increase therapeutic efficiency and reduce occurrence of resistance.[121] However, the application of several specific growth factor receptor inhibitors would also mean combining the respective adverse effects, resulting in a severe burden for patients and an increased risk for treatment discontinuation due to serious secondary effects. Therefore, this approach is highly unlikely to find application in the clinical context. Along this line, targeting several growth factor receptors by interfering with a common process during signal activation, rather than inhibiting individual kinase activities, would be a more favorable method accompanied by less adverse effects.

4.4 Cdk5 Interferes with Intracellular Trafficking to Inhibit Growth Factor Receptor Signaling

In this study we suggest targeting Cdk5 as a promising approach to increase the efficacy of Sorafenib in HCC. The results presented here provide direct evidence that an inhibition of Cdk5 enhances the therapeutic effect of Sorafenib by preventing the compensatory activation of growth factor receptors. We could confirm that Sorafenib treatment leads to an activation of the EGFR/Akt pathway. This compensatory activation could be prevented by Cdk5 inhibition. Like many other growth factor receptors, the EGFR pathway critically relies on endosomal trafficking.[81] In this study, we provided evidence that Cdk5 disturbs endosomal and autophagic trafficking causing an accumulation of respective cargos and an enlargement of endosomal vesicles, thereby critically interfering with receptor activity.

4.4.1 Endocytosis and Cancer

Endocytosis is a crucial mechanism for cells to regulate intracellular homeostasis and to communicate with their environment. Cells use endocytic trafficking to internalize ligand-bound surface receptors, nutrients, immunoglobulins and a variety of other extracellular molecules.[143] The endocytic circuitries are tightly regulated by the Rab proteins, a family of small GTPases which control various processes of the endocytic cascade including formation of vesicles, directed movement of vesicles and vesicle fusion.[144] The activity of Rab proteins is in turn regulated by guanine nucleotide exchange factors (GEFs) which mediate the exchange of GDP for GTP and GTPase-activating proteins (GAPs) which initiate GTP hydrolysis.[145] Especially, Rab 5, 7 and 11 play a critical role in surface internalization, vesicle maturation and recycling. In the context of surface receptors, endocytosis plays a pivotal role in mediating signaling.[146] Growth factor receptors are internalized via endosomes after activation and are then targeted to different fates via endosomal sorting. The receptor signaling is either terminated by degrading the receptor via lysosomes or maintained through recycling to the plasma membrane.[81]

In recent years evidence accumulated that cancer cells manipulate endocytosis to alter intracellular trafficking to their advantage.[147] By rerouting endosomal vesicles containing growth factor receptors destined for degradation back to the plasma membrane via recycling pathways, cancer cells sustain growth factor receptor signaling and avoid receptor downregulation.[148] The mechanisms used by cancer cells to sustain receptor signaling are diverse. In the case of EGFR, activation through EGF mainly leads to receptor degradation via lysosomes, while binding to TGF-α favours the recycling route.[149] Consequently, tumors expressing TGF-α can use autocrine feedback loops to avoid EGFR downregulation. Another way to sustain receptor activity is the impairment of ubiquitylation. The binding of ubiquitin

significantly influences the fate of internalized cargos and decides between degradation and recycling.[150] In glioblastoma, EGFR was shown to have an oncogenic deletion mutation (EGFRvIII), which leads to hypo-ubiquitylation and thereby to reduced internalization and increased recycling.[151] Further, receptor fate can be altered at the last stage of intracellular sorting. In multivesicular bodies (MVB), endosomal sorting complexes required for transport (ESCRTs) proteins are required to deliver ubiquitinylated cargos to lysosomes for degradation.[152] Studies have shown that a downregulation of ESCRT proteins led to substantially reduced degradation of EGFR followed by continued signaling.[153,154] Despite being the best characterized receptor in this context, these findings are not exclusive to the EGFR and affect other growth factor receptors as well.[148] Apart from the EGFR, especially the IGF-, FGF- and HGF-receptors play a very important role in Sorafenib treatment escape in HCC and also critically dependent on endocytic trafficking.[79,80]

Another group of proteins that is critically dependent on endocytosis and associated with cancer is the integrin family, a group of transmembrane receptors promoting cell-to-extracellular matrix adhesions. After binding to their extracellular ligand, integrins are internalized similar to growth factor receptors and degraded via lysosomes. Similar to growth factor receptor trafficking, integrin degradation and recycling is regulated by Rab proteins. Cells with a migratory phenotype have to sustain a constant fluctuation of integrins from the plasma membrane back to the leading edge of movement (reviewed in [155]). Especially for highly invasive and motile cancer cells it is imperative to maintain a continuous recycling of integrins rather than directing them to degradation. Along this line integrins mediate crucial steps in metastatic processes (reviewed in [156]). Another important mechanism for cancer cells to gain invasive capabilities is the epithelial-to-mesenchymal transition (EMT). Through EMT cancer cells lose their epithelial phenotype through the loss of E-cadherin and tight junction proteins, and gain mesenchymal traits, characterized by migratory and invasive behavior. This is an essential process in the formation of distant metastasis, which is highly dependent on and interconnected in endocytic circuitries (reviewed in [157]).

In summary, the endosomal system is commonly hijacked by cancer cells to redistribute intracellular cargo and is therefore a promising target for cancer treatment.[147] On this basis several preclinical studies showed promising anti-cancer effects by interfering with endocytosis and thereby gave valuable insights into new opportunities presented by targeting intracellular trafficking.[158-160] However, these studies used experimental drugs, which are not yet approved for the treatment of patients. In this study we suggest targeting Cdk5, a protein with clinically evaluated inhibitors ready at hand, as an effective strategy to interfere with intracellular trafficking. By inhibiting Cdk5 the incorrect transport and aberrant activation of growth factor receptors and integrins can be prevented, thereby impeding both cancer cell proliferation and migration.

4.4.2 Cdk5 is important for vesicle trafficking

In cancer cells Cdk5 has not yet been associated with endocytic trafficking, but there is evidence for the vital role of Cdk5 in the regulation of endocytosis in the neuronal system.[161] The role of Cdk5 in neurons has been extensively studied and Cdk5 has been established as a central regulator of endocytosis in the central nervous system. Cdk5 was shown to play an essential role in the endocytosis of clathrin coated vesicles in synapses by cophosphorylating the dephosphins amphiphysin I, dynamin I and synaptojanin and thereby enabling vesicle fission and formation.[161,162] Further, Cdk5 is involved in vesicle and membrane trafficking at presynaptic and postsynaptic sites. At presynaptic sites, Cdk5 mediates the release of neurotransmitters by regulating the vesicle pool composition and phosphorylating neurotransmitter-releasing substrates. At postsynaptic sites, Cdk5 is responsible for the phosphorylation of numerous substrates regulating the endocytosis of membrane receptors like the N-methyl-D-aspartate (NMDA) receptor (reviewed in [163]). Recently, Cdk5 has been shown to regulate the Rab8-Rab11 cascade in axon outgrowth by directly phosphorylating GRAB, a GEF of Rab8, thus creating a link between Cdk5 and the regulation of Rab proteins.[164] Thus, Cdk5 might regulate the activity of other Rab proteins by a similar mechanism, thereby influencing endocytosis and autophagy. This represents an interesting question for future research.

4.5 Dinaciclib, a Clinically Available Cdk5 Inhibitor

Targeting Cdks is a promising approach in cancer therapy. For example, inhibitors of Cdk4 and 6, Palbociclib[165], Ribociclib[166] and Abemaciclib[167], are approved for the treatment of advanced or metastatic breast cancer in combination with Letrozole. Along this line, Palbociclib showed promising results in a preclinical HCC study and could enhance Sorafenib efficacy in an HCC mouse model.[168] The notion of targeting Cdk5 was based on the involvement in the pathogenesis of neuronal diseases like Alzheimer's and Parkinson's disease.[33] Therefore an inhibition of Cdk5 has been a desirable goal and led to the development of a wide range of Cdk inhibitors, which are primarily selective for Cdk5. Recently, the role of Cdk5 extended beyond the neuronal system[169], which led to the evaluation of Cdk5 inhibitors in a variety of diseases. Roscovitine was evaluated in phase I and II clinical trials for the treatment of advanced solid tumors and non-small cell lung cancer, however with little success. Further the small molecule Cdk5 inhibitor AT7519 has been tested in patients with advanced or metastatic tumors in a phase I trial and in patients with relapsed or refractory chronic lymphocytic leukemia (CLL) and mantle cell lymphoma (MCL) in a phase II trial (reviewed in [170]). However, the phase II trials in CLL and MCL only revealed mediocre results for AT7519 as a single agent.[171]

In this context the role of Dinaciclib in recent clinical history has to be emphasized. Dinaciclib is a small molecule Cdk5 inhibitor that offered encouraging anti-cancer effects in combination with an acceptable profile of adverse effects in clinical trials. Especially in hematologic malignancies Dinaciclib could achieve good results. A phase III clinical trial successfully evaluated the efficacy of Dinaciclib as a therapy for chronic lymphocytic leukemia.[172] This achievement led to the clinical investigation of Dinaciclib for the treatment of other forms of leukemia.[173] In summary Dinaciclib is expected to have a clinical impact in the foreseeable future and in accordance with our study, Dinaciclib offers a promising therapeutic approach to limit treatment escape and increase the efficacy of Sorafenib in advanced HCC patients.

4.6 Conclusion and Outlook

What are the new findings?

Cdk5 inhibition is elucidated as a promising approach to improve Sorafenib responsiveness in HCC as:

- Cdk5 inhibition in combination with Sorafenib has a synergistic effect on HCC progression *in vitro* as well as *in vivo*
- Cdk5 inhibition interferes with the Sorafenib-induced compensatory activation of growth factor receptors

Importantly, Cdk5 inhibition was revealed to exert a mode of action that is different from classical growth factor receptor inhibitors as:

- Cdk5 inhibition interferes with intracellular trafficking
- Cdk5 inhibition therefore offers a comprehensive approach to globally block the activation of growth factor receptors in general

What is the impact of our findings on clinical practice in the foreseeable future?

- Cdk5 inhibition is a ground-breaking and valuable strategy to prevent Sorafenib treatment escape.
- As with Dinaciclib a clinically tested Cdk5 inhibitor is available, evaluating the combination of Sorafenib and Cdk5 inhibition to improve the therapeutic situation for advanced-stage HCC patients turns out to become realistic.

REFERENCES

5 REFERENCES

1 Llovet, J. M., Burroughs, A. & Bruix, J. Hepatocellular carcinoma. *Lancet* **362**, 1907-1917, doi:10.1016/S0140-6736(03)14964-1 (2003).

2 Caldwell, S. & Park, S. H. The epidemiology of hepatocellular cancer: from the perspectives of public health problem to tumor biology. *J Gastroenterol* **44 Suppl 19**, 96-101, doi:10.1007/s00535-008-2258-6 (2009).

3 Alazawi, W., Cunningham, M., Dearden, J. & Foster, G. R. Systematic review: outcome of compensated cirrhosis due to chronic hepatitis C infection. *Aliment Pharmacol Ther* **32**, 344-355, doi:10.1111/j.1365-2036.2010.04370.x (2010).

4 Sherman, M. Hepatocellular carcinoma: epidemiology, surveillance, and diagnosis. *Semin Liver Dis* **30**, 3-16, doi:10.1055/s-0030-1247128 (2010).

5 El-Serag, H. B. Hepatocellular carcinoma. *N Engl J Med* **365**, 1118-1127, doi:10.1056/NEJMra1001683 (2011).

6 El-Serag, H. B. Epidemiology of viral hepatitis and hepatocellular carcinoma. *Gastroenterology* **142**, 1264-1273 e1261, doi:10.1053/j.gastro.2011.12.061 (2012).

7 Inokawa, Y. *et al.* Molecular alterations in the carcinogenesis and progression of hepatocellular carcinoma: Tumor factors and background liver factors. *Oncol Lett* **12**, 3662-3668, doi:10.3892/ol.2016.5141 (2016).

8 Hsu, H., Peng, S., Lai, P., Chu, J. & Lee, P. Mutations of p53 gene in hepatocellular-carcinoma (hcc) correlate with tumor progression and patient prognosis - a study of 138 patients with unifocal hcc. *Int J Oncol* **4**, 1341-1347 (1994).

9 Giles, R. H., van Es, J. H. & Clevers, H. Caught up in a Wnt storm: Wnt signaling in cancer. *Biochim Biophys Acta* **1653**, 1-24 (2003).

10 Kim, M. *et al.* Functional interaction between Wnt3 and Frizzled-7 leads to activation of the Wnt/beta-catenin signaling pathway in hepatocellular carcinoma cells. *J Hepatol* **48**, 780-791, doi:10.1016/j.jhep.2007.12.020 (2008).

11 Llovet, J. M., Bru, C. & Bruix, J. Prognosis of hepatocellular carcinoma: the BCLC staging classification. *Semin Liver Dis* **19**, 329-338, doi:10.1055/s-2007-1007122 (1999).

12 Pugh, R. N., Murray-Lyon, I. M., Dawson, J. L., Pietroni, M. C. & Williams, R. Transection of the oesophagus for bleeding oesophageal varices. *Br J Surg* **60**, 646-649 (1973).

13 Lin, S., Hoffmann, K. & Schemmer, P. Treatment of hepatocellular carcinoma: a systematic review. *Liver Cancer* **1**, 144-158, doi:10.1159/000343828 (2012).

14 Bruix, J., Sherman, M. & American Association for the Study of Liver, D. Management of hepatocellular carcinoma: an update. *Hepatology* **53**, 1020-1022, doi:10.1002/hep.24199 (2011).

15 Llovet, J. M. *et al.* Liver transplantation for small hepatocellular carcinoma: the tumor-node-metastasis classification does not have prognostic power. *Hepatology* **27**, 1572-1577, doi:10.1002/hep.510270616 (1998).

16 Han, K. & Kim, J. H. Transarterial chemoembolization in hepatocellular carcinoma treatment: Barcelona clinic liver cancer staging system. *World J Gastroenterol* **21**, 10327-10335, doi:10.3748/wjg.v21.i36.10327 (2015).

17 El-Serag, H. B., Marrero, J. A., Rudolph, L. & Reddy, K. R. Diagnosis and treatment of hepatocellular carcinoma. *Gastroenterology* **134**, 1752-1763, doi:10.1053/j.gastro.2008.02.090 (2008).

18 Asghar, U. & Meyer, T. Are there opportunities for chemotherapy in the treatment of hepatocellular cancer? *J Hepatol* **56**, 686-695, doi:10.1016/j.jhep.2011.07.031 (2012).

19 Llovet, J. M. *et al.* Sorafenib in advanced hepatocellular carcinoma. *N Engl J Med* **359**, 378-390, doi:10.1056/NEJMoa0708857 (2008).

20 Forner, A., Gilabert, M., Bruix, J. & Raoul, J. L. Treatment of intermediate-stage hepatocellular carcinoma. *Nat Rev Clin Oncol* **11**, 525-535, doi:10.1038/nrclinonc.2014.122 (2014).

21 Abdel-Rahman, O. & Fouad, M. Sorafenib-based combination as a first line treatment for advanced hepatocellular carcinoma: a systematic review of the literature. *Crit Rev Oncol Hematol* **91**, 1-8, doi:10.1016/j.critrevonc.2013.12.013 (2014).

22 Adnane, L., Trail, P. A., Taylor, I. & Wilhelm, S. M. Sorafenib (BAY 43-9006, Nexavar), a dual-action inhibitor that targets RAF/MEK/ERK pathway in tumor cells and tyrosine kinases VEGFR/PDGFR in tumor vasculature. *Methods Enzymol* **407**, 597-612, doi:10.1016/S0076-6879(05)07047-3 (2006).

23 Wilhelm, S. M. *et al.* BAY 43-9006 exhibits broad spectrum oral antitumor activity and targets the RAF/MEK/ERK pathway and receptor tyrosine kinases involved in tumor progression and angiogenesis. *Cancer Res* **64**, 7099-7109, doi:10.1158/0008-5472.CAN-04-1443 (2004).

24 Cheng, A. L. *et al.* Efficacy and safety of sorafenib in patients in the Asia-Pacific region with advanced hepatocellular carcinoma: a phase III randomised, double-blind, placebo-controlled trial. *Lancet Oncol* **10**, 25-34, doi:10.1016/S1470-2045(08)70285-7 (2009).

25 Doyle, A. *et al.* Sorafenib in the treatment of hepatocellular carcinoma: a multi-centre real-world study. *Scand J Gastroenterol* **51**, 979-985, doi:10.3109/00365521.2016.1166518 (2016).

26 Ehrlich, S. M. *et al.* Targeting cyclin dependent kinase 5 in hepatocellular carcinoma--A novel therapeutic approach. *J Hepatol* **63**, 102-113, doi:10.1016/j.jhep.2015.01.031 (2015).

27 Malumbres, M. & Barbacid, M. Mammalian cyclin-dependent kinases. *Trends Biochem Sci* **30**, 630-641, doi:10.1016/j.tibs.2005.09.005 (2005).

28 Dhavan, R. & Tsai, L. H. A decade of CDK5. *Nat Rev Mol Cell Biol* **2**, 749-759, doi:10.1038/35096019 (2001).

29 Lew, J., Beaudette, K., Litwin, C. M. & Wang, J. H. Purification and characterization of a novel proline-directed protein kinase from bovine brain. *J Biol Chem* **267**, 13383-13390 (1992).

30 Liebl, J., Furst, R., Vollmar, A. M. & Zahler, S. Twice switched at birth: cell cycle-independent roles of the "neuron-specific" cyclin-dependent kinase 5 (Cdk5) in non-neuronal cells. *Cell Signal* **23**, 1698-1707, doi:10.1016/j.cellsig.2011.06.020 (2011).

31 Hirasawa, M. *et al.* Perinatal abrogation of Cdk5 expression in brain results in neuronal migration defects. *Proc Natl Acad Sci U S A* **101**, 6249-6254, doi:10.1073/pnas.0307322101 (2004).

32 Chergui, K., Svenningsson, P. & Greengard, P. Cyclin-dependent kinase 5 regulates dopaminergic and glutamatergic transmission in the striatum. *Proc Natl Acad Sci U S A* **101**, 2191-2196, doi:10.1073/pnas.0308652100 (2004).

33 Cheung, Z. H. & Ip, N. Y. Cdk5: a multifaceted kinase in neurodegenerative diseases. *Trends Cell Biol* **22**, 169-175, doi:10.1016/j.tcb.2011.11.003 (2012).

34 Noble, W. *et al.* Cdk5 is a key factor in tau aggregation and tangle formation in vivo. *Neuron* **38**, 555-565 (2003).

35 Zhang, P. *et al.* Cdk5-Dependent Activation of Neuronal Inflammasomes in Parkinson's Disease. *Mov Disord* **31**, 366-376, doi:10.1002/mds.26488 (2016).

36 Wong, A. S. *et al.* Cdk5-mediated phosphorylation of endophilin B1 is required for induced autophagy in models of Parkinson's disease. *Nat Cell Biol* **13**, 568-579, doi:10.1038/ncb2217 (2011).

37 Ko, J. *et al.* p35 and p39 are essential for cyclin-dependent kinase 5 function during neurodevelopment. *J Neurosci* **21**, 6758-6771 (2001).

38 Humbert, S., Dhavan, R. & Tsai, L. p39 activates cdk5 in neurons, and is associated with the actin cytoskeleton. *J Cell Sci* **113 (Pt 6)**, 975-983 (2000).

39 Zukerberg, L. R. *et al.* Cables links Cdk5 and c-Abl and facilitates Cdk5 tyrosine phosphorylation, kinase upregulation, and neurite outgrowth. *Neuron* **26**, 633-646 (2000).

40 Sasaki, Y. *et al.* Fyn and Cdk5 mediate semaphorin-3A signaling, which is involved in regulation of dendrite orientation in cerebral cortex. *Neuron* **35**, 907-920 (2002).

41 Kobayashi, H. *et al.* Phosphorylation of cyclin-dependent kinase 5 (Cdk5) at Tyr-15 is inhibited by Cdk5 activators and does not contribute to the activation of Cdk5. *J Biol Chem* **289**, 19627-19636, doi:10.1074/jbc.M113.501148 (2014).

42 Kimura, T., Ishiguro, K. & Hisanaga, S. Physiological and pathological phosphorylation of tau by Cdk5. *Front Mol Neurosci* **7**, 65, doi:10.3389/fnmol.2014.00065 (2014).

43 Arif, A. Extraneuronal activities and regulatory mechanisms of the atypical cyclin-dependent kinase Cdk5. *Biochem Pharmacol* **84**, 985-993, doi:10.1016/j.bcp.2012.06.027 (2012).

44 Tarricone, C. *et al.* Structure and regulation of the CDK5-p25(nck5a) complex. *Mol Cell* **8**, 657-669 (2001).

45 Pozo, K. & Bibb, J. A. The Emerging Role of Cdk5 in Cancer. *Trends Cancer* **2**, 606-618, doi:10.1016/j.trecan.2016.09.001 (2016).

46 Choi, H. S. *et al.* Single-nucleotide polymorphisms in the promoter of the CDK5 gene and lung cancer risk in a Korean population. *J Hum Genet* **54**, 298-303, doi:10.1038/jhg.2009.29 (2009).

47 Kibel, A. S. *et al.* Genetic variants in cell cycle control pathway confer susceptibility to aggressive prostate carcinoma. *Prostate* **76**, 479-490, doi:10.1002/pros.23139 (2016).

48 Liu, J. L. *et al.* Expression of CDK5/p35 in resected patients with non-small cell lung cancer: relation to prognosis. *Med Oncol* **28**, 673-678, doi:10.1007/s12032-010-9510-7 (2011).

49 Catania, A. *et al.* Expression and localization of cyclin-dependent kinase 5 in apoptotic human glioma cells. *Neuro Oncol* **3**, 89-98 (2001).

50 Zhang, X. *et al.* Aberrant expression of CDK5 infers poor outcomes for nasopharyngeal carcinoma patients. *Int J Clin Exp Pathol* **8**, 8066-8074 (2015).

51 Chiker, S. *et al.* Cdk5 promotes DNA replication stress checkpoint activation through RPA-32 phosphorylation, and impacts on metastasis free survival in breast cancer patients. *Cell Cycle* **14**, 3066-3078, doi:10.1080/15384101.2015.1078020 (2015).

52 Futatsugi, A. *et al.* Cyclin-dependent kinase 5 regulates E2F transcription factor through phosphorylation of Rb protein in neurons. *Cell Cycle* **11**, 1603-1610, doi:10.4161/cc.20009 (2012).

53 Pozo, K. *et al.* The role of Cdk5 in neuroendocrine thyroid cancer. *Cancer Cell* **24**, 499-511, doi:10.1016/j.ccr.2013.08.027 (2013).

54 Hsu, F. N. *et al.* Cyclin-dependent kinase 5 modulates STAT3 and androgen receptor activation through phosphorylation of Ser(7)(2)(7) on STAT3 in prostate cancer cells. *Am J Physiol Endocrinol Metab* **305**, E975-986, doi:10.1152/ajpendo.00615.2012 (2013).

55 Lindqvist, J. *et al.* Cyclin-dependent kinase 5 acts as a critical determinant of AKT-dependent proliferation and regulates differential gene expression by the androgen receptor in prostate cancer cells. *Mol Biol Cell* **26**, 1971-1984, doi:10.1091/mbc.E14-12-1634 (2015).

56 Sharma, M. R., Tuszynski, G. P. & Sharma, M. C. Angiostatin-induced inhibition of endothelial cell proliferation/apoptosis is associated with the down-regulation of cell cycle regulatory protein cdk5. *J Cell Biochem* **91**, 398-409, doi:10.1002/jcb.10762 (2004).

57 Liebl, J. *et al.* Cyclin-dependent kinase 5 regulates endothelial cell migration and angiogenesis. *J Biol Chem* **285**, 35932-35943, doi:10.1074/jbc.M110.126177 (2010).

58 Merk, H. *et al.* Inhibition of endothelial Cdk5 reduces tumor growth by promoting non-productive angiogenesis. *Oncotarget* **7**, 6088-6104, doi:10.18632/oncotarget.6842 (2016).

59 Malumbres, M. & Barbacid, M. To cycle or not to cycle: a critical decision in cancer. *Nat Rev Cancer* **1**, 222-231, doi:10.1038/35106065 (2001).

60 Malumbres, M. & Barbacid, M. Cell cycle, CDKs and cancer: a changing paradigm. *Nat Rev Cancer* **9**, 153-166, doi:10.1038/nrc2602 (2009).

61 Bach, S. *et al.* Roscovitine targets, protein kinases and pyridoxal kinase. *J Biol Chem* **280**, 31208-31219, doi:10.1074/jbc.M500806200 (2005).

62 Weishaupt, J. H. *et al.* Inhibition of CDK5 is protective in necrotic and apoptotic paradigms of neuronal cell death and prevents mitochondrial dysfunction. *Mol Cell Neurosci* **24**, 489-502 (2003).

63 Helal, C. J. *et al.* Potent and cellularly active 4-aminoimidazole inhibitors of cyclin-dependent kinase 5/p25 for the treatment of Alzheimer's disease. *Bioorg Med Chem Lett* **19**, 5703-5707, doi:10.1016/j.bmcl.2009.08.019 (2009).

64 Parry, D. *et al.* Dinaciclib (SCH 727965), a novel and potent cyclin-dependent kinase inhibitor. *Mol Cancer Ther* **9**, 2344-2353, doi:10.1158/1535-7163.MCT-10-0324 (2010).

65 Ran, F. A. *et al.* Genome engineering using the CRISPR-Cas9 system. *Nat Protoc* **8**, 2281-2308, doi:10.1038/nprot.2013.143 (2013).

66 Haeussler, M. *et al.* Evaluation of off-target and on-target scoring algorithms and integration into the guide RNA selection tool CRISPOR. *Genome Biol* **17**, 148, doi:10.1186/s13059-016-1012-2 (2016).

67 Slaymaker, I. M. *et al.* Rationally engineered Cas9 nucleases with improved specificity. *Science* **351**, 84-88, doi:10.1126/science.aad5227 (2016).

68 Laemmli, U. K. Cleavage of structural proteins during the assembly of the head of bacteriophage T4. *Nature* **227**, 680-685 (1970).

69 Kurien, B. T. & Scofield, R. H. Protein blotting: a review. *J Immunol Methods* **274**, 1-15 (2003).

70 Fleige, S. *et al.* Comparison of relative mRNA quantification models and the impact of RNA integrity in quantitative real-time RT-PCR. *Biotechnol Lett* **28**, 1601-1613, doi:10.1007/s10529-006-9127-2 (2006).

71 Berenbaum, M. C. What is synergy? *Pharmacol Rev* **41**, 93-141 (1989).

72 Nicoletti, I., Migliorati, G., Pagliacci, M. C., Grignani, F. & Riccardi, C. A rapid and simple method for measuring thymocyte apoptosis by propidium iodide staining and flow cytometry. *J Immunol Methods* **139**, 271-279 (1991).

73 Remmele, W. & Stegner, H. E. [Recommendation for uniform definition of an immunoreactive score (IRS) for immunohistochemical estrogen receptor detection (ER-ICA) in breast cancer tissue]. *Pathologe* **8**, 138-140 (1987).

74 Weitensteiner, S. B. *et al.* Trisubstituted pyrazolopyrimidines as novel angiogenesis inhibitors. *PLoS One* **8**, e54607, doi:10.1371/journal.pone.0054607 (2013).

75 Foucquier, J. & Guedj, M. Analysis of drug combinations: current methodological landscape. *Pharmacol Res Perspect* **3**, e00149, doi:10.1002/prp2.149 (2015).

76 McDaniel, K. *et al.* Lin28 and let-7: roles and regulation in liver diseases. *Am J Physiol Gastrointest Liver Physiol* **310**, G757-765, doi:10.1152/ajpgi.00080.2016 (2016).

77 Ito, Y. *et al.* Expression and clinical significance of erb-B receptor family in hepatocellular carcinoma. *Br J Cancer* **84**, 1377-1383, doi:10.1054/bjoc.2000.1580 (2001).

78 Blivet-Van Eggelpoel, M. J. *et al.* Epidermal growth factor receptor and HER-3 restrict cell response to sorafenib in hepatocellular carcinoma cells. *J Hepatol* **57**, 108-115, doi:10.1016/j.jhep.2012.02.019 (2012).

79 Firtina Karagonlar, Z., Koc, D., Iscan, E., Erdal, E. & Atabey, N. Elevated hepatocyte growth factor expression as an autocrine c-Met activation mechanism in acquired resistance to sorafenib in hepatocellular carcinoma cells. *Cancer Sci* **107**, 407-416, doi:10.1111/cas.12891 (2016).

80 Tovar, V. *et al.* Tumour initiating cells and IGF/FGF signalling contribute to sorafenib resistance in hepatocellular carcinoma. *Gut* **66**, 530-540, doi:10.1136/gutjnl-2015-309501 (2017).

81 Sigismund, S. *et al.* Endocytosis and signaling: cell logistics shape the eukaryotic cell plan. *Physiol Rev* **92**, 273-366, doi:10.1152/physrev.00005.2011 (2012).

82 Giordano, S. & Columbano, A. Met as a therapeutic target in HCC: facts and hopes. *J Hepatol* **60**, 442-452, doi:10.1016/j.jhep.2013.09.009 (2014).

83 Llovet, J. M. *et al.* Design and endpoints of clinical trials in hepatocellular carcinoma. *J Natl Cancer Inst* **100**, 698-711, doi:10.1093/jnci/djn134 (2008).

84 Hsu, C. H. *et al.* Phase II study of combining sorafenib with metronomic tegafur/uracil for advanced hepatocellular carcinoma. *J Hepatol* **53**, 126-131, doi:10.1016/j.jhep.2010.01.035 (2010).

85 Petrini, I. *et al.* Phase II trial of sorafenib in combination with 5-fluorouracil infusion in advanced hepatocellular carcinoma. *Cancer Chemother Pharmacol* **69**, 773-780, doi:10.1007/s00280-011-1753-2 (2012).

86 Abou-Alfa, G. K. *et al.* Doxorubicin plus sorafenib vs doxorubicin alone in patients with advanced hepatocellular carcinoma: a randomized trial. *JAMA* **304**, 2154-2160, doi:10.1001/jama.2010.1672 (2010).

87 Richly, H. *et al.* Combination of sorafenib and doxorubicin in patients with advanced hepatocellular carcinoma: results from a phase I extension trial. *Eur J Cancer* **45**, 579-587, doi:10.1016/j.ejca.2008.10.039 (2009).

88 Gomez-Martin, C. *et al.* Efficacy and safety of sorafenib in combination with mammalian target of rapamycin inhibitors for recurrent hepatocellular carcinoma after liver transplantation. *Liver Transpl* **18**, 45-52, doi:10.1002/lt.22434 (2012).

89 Finn, R. S. *et al.* Phase I study investigating everolimus combined with sorafenib in patients with advanced hepatocellular carcinoma. *J Hepatol* **59**, 1271-1277, doi:10.1016/j.jhep.2013.07.029 (2013).

90 Cheng, A. L. *et al.* Sunitinib versus sorafenib in advanced hepatocellular cancer: results of a randomized phase III trial. *J Clin Oncol* **31**, 4067-4075, doi:10.1200/JCO.2012.45.8372 (2013).

91 Johnson, P. J. *et al.* Brivanib versus sorafenib as first-line therapy in patients with unresectable, advanced hepatocellular carcinoma: results from the randomized phase III BRISK-FL study. *J Clin Oncol* **31**, 3517-3524, doi:10.1200/JCO.2012.48.4410 (2013).

92 Cainap, C. *et al.* Linifanib versus Sorafenib in patients with advanced hepatocellular carcinoma: results of a randomized phase III trial. *J Clin Oncol* **33**, 172-179, doi:10.1200/JCO.2013.54.3298 (2015).

93 Llovet, J. M. *et al.* Brivanib in patients with advanced hepatocellular carcinoma who were intolerant to sorafenib or for whom sorafenib failed: results from the randomized phase III BRISK-PS study. *J Clin Oncol* **31**, 3509-3516, doi:10.1200/JCO.2012.47.3009 (2013).

94 Zhu, A. X. *et al.* Effect of everolimus on survival in advanced hepatocellular carcinoma after failure of sorafenib: the EVOLVE-1 randomized clinical trial. *JAMA* **312**, 57-67, doi:10.1001/jama.2014.7189 (2014).

95 Zhu, A. X. *et al.* Ramucirumab versus placebo as second-line treatment in patients with advanced hepatocellular carcinoma following first-line therapy with sorafenib (REACH): a randomised, double-blind, multicentre, phase 3 trial. *Lancet Oncol* **16**, 859-870, doi:10.1016/S1470-2045(15)00050-9 (2015).

96 Bruix, J. *et al.* Regorafenib for patients with hepatocellular carcinoma who progressed on sorafenib treatment (RESORCE): a randomised, double-blind, placebo-controlled, phase 3 trial. *Lancet* **389**, 56-66, doi:10.1016/S0140-6736(16)32453-9 (2017).

97 Ikeda, K. *et al.* Phase 2 study of lenvatinib in patients with advanced hepatocellular carcinoma. *J Gastroenterol* **52**, 512-519, doi:10.1007/s00535-016-1263-4 (2017).

98 Kudo, M. *et al.* Lenvatinib versus sorafenib in first-line treatment of patients with unresectable hepatocellular carcinoma: a randomised phase 3 non-inferiority trial. *Lancet*, doi:10.1016/S0140-6736(18)30207-1 (2018).

99 Calderaro, J. *et al.* Programmed death ligand 1 expression in hepatocellular carcinoma: Relationship With clinical and pathological features. *Hepatology* **64**, 2038-2046, doi:10.1002/hep.28710 (2016).

100 El-Khoueiry, A. B. *et al.* Nivolumab in patients with advanced hepatocellular carcinoma (CheckMate 040): an open-label, non-comparative, phase 1/2 dose escalation and expansion trial. *Lancet* **389**, 2492-2502, doi:10.1016/S0140-6736(17)31046-2 (2017).

101 Engelman, J. A. *et al.* MET amplification leads to gefitinib resistance in lung cancer by activating ERBB3 signaling. *Science* **316**, 1039-1043, doi:10.1126/science.1141478 (2007).

102 Gao, J. J., Shi, Z. Y., Xia, J. F., Inagaki, Y. & Tang, W. Sorafenib-based combined molecule targeting in treatment of hepatocellular carcinoma. *World J Gastroenterol* **21**, 12059-12070, doi:10.3748/wjg.v21.i42.12059 (2015).

103 Huynh, H. *et al.* AZD6244 enhances the anti-tumor activity of sorafenib in ectopic and orthotopic models of human hepatocellular carcinoma (HCC). *J Hepatol* **52**, 79-87, doi:10.1016/j.jhep.2009.10.008 (2010).

104 Schmieder, R. *et al.* Allosteric MEK1/2 inhibitor refametinib (BAY 86-9766) in combination with sorafenib exhibits antitumor activity in preclinical murine and rat models of hepatocellular carcinoma. *Neoplasia* **15**, 1161-1171 (2013).

105 Lim, H. Y. *et al.* A phase II study of the efficacy and safety of the combination therapy of the MEK inhibitor refametinib (BAY 86-9766) plus sorafenib for Asian patients with unresectable hepatocellular carcinoma. *Clin Cancer Res* **20**, 5976-5985, doi:10.1158/1078-0432.CCR-13-3445 (2014).

106 Rudalska, R. *et al.* In vivo RNAi screening identifies a mechanism of sorafenib resistance in liver cancer. *Nat Med* **20**, 1138-1146, doi:10.1038/nm.3679 (2014).

107 Villanueva, A. *et al.* Pivotal role of mTOR signaling in hepatocellular carcinoma. *Gastroenterology* **135**, 1972-1983, 1983 e1971-1911, doi:10.1053/j.gastro.2008.08.008 (2008).

108 Zhu, A. X. *et al.* Phase 1/2 study of everolimus in advanced hepatocellular carcinoma. *Cancer* **117**, 5094-5102, doi:10.1002/cncr.26165 (2011).

109 Koeberle, D. *et al.* Sorafenib with or without everolimus in patients with advanced hepatocellular carcinoma (HCC): a randomized multicenter, multinational phase II trial (SAKK 77/08 and SASL 29). *Ann Oncol* **27**, 856-861, doi:10.1093/annonc/mdw054 (2016).

110 Berasain, C. & Avila, M. A. The EGFR signalling system in the liver: from hepatoprotection to hepatocarcinogenesis. *J Gastroenterol* **49**, 9-23, doi:10.1007/s00535-013-0907-x (2014).

111 Carracedo, A. *et al.* Inhibition of mTORC1 leads to MAPK pathway activation through a PI3K-dependent feedback loop in human cancer. *J Clin Invest* **118**, 3065-3074, doi:10.1172/JCI34739 (2008).

112 Gedaly, R. *et al.* PI-103 and sorafenib inhibit hepatocellular carcinoma cell proliferation by blocking Ras/Raf/MAPK and PI3K/AKT/mTOR pathways. *Anticancer Res* **30**, 4951-4958 (2010).

113 Masuda, M. *et al.* Alternative mammalian target of rapamycin (mTOR) signal activation in sorafenib-resistant hepatocellular carcinoma cells revealed by array-based pathway profiling. *Mol Cell Proteomics* **13**, 1429-1438, doi:10.1074/mcp.M113.033845 (2014).

114 Rose, A. *et al.* Stimulatory effects of the multi-kinase inhibitor sorafenib on human bladder cancer cells. *Br J Pharmacol* **160**, 1690-1698, doi:10.1111/j.1476-5381.2010.00838.x (2010).

115 Wang, H. *et al.* Activation of phosphatidylinositol 3-kinase/Akt signaling mediates sorafenib-induced invasion and metastasis in hepatocellular carcinoma. *Oncol Rep* **32**, 1465-1472, doi:10.3892/or.2014.3352 (2014).

116 de Larco, J. E. & Todaro, G. J. Epithelioid and fibroblastic rat kidney cell clones: epidermal growth factor (EGF) receptors and the effect of mouse sarcoma virus transformation. *J Cell Physiol* **94**, 335-342, doi:10.1002/jcp.1040940311 (1978).

117 Yarden, Y. & Sliwkowski, M. X. Untangling the ErbB signalling network. *Nat Rev Mol Cell Biol* **2**, 127-137, doi:10.1038/35052073 (2001).

118 Yewale, C., Baradia, D., Vhora, I., Patil, S. & Misra, A. Epidermal growth factor receptor targeting in cancer: a review of trends and strategies. *Biomaterials* **34**, 8690-8707, doi:10.1016/j.biomaterials.2013.07.100 (2013).

119 Kira, S. *et al.* Expression of transforming growth factor alpha and epidermal growth factor receptor in human hepatocellular carcinoma. *Liver* **17**, 177-182 (1997).

120 Daveau, M. *et al.* Hepatocyte growth factor, transforming growth factor alpha, and their receptors as combined markers of prognosis in hepatocellular carcinoma. *Mol Carcinog* **36**, 130-141, doi:10.1002/mc.10103 (2003).

121 Komposch, K. & Sibilia, M. EGFR Signaling in Liver Diseases. *Int J Mol Sci* **17**, doi:10.3390/ijms17010030 (2015).

122 Huether, A., Hopfner, M., Baradari, V., Schuppan, D. & Scherubl, H. EGFR blockade by cetuximab alone or as combination therapy for growth control of hepatocellular cancer. *Biochem Pharmacol* **70**, 1568-1578, doi:10.1016/j.bcp.2005.09.007 (2005).

123 Huether, A., Hopfner, M., Sutter, A. P., Schuppan, D. & Scherubl, H. Erlotinib induces cell cycle arrest and apoptosis in hepatocellular cancer cells and enhances chemosensitivity towards cytostatics. *J Hepatol* **43**, 661-669, doi:10.1016/j.jhep.2005.02.040 (2005).

124 Okano, J., Matsumoto, K., Nagahara, T. & Murawaki, Y. Gefitinib and the modulation of the signaling pathways downstream of epidermal growth factor receptor in human liver cancer cells. *J Gastroenterol* **41**, 166-176, doi:10.1007/s00535-005-1736-3 (2006).

125 Huether, A. *et al.* Signaling pathways involved in the inhibition of epidermal growth factor receptor by erlotinib in hepatocellular cancer. *World J Gastroenterol* **12**, 5160-5167 (2006).

126 Fuchs, B. C. *et al.* Epidermal growth factor receptor inhibition attenuates liver fibrosis and development of hepatocellular carcinoma. *Hepatology* **59**, 1577-1590, doi:10.1002/hep.26898 (2014).

127 Matsuo, M., Sakurai, H. & Saiki, I. ZD1839, a selective epidermal growth factor receptor tyrosine kinase inhibitor, shows antimetastatic activity using a hepatocellular carcinoma model. *Mol Cancer Ther* **2**, 557-561 (2003).

128 Zhu, B. D. *et al.* Antitumor effect of Gefitinib, an epidermal growth factor receptor tyrosine kinase inhibitor, combined with cytotoxic agent on murine hepatocellular carcinoma. *World J Gastroenterol* **11**, 1382-1386 (2005).

129 Baselga, J. & Arteaga, C. L. Critical update and emerging trends in epidermal growth factor receptor targeting in cancer. *J Clin Oncol* **23**, 2445-2459, doi:10.1200/JCO.2005.11.890 (2005).

130 Marshall, J. Clinical implications of the mechanism of epidermal growth factor receptor inhibitors. *Cancer* **107**, 1207-1218, doi:10.1002/cncr.22133 (2006).

131 Ramanathan, R. K. *et al.* A phase II study of lapatinib in patients with advanced biliary tree and hepatocellular cancer. *Cancer Chemother Pharmacol* **64**, 777-783, doi:10.1007/s00280-009-0927-7 (2009).

132 Llovet, J. M. & Bruix, J. Molecular targeted therapies in hepatocellular carcinoma. *Hepatology* **48**, 1312-1327, doi:10.1002/hep.22506 (2008).

133 Thomas, M. B. *et al.* Phase 2 study of erlotinib in patients with unresectable hepatocellular carcinoma. *Cancer* **110**, 1059-1067, doi:10.1002/cncr.22886 (2007).

134 Zhu, A. X. *et al.* Phase 2 study of cetuximab in patients with advanced hepatocellular carcinoma. *Cancer* **110**, 581-589, doi:10.1002/cncr.22829 (2007).

135 Asnacios, A. *et al.* Gemcitabine plus oxaliplatin (GEMOX) combined with cetuximab in patients with progressive advanced stage hepatocellular carcinoma: results of a multicenter phase 2 study. *Cancer* **112**, 2733-2739, doi:10.1002/cncr.23489 (2008).

136 Hsu, C. H. *et al.* Bevacizumab with erlotinib as first-line therapy in Asian patients with advanced hepatocellular carcinoma: a multicenter phase II study. *Oncology* **85**, 44-52, doi:10.1159/000350841 (2013).

137 Zhu, A. X. *et al.* SEARCH: a phase III, randomized, double-blind, placebo-controlled trial of sorafenib plus erlotinib in patients with advanced hepatocellular carcinoma. *J Clin Oncol* **33**, 559-566, doi:10.1200/JCO.2013.53.7746 (2015).

138 Sakata, H. *et al.* Hepatocyte growth factor/scatter factor overexpression induces growth, abnormal development, and tumor formation in transgenic mouse livers. *Cell Growth Differ* **7**, 1513-1523 (1996).

139 Wang, R., Ferrell, L. D., Faouzi, S., Maher, J. J. & Bishop, J. M. Activation of the Met receptor by cell attachment induces and sustains hepatocellular carcinomas in transgenic mice. *J Cell Biol* **153**, 1023-1034 (2001).

140 Jo, M. *et al.* Cross-talk between epidermal growth factor receptor and c-Met signal pathways in transformed cells. *J Biol Chem* **275**, 8806-8811 (2000).

141 Desbois-Mouthon, C. *et al.* Insulin-like growth factor-1 receptor inhibition induces a resistance mechanism via the epidermal growth factor receptor/HER3/AKT signaling pathway: rational basis for cotargeting insulin-like growth factor-1 receptor and epidermal growth factor receptor in hepatocellular carcinoma. *Clin Cancer Res* **15**, 5445-5456, doi:10.1158/1078-0432.CCR-08-2980 (2009).

142 Desbois-Mouthon, C. *et al.* Impact of IGF-1R/EGFR cross-talks on hepatoma cell sensitivity to gefitinib. *Int J Cancer* **119**, 2557-2566, doi:10.1002/ijc.22221 (2006).

143 Lanzetti, L. & Di Fiore, P. P. Endocytosis and cancer: an 'insider' network with dangerous liaisons. *Traffic* **9**, 2011-2021, doi:10.1111/j.1600-0854.2008.00816.x (2008).

144 Rink, J., Ghigo, E., Kalaidzidis, Y. & Zerial, M. Rab conversion as a mechanism of progression from early to late endosomes. *Cell* **122**, 735-749, doi:10.1016/j.cell.2005.06.043 (2005).

145 Stenmark, H. Rab GTPases as coordinators of vesicle traffic. *Nat Rev Mol Cell Biol* **10**, 513-525, doi:10.1038/nrm2728 (2009).

146 Porther, N. & Barbieri, M. A. The role of endocytic Rab GTPases in regulation of growth factor signaling and the migration and invasion of tumor cells. *Small GTPases* **6**, 135-144, doi:10.1080/21541248.2015.1050152 (2015).

147 Mellman, I. & Yarden, Y. Endocytosis and cancer. *Cold Spring Harb Perspect Biol* **5**, a016949, doi:10.1101/cshperspect.a016949 (2013).

148 Mosesson, Y., Mills, G. B. & Yarden, Y. Derailed endocytosis: an emerging feature of cancer. *Nat Rev Cancer* **8**, 835-850, doi:10.1038/nrc2521 (2008).

149 Ebner, R. & Derynck, R. Epidermal growth factor and transforming growth factor-alpha: differential intracellular routing and processing of ligand-receptor complexes. *Cell Regul* **2**, 599-612 (1991).

150 Huangfu, W. C. & Fuchs, S. Y. Ubiquitination-dependent regulation of signaling receptors in cancer. *Genes Cancer* **1**, 725-734, doi:10.1177/1947601910382901 (2010).

151 Grandal, M. V. *et al.* EGFRvIII escapes down-regulation due to impaired internalization and sorting to lysosomes. *Carcinogenesis* **28**, 1408-1417, doi:10.1093/carcin/bgm058 (2007).

152 Katzmann, D. J., Odorizzi, G. & Emr, S. D. Receptor downregulation and multivesicular-body sorting. *Nat Rev Mol Cell Biol* **3**, 893-905, doi:10.1038/nrm973 (2002).

153 Doyotte, A., Russell, M. R., Hopkins, C. R. & Woodman, P. G. Depletion of TSG101 forms a mammalian "Class E" compartment: a multicisternal early endosome with multiple sorting defects. *J Cell Sci* **118**, 3003-3017, doi:10.1242/jcs.02421 (2005).

154 Bache, K. G. *et al.* The ESCRT-III subunit hVps24 is required for degradation but not silencing of the epidermal growth factor receptor. *Mol Biol Cell* **17**, 2513-2523, doi:10.1091/mbc.E05-10-0915 (2006).

155 Paul, N. R., Jacquemet, G. & Caswell, P. T. Endocytic Trafficking of Integrins in Cell Migration. *Curr Biol* **25**, R1092-1105, doi:10.1016/j.cub.2015.09.049 (2015).

156 Seguin, L., Desgrosellier, J. S., Weis, S. M. & Cheresh, D. A. Integrins and cancer: regulators of cancer stemness, metastasis, and drug resistance. *Trends Cell Biol* **25**, 234-240, doi:10.1016/j.tcb.2014.12.006 (2015).

157 Corallino, S., Malabarba, M. G., Zobel, M., Di Fiore, P. P. & Scita, G. Epithelial-to-Mesenchymal Plasticity Harnesses Endocytic Circuitries. *Front Oncol* **5**, 45, doi:10.3389/fonc.2015.00045 (2015).

158 Wiedmann, R. M. *et al.* The V-ATPase-inhibitor archazolid abrogates tumor metastasis via inhibition of endocytic activation of the Rho-GTPase Rac1. *Cancer Res* **72**, 5976-5987, doi:10.1158/0008-5472.CAN-12-1772 (2012).

159 Schneider, L. S. *et al.* Vacuolar-ATPase Inhibition Blocks Iron Metabolism to Mediate Therapeutic Effects in Breast Cancer. *Cancer Res* **75**, 2863-2874, doi:10.1158/0008-5472.CAN-14-2097 (2015).

160 Merk, H. *et al.* Inhibition of the V-ATPase by Archazolid A: A New Strategy to Inhibit EMT. *Mol Cancer Ther* **16**, 2329-2339, doi:10.1158/1535-7163.MCT-17-0129 (2017).

161 Tan, T. C. *et al.* Cdk5 is essential for synaptic vesicle endocytosis. *Nat Cell Biol* **5**, 701-710, doi:10.1038/ncb1020 (2003).

162 Tomizawa, K. *et al.* Cophosphorylation of amphiphysin I and dynamin I by Cdk5 regulates clathrin-mediated endocytosis of synaptic vesicles. *J Cell Biol* **163**, 813-824, doi:10.1083/jcb.200308110 (2003).

163 Kawauchi, T. Cdk5 regulates multiple cellular events in neural development, function and disease. *Dev Growth Differ* **56**, 335-348, doi:10.1111/dgd.12138 (2014).

164 Furusawa, K. *et al.* Cdk5 Regulation of the GRAB-Mediated Rab8-Rab11 Cascade in Axon Outgrowth. *J Neurosci* **37**, 790-806, doi:10.1523/JNEUROSCI.2197-16.2016 (2017).

165 Finn, R. S. *et al.* Palbociclib and Letrozole in Advanced Breast Cancer. *N Engl J Med* **375**, 1925-1936, doi:10.1056/NEJMoa1607303 (2016).

166 Hortobagyi, G. N. *et al.* Ribociclib as First-Line Therapy for HR-Positive, Advanced Breast Cancer. *N Engl J Med* **375**, 1738-1748, doi:10.1056/NEJMoa1609709 (2016).

167 Goetz, M. P. *et al.* MONARCH 3: Abemaciclib As Initial Therapy for Advanced Breast Cancer. *J Clin Oncol* **35**, 3638-3646, doi:10.1200/JCO.2017.75.6155 (2017).

168 Bollard, J. *et al.* Palbociclib (PD-0332991), a selective CDK4/6 inhibitor, restricts tumour growth in preclinical models of hepatocellular carcinoma. *Gut* **66**, 1286-1296, doi:10.1136/gutjnl-2016-312268 (2017).

169 Contreras-Vallejos, E., Utreras, E. & Gonzalez-Billault, C. Going out of the brain: non-nervous system physiological and pathological functions of Cdk5. *Cell Signal* **24**, 44-52, doi:10.1016/j.cellsig.2011.08.022 (2012).

170 Shupp, A., Casimiro, M. C. & Pestell, R. G. Biological functions of CDK5 and potential CDK5 targeted clinical treatments. *Oncotarget* **8**, 17373-17382, doi:10.18632/oncotarget.14538 (2017).

171 Seftel, M. D. *et al.* The CDK inhibitor AT7519M in patients with relapsed or refractory chronic lymphocytic leukemia (CLL) and mantle cell lymphoma. A Phase II study of the Canadian Cancer Trials Group. *Leuk Lymphoma* **58**, 1358-1365, doi:10.1080/10428194.2016.1239259 (2017).

172 Ghia, P. *et al.* Efficacy and safety of dinaciclib vs ofatumumab in patients with relapsed/refractory chronic lymphocytic leukemia. *Blood* **129**, 1876-1878, doi:10.1182/blood-2016-10-748210 (2017).

173 Kumar, S. K. *et al.* Dinaciclib, a novel CDK inhibitor, demonstrates encouraging single-agent activity in patients with relapsed multiple myeloma. *Blood* **125**, 443-448, doi:10.1182/blood-2014-05-573741 (2015).

APPENDIX

6 APPENDIX

6.1 Supplementary Figures

a

Protein names	Gene names	x-fold change	t-test p-value
DNA dC->dU-editing enzyme APOBEC-3G	APOBEC3G	0.36	0.00263
Lymphokine-activated killer T-cell-originated protein kinase	PBK	0.51	0.00295
F-box only protein 2	FBXO2	0.55	2.01E-06
Hypoxanthine-guanine phosphoribosyltransferase	HPRT1	0.55	2.26E-05
Epiplakin	EPPK1	0.57	1.91E-06
Core histone macro-H2A.1;Histone H2A	H2AFY	0.58	1.97E-09
Bifunctional ATP-dependent dihydroxyacetone kinase/FAD-AMP lyase (cyclizing)	DAK	0.59	0.00665
Importin subunit alpha	KPNA2	0.59	7.62E-05
Protein lin-28 homolog B	LIN28B	0.59	8.00E-07
DNA topoisomerase 2-alpha	TOP2A	0.60	3.41E-06
Alpha-fetoprotein	AFP	0.61	0.00639
Carbonic anhydrase 2	CA2	0.61	1.24E-05
Aflatoxin B1 aldehyde reductase member 2	AKR7A2	0.62	0.00023
Vacuolar protein sorting-associated protein VTA1 homolog	VTA1	0.63	7.07E-08
Exportin-7	XPO7	0.63	2.11E-05
14-3-3 protein sigma	SFN	0.64	0.02276
Pyrroline-5-carboxylate reductase 1. mitochondrial	PYCR1	0.64	5.71E-05
Glycine dehydrogenase [decarboxylating]. mitochondrial	GLDC	0.64	7.68E-07
Prolyl 4-hydroxylase subunit alpha-1	P4HA1	0.65	0.00070
ADP-ribosylation factor 5	ARF5	0.65	0.00062
Epidermal growth factor receptor	EGFR	1.44	2.95E-05
Protein FAM151A	FAM151A	1.52	0.00627
Fibronectin	FN1	1.52	0.00335
Ectonucleoside triphosphate diphosphohydrolase 5	ENTPD5	1.53	9.08E-05
Serotransferrin	TF	1.54	0.00154
Fatty acid-binding protein. epidermal	FABP5	1.55	7.90E-05
Glucose-6-phosphate 1-dehydrogenase	G6PD	1.56	1.59E-07
Bile salt sulfotransferase	SULT2A1	1.59	0.00454
Syntenin-1	SDCBP	1.60	0.01119
Myc box-dependent-interacting protein 1	BIN1	1.65	2.07E-08
Peroxisomal multifunctional enzyme type 2	HSD17B4	1.66	0.00117
NAD(P)H dehydrogenase [quinone] 1	NQO1	1.68	0.00026
Vimentin	VIM	1.70	0.00085
Scavenger receptor class B member 1	SCARB1	1.70	0.00059
Amyloid beta A4 protein	APP	1.71	0.00840
Multidrug resistance protein 1	ABCB1	1.71	0.00011
Angiotensinogen	AGT	1.73	0.00424
Protein S100-P	S100P	1.75	0.00131
Claudin-6	CLDN6	1.77	0.03187
Reticulocalbin-1	RCN1	1.80	0.00014
Epoxide hydrolase 1	EPHX1	1.97	0.00036
Aminopeptidase N	ANPEP	1.99	2.82E-10
Galectin-3	LGALS3	2.04	1.67E-05
Calcium-regulated heat stable protein 1	CARHSP1	2.33	6.35E-07
Ferritin;Ferritin light chain	FTL	2.35	0.02201
Sequestosome-1	SQSTM1	2.46	4.46E-05
Ferritin;Ferritin heavy chain	FTH1	2.49	0.03318
Aldo-keto reductase family 1 member C2	AKR1C2	2.62	0.00323
Clathrin interactor 1	CLINT1	3.20	0.00018

b

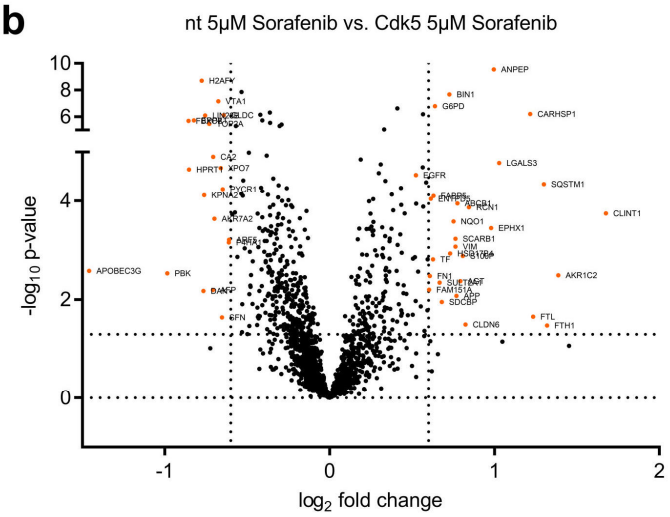

c

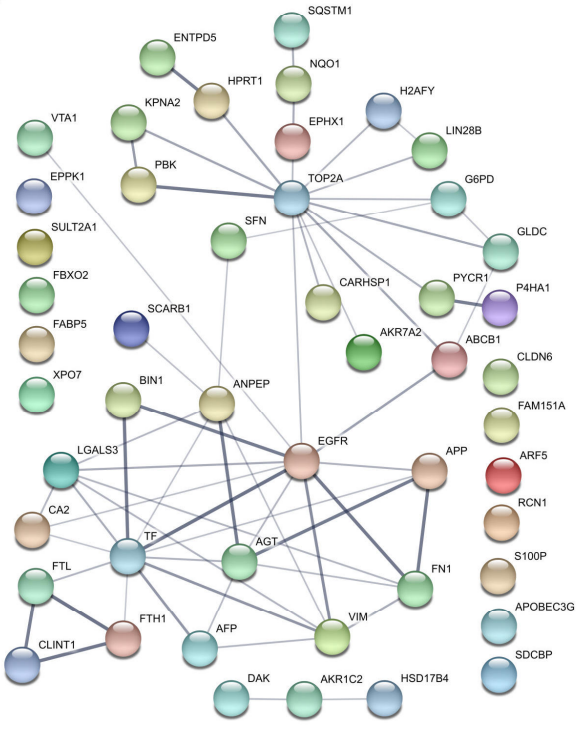

Supplementary Figure 1 - Proteomic analysis of Cdk5 knockdown cells treated with Sorafenib. **(**a) Table of proteins showing alterations of protein abundance (*P*-value < 0.05; log2-fold change > |0.6|) between nt and Cdk5 shRNA cells treated with Sorafenib together with their respective gene names, x-fold changes (nt 5 µM Sorafenib vs. Cdk5 5 µM Sorafenib) and *P*-values. (**b**) Volcano Plot visualizing the protein hits given in **a** is shown. (**c**) Protein interaction map of protein hits given in **a** created with string-db.org. (protein-protein interaction enrichment *P*-value: $1.57*10^{-6}$).

a

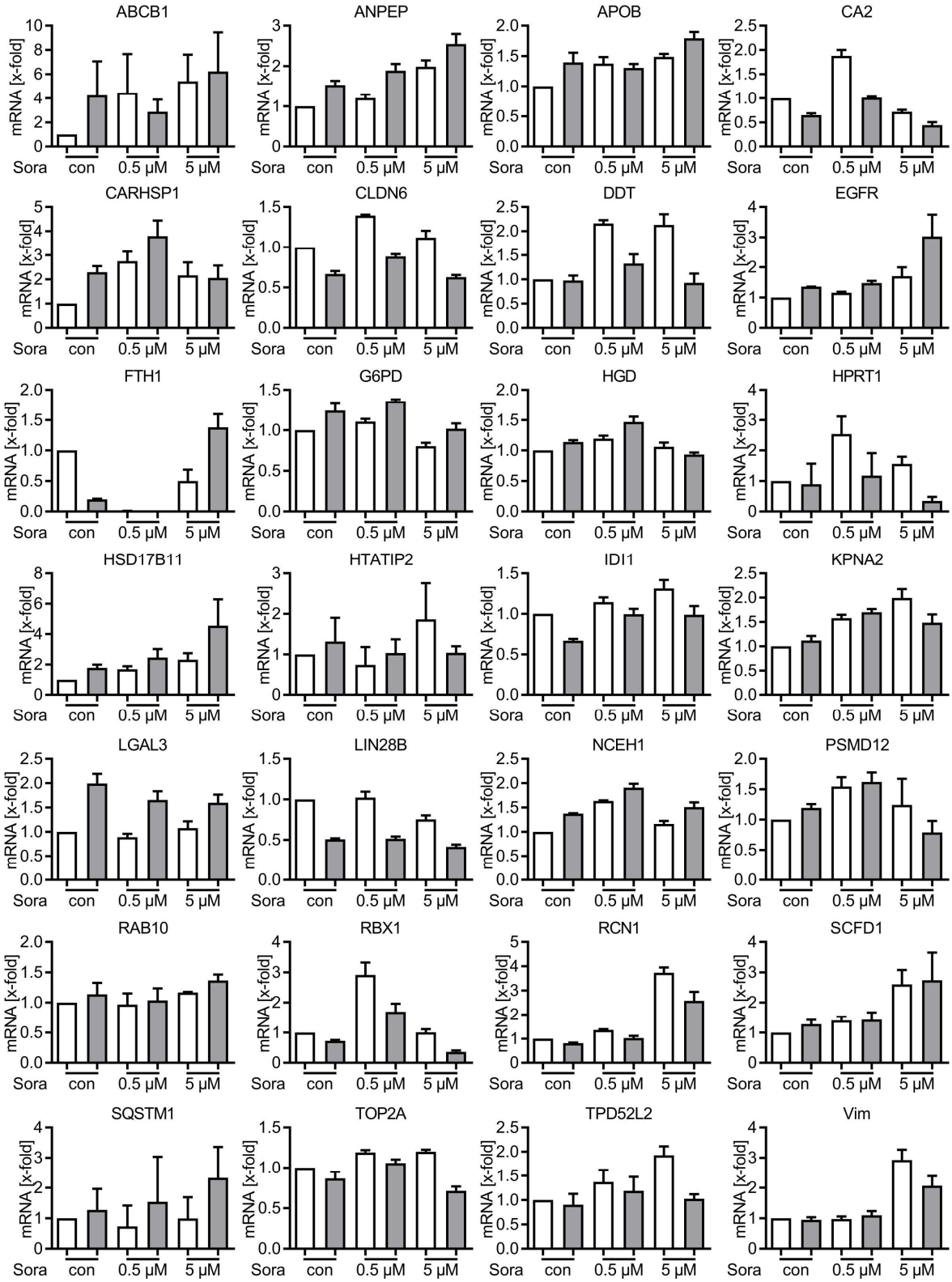
ABCB1
ANPEP
APOB
CA2
CARHSP1
CLDN6
DDT
EGFR
FTH1
G6PD
HGD
HPRT1
HSD17B11
HTATIP2
IDI1
KPNA2
LGAL3
LIN28B
NCEH1
PSMD12
RAB10
RBX1
RCN1
SCFD1
SQSTM1
TOP2A
TPD52L2
Vim
mRNA [x-fold]
Sora
con
0.5 µM
5 µM

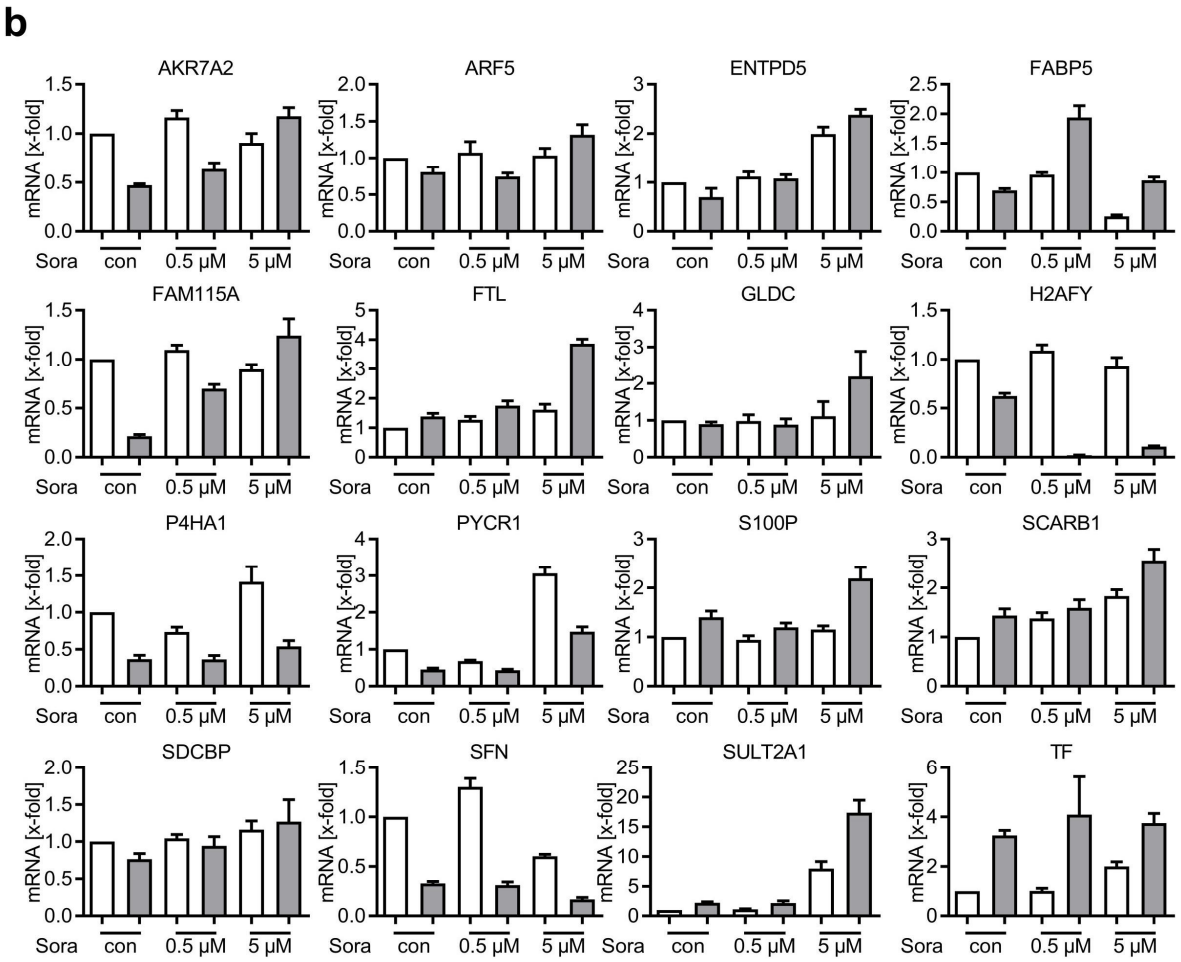

Supplementary Figure 2 - qPCR analysis of targets from the proteomics screen. mRNA expression of selected proteins yielded from the proteomic analysis of untreated (**a**) or Sorafenib treated (**b**) nt (white bars) and Cdk5 (grey bars) shRNA HUH7 cells.

6.2 Supplementary Table

Supplementary Table 1 - Correlation of EGFR staining with clinical parameters. Contingency tables correlating percentage of EGFR positive cells, EGFR staining intensity and EGFR IRS with r-classification (R0: no residual tumor, R1: residual tumor, X: N/A) (**a**), frequency of recurrence (0: no tumor recurrence, 1: tumor recurrence) (**b**), cause of death (**c**), tumor stage (**d**) and tumor grading (**e**) are shown.

a

R-classification					
		frequency	percentage	valid percentage	cumulated percentage
valid	R0	54	85.7	85.7	85.7
	R1	5	7.9	7.9	93.7
	X	4	6.3	6.3	100
	total	63	100	100	

R-classification * EGFR percentage of positive cells - contingency table								
number								
		EGFR percentage of positive cells						total
		negative	< 10%	11-50%	51-80%	> 80%	missing	
R-classification	R0	17	2	4	5	23	3	54
	R1	2	0	0	0	3	0	5
	X	1	0	1	0	2	0	4
total		20	2	5	5	28	3	63

chi-squared test			
	value	df	Asymptotic significance (two-sided)
Chi-squared (Pearson)	4.058[a]	10	0.945
Likelihood-Quotient	5.302	10	0.87
Number of valid cases	63		
a. 16 cells (88.9%) have an expected frequency of 5 or less. The smallest expected frequency is 0.13.			

R-classification * EGFR staining intensity – contingency table							
number							
		EGFR staining intensity					total
		0	weak	intermediate	strong	missing	
R-classification	R0	17	11	13	10	3	54
	R1	2	1	0	2	0	5
	X	1	1	0	2	0	4
total		20	13	13	14	3	63

chi-squared test			
	value	df	Asymptotic significance (two-sided)
Chi-squared (Pearson)	5.306[a]	8	0.724
Likelihood-Quotient	7.081	8	0.528
Number of valid cases	63		
a. 11 cells (88.9%) have an expected frequency of 5 or less. The smallest expected frequency is 0.19.			

r-classification * EGFR IRS – contingency table											
number											
		EGFR – IRS									total
		0	1	2	4	5	6	8	9	12	
R-calssification	R0	17	1	4	8	3	3	9	2	7	54
	R1	2	0	0	1	0	0	0	0	2	5
	X	1	0	1	0	0	0	0	0	2	4
total		20	1	5	9	3	3	9	2	11	63

chi-squared test			
	value	df	Asymptotic significance (two-sided)
Chi-squared (Pearson)	10.252[a]	16	0.853
Likelihood-Quotient	12.064	16	0.74
Number of valid cases	63		
a. 23 cells (85.2%) have an expected frequency of 5 or less. The smallest expected frequency is 0.06.			

b

Frequency of recurrence					
		frequency	percentage	valid percentage	cumulated percentage
valid	0	40	63.5	63.5	63.5
	1	17	27	27	90.5
	n.s.	6	9.5	9.5	100
	total	63	100	100	

Frequency of recurrance * EGFR percentage of positive cells - contingency table								
number								
		EGFR percentage of positive cells						total
		negative	< 10%	11-50%	51-80%	> 80%	missing	
frequency of recurrance	0	12	2	5	4	16	1	40
	1	7	0	0	1	8	1	17
	n.s.	1	0	0	0	4	1	6
total		20	2	5	5	28	3	63

chi-squared test			
	value	df	Asymptotic significance (two-sided)
Chi-squared (Pearson)	8.881[a]	10	0.543
Likelihood-Quotient	11.031	10	0.355
Number of valid cases	63		
a. 14 cells (77.8%) have an expected frequency of 5 or less. The smallest expected frequency is 0.19.			

Frequency of recurrence * EGFR staining intensity – contingency table							
number							
		EGFR staining intensity					total
		0	weak	intermediate	strong	missing	
frequency of recurrence	0	12	9	11	7	1	40
	1	7	4	1	4	1	17
	n.s.	1	0	1	3	1	6
total		20	13	13	14	3	63

chi-squared test			
	value	df	Asymptotic significance (two-sided)
Chi-squared (Pearson)	9.829[a]	8	0.277
Likelihood-Quotient	10.602	8	0.225
Number of valid cases	63		
a. 10 cells (66.7%) have an expected frequency of 5 or less. The smallest expected frequency is 0.29.			

Frequency of recurrence * EGFR IRS – contingency table											
number											
		EGFR – IRS									total
		0	1	2	4	5	6	8	9	12	
frequency of recurrance	0	12	1	5	5	1	2	8	2	4	40
	1	7	0	0	4	1	1	0	0	4	17
	n.s.	1	0	0	0	1	0	1	0	3	6
total		20	1	5	9	3	3	9	2	11	63

chi-squared test			
	value	df	Asymptotic significance (two-sided)
Chi-squared (Pearson)	18.742[a]	16	0.282
Likelihood-Quotient	23.109	16	0.111
Number of valid cases	63		
a. 22 cells (81.5%) have an expected frequency of 5 or less. The smallest expected frequency is 0.10.			

c

cause of death					
		frequency	percentage	valid percentage	cumulated percentage
valid	not determined	42	66.7	66.7	66.7
	tumor unrelated	2	3.2	3.2	69.8
	tumor related	14	22.2	22.2	92.1
	n.s.	5	7.9	7.9	100
	total	63	100	100	

cause of death * EGFR percentage of positive cells - contingency table								
number								
		EGFR percentage of positive cells						total
		negative	<10%	11-50%	51-80%	> 80%	missing	
cause of death	not determined	11	1	4	5	19	2	42
	tumor unrelated	1	0	0	0	1	0	2
	tumor related	7	1	1	0	4	1	14
	n.s.	1	0	0	0	4	0	5
total		20	2	5	5	28	3	63

chi-squared test			
	value	df	Asymptotic significance (two-sided)
Chi-squared (Pearson)	9.241[a]	15	0.865
Likelihood-Quotient	11.348	15	0.728
Number of valid cases	63		
a. 21 cells (87.5%) have an expected frequency of 5 or less. The smallest expected frequency is 0.06.			

cause of death * EGFR staining intensity – contingency table							
number							
		EGFR staining intensity					total
		0	weak	intermediate	strong	missing	
cause of death	not determined	11	11	10	8	2	42
	tumor unrelated	1	0	0	1	0	2
	tumor related	7	2	2	2	1	14
	n.s.	1	0	1	3	0	5
total		20	13	13	14	3	63

chi-squared test			
	value	df	Asymptotic significance (two-sided)
Chi-squared (Pearson)	10.536[a]	12	0.569
Likelihood-Quotient	11.373	12	0.497
Number of valid cases	63		
a. 16 cells (80.0%) have an expected frequency of 5 or less. The smallest expected frequency is 0.1.			

cause of death * EGFR IRS – contingency table											
number											
		EGFR – IRS									total
		0	1	2	4	5	6	8	9	12	
cause of death	not determined	11	1	3	8	2	3	7	2	5	42
	tumor unrelated	1	0	0	0	0	0	0	0	1	2
	tumor related	7	0	2	1	1	0	1	0	2	14
	n.s.	1	0	0	0	0	0	1	0	3	5
total		20	1	5	9	3	3	9	2	11	63

chi-squared test			
	value	df	Asymptotic significance (two-sided)
Chi-squared (Pearson)	17.557[a]	24	0.824
Likelihood-Quotient	19.047	24	0.749
Number of valid cases	63		
a. 32 cells (88.9%) have an expected frequency of 5 or less. The smallest expected frequency is 0.03.			

d

tumor score					
		frequency	percentage	valid percentage	cumulated percentage
valid	1	27	42.9	42.9	42.9
	2	17	27.0	27.0	69.8
	2a	2	3.2	3.2	73.0
	2b	2	3.2	3.2	76.2
	3	1	1.6	1.6	77.8
	3a	6	9.5	9.5	87.3
	3b	1	1.6	1.6	88.9
	4	1	1.6	1.6	90.5
	X	6	9.5	9.5	100.0
	total	63	100	100.0	

tumor score * EGFR percentage of positive cells - contingency table								
number								
		EGFR percentage of positive cells						total
		negative	< 10%	11-50%	51-80%	> 80%	missing	
valid	1	10	1	1	2	12	1	27
	2	5	1	3	1	6	1	17
	2a	0	0	0	1	1	0	2
	2b	1	0	0	1	0	0	2
	3	0	0	0	0	0	1	1
	3a	1	0	0	0	5	0	6
	3b	1	0	0	0	0	0	1
	4	0	0	0	0	1	0	1
	X	2	0	1	0	3	0	6
	total	20	2	5	5	28	3	63

chi-squared test			
	value	df	Asymptotic significance (two-sided)
Chi-squared (Pearson)	44.017[a]	40	0.305
Likelihood-Quotient	29.305	40	0.894
Number of valid cases	63		
a. 50 cells (92.6%) have an expected frequency of 5 or less. The smallest expected frequency is 0.03.			

tumor score * EGFR staining intensity – contingency table							
number							
		EGFR staining intensity					total
		0	weak	intermediate	strong	missing	
valid	1	10	5	5	6	1	27
	2	5	3	6	2	1	17
	2a	0	0	1	1	0	2
	2b	1	0	1	0	0	2
	3	0	0	0	0	1	1
	3a	1	3	0	2	0	6
	3b	1	0	0	0	0	1
	4	0	0	0	1	0	1
	X	2	2	0	2	0	6
	total	20	13	13	14	3	63

chi-squared test			
	value	df	Asymptotic significance (two-sided)
Chi-squared (Pearson)	40.619[a]	32	0.141
Likelihood-Quotient	29.875	32	0.575
Number of valid cases	63		
a. 40 cells (88.9%) have an expected frequency of 5 or less. The smallest expected frequency is 0.05.			

tumor score * EGFR IRS – contingency table											
number											
		EGFR – IRS									total
		0	1	2	4	5	6	8	9	12	
valid	1	10	1	1	3	1	0	5	2	4	27
	2	5	0	3	2	1	1	3	0	2	17
	2a	0	0	0	0	0	1	0	0	1	2
	2b	1	0	0	0	0	1	0	0	0	2
	3	0	0	0	0	1	0	0	0	0	1
	3a	1	0	0	3	0	0	1	0	1	6
	3b	1	0	0	0	0	0	0	0	0	1
	4	0	0	0	0	0	0	0	0	1	1
	X	2	0	1	1	0	0	0	0	2	6
	total	20	1	5	9	3	3	9	2	11	63

chi-squared test			
	value	df	Asymptotic significance (two-sided)
Chi-squared (Pearson)	67.241[a]	64	0.367
Likelihood-Quotient	45.01	64	0.966
Number of valid cases	63		
a. 79 cells (97.5 %) have an expected frequency of 5 or less. The smallest expected frequency is 0.02.			

e

tumor grading					
		frequency	percentage	valid percentage	cumulated percentage
valid	no grading or missing	6	9.5	9.5	9.5
	Well-differentiated	11	17.5	17.5	27.0
	moderatly-differentiated	29	46.0	46.0	73.0
	poorly-differentiated	17	27.0	27.0	100.0
	total	63	100	100	

tumor grading * EGFR percentage of positive cells - contingency table								
number								
		EGFR percentage of positive cells						total
		negative	<10%	11-50%	51-80%	> 80%	missing	
valid	no grading or missing	1	1	1	0	3	0	6
	Well-differentiated	2	0	1	2	6	0	11
	moderatly-differentiated	10	1	3	2	12	1	29
	poorly-differentiated	7	0	0	1	7	2	17
	total	20	2	5	5	28	3	63

chi-squared test			
	value	df	Asymptotic significance (two-sided)
Chi-squared (Pearson)	13.227[a]	15	0.585
Likelihood-Quotient	14.112	15	0.517
Number of valid cases	63		
a. 20 cells (83.3%) have an expected frequency of 5 or less. The smallest expected frequency is 0.19.			

tumor grading * EGFR staining intensity – contingency table							
number							
		EGFR staining intensity					total
		0	weak	intermediate	strong	missing	
valid	no grading or missing	1	3	0	2	0	6
	Well-differentiated	2	2	6	1	0	11
	moderatly-differentiated	10	6	4	8	1	29
	poorly-differentiated	7	2	3	3	2	17
	total	20	13	13	14	3	63

chi-squared test			
	value	df	Asymptotic significance (two-sided)
Chi-squared (Pearson)	17.287[a]	12	0.139
Likelihood-Quotient	16.752	12	0.159
Number of valid cases	63		
a. 15 cells (75.0%) have an expected frequency of 5 or less. The smallest expected frequency is 0.29.			

tumor grading * EGFR IRS – contingency table											
number											
		EGFR – IRS									total
		0	1	2	4	5	6	8	9	12	
valid	no grading or missing	1	1	1	1	0	0	0	0	2	6
	Well-differentiated	2	0	1	1	0	2	4	0	1	11
	moderatly-differentiated	10	0	3	5	1	0	2	2	6	29
	poorly-differentiated	7	0	0	2	2	1	3	0	2	17
	total	20	1	5	9	3	3	9	2	11	63

chi-squared test			
	value	df	Asymptotic significance (two-sided)
Chi-squared (Pearson)	32.283[a]	24	0.12
Likelihood-Quotient	29.759	24	0.193
Number of valid cases	63		
a. 33 cells (91.7%) have an expected frequency of 5 or less. The smallest expected frequency is 0.10.			

6.3 Abbreviations

2-DG	2-deoxy-D-glucose
ANOVA	Analysis of variance between groups
APS	Ammonium persulfate
AR	Androgen receptor
ATP	Adenosine triphosphate
BCLC	Barcelona clinic liver cancer staging
BSA	Bovine serum albumin
c-Abl	c-Abelson
Cdk5	Cyclin-dependent kinase 5
CLL	Chronic lymphatic leukemia
CNS	Central nervous system
ConcA	Concanamycin A
CTCF	Corrected total cell fluorescence
DEN	Diethylnitrosamine
DMEM	Dulbecco's modified eagle medium
DMSO	Dimethylsulfoxide
DNA	Deoxyribonucleic acid
DTT	Dithiothreitol
ECAR	Extracellular acidification rate
E. coli	Escherichia coli
EDTA	Ethylendiaminetetraacetic acid
EEA1	Early endosome antigen
EGF	Epidermal growth factor
EGFR	Epidermal growth factor receptor
EMT	Epithelial-to-mesenchymal transition
Erk	Extracellular signalling-regulated kinase
ESCRT	Endosomal sorting complex required for transport
FACS	Fluorescence activated cell sorter
FCS	Fetal calf serum
FGF	Fibroblast growth factor
FLT3	FMS-like tyrosine kinase 3
FS	Fluorochrome solution
GAP	GTPase-activating proteins
GDP	Guanosine diphosphate

GEF	Guanine nucleotide exchange factors
GFP	Green fluorescent protein
GTP	Guanosine triphosphate
HBV	Hepatitis B virus
HCC	Hepatocellular carcinoma
HCV	Hepatitis C virus
HDAC	Histone deacetylase
HGF	Hepatocyte growth factor
HGFR	Hepatocyte growth factor receptor
HRP	Horse radish peroxidase
IGF	Insulin-like growth factor
IGF1R	Insulin-like growth factor-1 receptor
IRS	Immunoreactive score
JCBR	Japanese collection of research bioresources
KO	Knock-Out
MAPK	Mitogen-activated protein kinase
MCL	Mantle cell lymphoma
MEK	MAPK/ERK kinase
MOI	Multiplicity of infection
mRNA	Messanger RNA
MTC	Medullary thyroid carcinoma
mTOR	Mammalian target of rapamycin
MVB	Multivesicluar body
Na_3VO_4	Sodium orthovanadate
NaF	Sodium fluoride
NMDA	N-methyl-D-aspartate
NSCLC	Non-small cell lung cancer
OCR	Oxygen consumption rate
PBS	Phosphate buffered saline
PD-1	Programmed cell death protein 1
PDGFR	Platlet derived growth factor receptor
PI	Propidium iodide
PI3K	Phosphatidylinositol-4,5-bisphosphate 3-kinase
PMSF	Phenylmethylsulfonyl fluoride
PPI	Protein-protein interaction
PVDF	Polyvinylidene difluoride
Rb	Retinoblastoma protein

RNA	Ribonucleic acid
rpm	Revolutions per minute
RT	Room temperatur
RT-qPCR	Realt time- quantitative polymerase chain reaction
SCID	Severe combined immunodeficiancy
SDS	Sodium dodecyl sulfate
SDS-PAGE	SDS-polyacrylamide gel electrophoresis
SEM	Standard error of the mean
sgRNA	Single guide RNA
shRNA	Short hairpin ribonucleic acid
Sora	Sorafenib
STAT3	Signal transducer and activator of transcription 3
TACE	Transarterial chemoembolization
TBS-T	Tris-buffered saline-Tween 20
TEMED	Tetramethylethylenediamine
TGF-α	Transforming growth factor alpha
TMA	Tissue microarray
VEGFR	Vascular endothelial growth factor receptor
Wnt	Wingless
wt	Wild-type

6.4 List of Publications and Conference Contributions

6.4.1 Articles

Inhibition of Cyclin-dependent Kinase 5 – a Novel Strategy to Improve Sorafenib Response in HCC Therapy
Maximilian A. Ardel, Thomas Fröhlich, Emanuele Martini, Martin Müller, Veronika Kanitz, Carina Atzberger, Petra Cantonati, Martina Meßner, Laura Posselt, Thorsten Lehr, Jan-Georg Wojtyniak, Melanie Ulrich, Georg J. Arnold, Lars König, Dario Parazzoli, Stefan Zahler, Simon Rothenfußer, Doris Mayr, Alexander Gerbes, Giorgio Scita, Angelika M. Vollmar, Johanna Pachmayr
Hepatology, 2018 July 23

Targeting cyclin dependent kinase 5 in hepatocellular carcinoma - A novel therapeutic approach
Sandra M. Ehrlich, Johanna Liebl, Maximilian A. Ardelt, Thorsten Lehr, Enrico N. De Toni, Doris Mayr, Lydia Brandl, Thomas Kirchner, Stefan Zahler, Alexander L. Gerbes, Angelika M. Vollmar
J Hepatol **63**, 102-113, 2015.

Inhibition of the V-ATPase by Archazolid A: A New Strategy to Inhibit EMT
Henriette Merk, Philipp Messer, Maximilian A. Ardelt, Don. C. Lamb, Stefan Zahler, Rolf Müller, Angelika M. Vollmar, Johanna Pachmayr
Mol Cancer Ther **16**, 2329-2339, 2017.

The long non-coding RNA H19 – a new player in HCC
Maximilian A. Ardelt, Johanna Pachmayr
Cell Stress **1**, 4-6, 2017

6.4.2 Presentations

Maximilian A. Ardelt, Thomas Fröhlich, Georg J. Arnold, Angelika M. Vollmar, Johanna Liebl; *Inhibition of Cyclin dependent kinase 5 sensitizes hepatocellular carcinoma cells for Sorafenib treatment*, International Liver Cancer Association 10th Annual Conference, Vancouver, Canada, September 9-11, 2016 (Unterstützt durch ein Stipendium der GlaxoSmithKline Stiftung)

Maximilian A. Ardelt, Thomas Fröhlich, Thorsten Lehr, Jan-Georg Wojtyniak, Georg J. Arnold, Angelika M. Vollmar, Johanna Liebl; *Inhibition of Cdk5 – a novel strategy to improve Sorafenib response in HCC therapy,* Annual Meeting of the German Pharmaceutical Society (DPhG), Munich, Germany, Oktober 4-7, 2016

Maximilian A. Ardelt, Thomas Fröhlich, Thorsten Lehr, Jan-Georg Wojtyniak, Georg J. Arnold, Giorgio Scita, Angelika M. Vollmar, Johanna Liebl; *Sorafenib response in HCC therapy – Introducing new possibilities with Cdk5 inhibition,* International PhD students/Postdocs meeting 2017 of the German Pharmaceutical Society (DPhG), Frankfurt am Main, Germany, March 29-31, 2017

6.5 Acknowledgements

An allererster Stelle möchte ich mich ganz herzlich bei Frau Prof. Dr. Angelika Vollmar dafür bedanken, dass sie es mir ermöglicht haben meine Doktorarbeit in Ihrer Arbeitsgruppe anzufertigen. Ihre hervorragende Betreuung, die produktiven Diskussionen in den Achievements, sowie Ihr offenes Ohr für schwierige persönliche sowie wissenschaftliche Belange haben die letzten drei Jahre zu etwas ganz Besonderem gemacht. Vielen Dank für Ihr Vertrauen in meine Arbeit und Ihre Geduld, die es mir ermöglichte meine Ideen umzusetzen.

Ein ganz besonderer Dank gebührt Frau Prof. Dr. Johanna Pachmayr, die mich seit dem Beginn meines Forschungspraktikums im Oktober 2013 bis heute betreut hat und mir auf meinem Weg stets mit Rat und Tat zur Seite stand. Vielen Dank, dass du immer an mich und meine Ideen geglaubt hast und die nötige Motivation vermittelt hast, wenn die Versuche mal nicht wie geplant funktioniert haben. Ich freue mich auf neue, gemeinsame Herausforderungen in Salzburg.

Außerdem möchte ich Herrn Prof. Dr. Zahler für die konstruktive Kritik an meiner Arbeit sowie für jegliche Unterstützung mit technischen Problemen danken.

Meinem Prüfungskomitee bestehend aus PD Dr. Hans Zischka, Prof. Dr. Franz Paintner, PD Dr. Dr. Christian Grimm und Prof. Dr. Franz Bracher gilt mein aufrichtiger Dank für Ihre Zeit und Mühe.

Vielen Dank an meine zahlreichen Kooperationspartner, die mir dabei geholfen haben, die Arbeit zu dem zu machen was sie ist:

Prof. Dr. Thorsten Lehr (Klinische Pharmazie, Universität des Saarlands), Prof. Dr. Doris Mayr und Dr. Veronika Kanitz (Pathologisches Institut, Klinikum der Universität München), Prof. Dr. Georg Arnold und Dr. Thomas Fröhlich (LAFUGA, Gen Zentrum, Universität München), Prof. Dr. Simon Rothenfußer, Dr. Lars König und Dr. Laura Posselt (Clinical Pharmacology, Klinikum der Universität München), Prof. Dr. Giorgio Scita, Dr. Dario Parazzoli and Dr. Emanuele Martini (Institute for Molecular Oncology, Universität Mailand) und Prof. Dr. Alexander Gerbes (Leberzentrum München, Klinikum der Universität München).

Besonders hervorgehoben werden muss die Leistung der Bachelor- und Masterstudenten, die ich in meiner Zeit betreut habe: Maximilian Schielein (B.Sc.), Martina Meßner (M.Sc.) und Martin Müller (M.Sc.). Vielen Dank für eure tatkräftige Hilfe im Labor und für eure hervorragende Arbeit.

Zudem möchte ich mich bei allen ehemaligen und aktuellen Mitgliedern des AK Vollmars für das herausragende Arbeitsklima bedanken, das es mir jeden einzelnen Tag der letzten Jahre einfach gemacht hat zur Arbeit zu gehen.

Vielen Dank an Jana und Kerstin, für die ich bereits zum Inventar gehört habe, für die schöne Zeit und die Hilfe im Labor.
Von den „Alt-Doktoranden“ möchte ich besonders Sandra, Henri, Lina, Julia und Katja dafür danken, dass sie mich so gut aufgenommen haben, mir bei Fragen immer geholfen haben und die Zeit in und um das Labor mit verschiedensten Aktivitäten besonders gestaltet haben. Besonders möchte ich mich hier bei Sandra für die Betreuung meiner Masterarbeit und bei Henri, der besten Laborboxpartnerin, bedanken.
Ebenfalls ein großes Dankeschön geht an meine Doktorandengeneration. Meli, Chrissi, Fabi, Karin und Lisa, vielen Dank für die schönen letzten drei Jahre.
Ein besonderes Dankeschön geht an Flo mit dem ich den Weg zum Doktortitel seit Tag 1 unseres Studiums gegangen bin. Vielen Dank für deine Freundschaft und die Unterstützung in den letzten 9 Jahren.
Zu guter Letzt möchte ich mich bei denjenigen bedanken, denen diese Arbeit gewidmet ist. Vielen Dank an meine Mutter, meinen Vater und meine Schwester für die immerwährende Unterstützung in jeder Lebenslage und das offene Ohr in schwierigen Zeiten. Ihr habt maßgeblich dazu beigetragen wo ich heute stehe und ohne eure Hilfe wäre das hier nicht möglich gewesen.